Urban Gamma Spectrometry: Report 1

Aage, Helle Karina; Kuukankorpi, Satu; Moring, Mikael; Smolander, Petri ; Toivonen, Harri

Publication date:
2009

Document Version
Publisher's PDF, also known as Version of record

nks

Nordisk kernesikkerhedsforskning
Norrænar kjarnöryggisrannsóknir
Pohjoismainen ydinturvallisuustutkimus
Nordisk kjernesikkerhetsforskning
Nordisk kärnsäkerhetsforskning
Nordic nuclear safety research

NKS-190
ISBN 978-87-7893-257-0

Urban Gamma Spectrometry: Report 1

[1]Helle Karina Aage, [2]Satu Kuukankorpi, [2]Mikael Moring, [2]Petri Smolander and [2]Harri Toivonen

1) Technical University of Denmark, Kgs. Lyngby, Denmark
2) Radiation and Nuclear Safety Authority, Helsinki, Finland

June 2009

Abstract

This report contains the present status and results for the NKS UGS-project per 1 June 2006 for NKS partners DTU, Denmark, and STUK, Finland.
The Danish and Finnish CGS systems are not of similar types. The Danish CGS system(s) only make use of one NaI(Tl) detector whereas the Finnish CGS system consists of several detectors, NaI(Tl) and HPGe both and as an additional feature the Finnish detectors have position dependent different fields of view. Furthermore, the Finnish system is equipped with an air sampling system. In terms of operation, the Danish detector is located r on the rooftop whereas the Finnish detectors are located inside the vehicle.
The Finnish and the Danish team use different methods for data processing. STUK uses a hypothesis test method to get robust real time alarms (within 10 seconds) when significant peaks from a previously defined set of nuclides are detected. An alarm for a significantly elevated total pulse rate is sent if none of the predefined nuclides is identified. All data are stored to the LINSSI database, which facilitates easy data retrieval for post processing.
DEMA/DTU bases their calculations on full spectrum fitting using NASVD and the Danish software NucSpec. Source signals are found from spectrum fitting residuals or from stripping of energy windows – either by the standard 4-windows method or by a measurement based method where stripping factors for any window of interest can be derived from the measurements themselves.
A thorough description of the two systems and data processing methods (including mathematics) are described in this report.
For the Danish methods of data processing some comparisons have been made, but no final conclusion has been reached yet. Raw urban data has been investigated along with urban data sets to which source signals have been added and searched for.
For the Finnish method calibration plots of the minimum detection limits for two different detector types have been made so far, and survey significance plots from drives around Helsinki during the Athletics World Championship in 2005 are presented.

Key words

Urban Carborne Gamma Spectrometry, Spectrum Stripping, Peak hypothesis, LINSSI, FSC, ASSS, NASVD

NKS-190
ISBN 978-87-7893-257-0

Electronic report, June 2009

NKS Secretariat
NKS-776
P.O. Box 49
DK - 4000 Roskilde, Denmark

Phone +45 4677 4045
Fax +45 4677 4046
www.nks.org
e-mail nks@nks.org

URBAN GAMMA SPECTROMETRY

NKS
Nordic Nuclear Safety Research

Report 1 from the AFT/B(06)3 project group
01 June 2006

Helle Karina Aage[1)]
Satu Kuukankorpi[2)]
Mikael Moring[2)]
Petri Smolander[2)]
Harri Toivonon[2)]

1) Technical University of Denmark, Lyngby, Denmark
2) Radiation and Nuclear Safety Authority, Helsinki, Finland

1 SUMMARY

This report contains the present status and results for the NKS UGS-project per 1 June 2006. A comparison of the data treatment methods – Finnish method on Danish data material and vice versa -will take place in the second part of the project, which will also include data from SSI custom control CGS systems.

The Danish and Finnish CGS systems are not of similar types. The Danish CGS system(s) only make use of one NaI(Tl) detector whereas the Finnish CGS system consists of several detectors, NaI(Tl) and HPGe both and as an additional feature the Finnish detectors have position dependent different fields of view. Furthermore, the Finnish system is equipped with an air sampling system.

In terms of personnel, The Danish preference has been to have 3 simple CGS systems, that can be operated (with some introduction) by unskilled persons if necessary whereas the Finnish system is operated by experts.
In terms of operation, the Danish detector is located outdoor on the rooftop whereas the Finnish detectors are located inside the vehicle.

As a consequence of the different types and positions of detectors, one can say for certain that if the two different systems surveyed the same route, the results in terms of measurements would be far from identical.

The Finnish and the Danish teams use different methods for data processing.

STUK uses a hypothesis test method to get robust real time alarms (within 10 seconds) when significant peaks from a previously defined set of nuclides are detected. An alarm for a significantly elevated total pulse rate is sent if none of the predefined nuclides is identified. All data are stored to the LINSSI database, which facilitates easy data retrieval for post processing.
DEMA/DTU bases their calculations on full spectrum fitting using NASVD and the Danish software NucSpec. Source signals are found from spectrum fitting residuals or from stripping of energy windows – either by the standard 4-windows method or by a measurement based method where stripping factors for any window of interest can be derived from the measurements themselves.

Measurements from two different systems are available to be processed with three different data processing tools. This gives the participants a great opportunity to test the limits of their data processing methods that has previously only been used on own data material, i.e. are the data processing methods to be recommended for other users?

A thorough description of the two systems and data processing methods (including mathematics) are described in this report.

For the Danish methods of data processing some comparisons have been made, but no final conclusion has been reached yet. Raw urban data has been investigated along with urban data sets to which source signals have been added and searched for.
For the Finnish method calibration plots of the minimum detection limits for two different detector types have been made so far, and survey significance plots from drives around Helsinki during the Athletics World Championship in 2005 are presented.

CONTENTS PAGE

2 INTRODUCTION

Urban gamma spectrometry has been given only minor attention with the focus being on rural gamma spectrometry. However, in recent years the Nordic emergency management agencies have turned focus towards border controls and the topic of lost sources. Gamma spectra measured in urban areas are characterized by a wide variety of spectrum shapes and very fast changes in environmental background values.

In 2004 a Danish CGS survey in the capitol Copenhagen took place. It was found that gamma spectrometry in urban areas is far more complicated to interpret than had previously been thought. Known and available methods of data processing were not enough to interpret the results and a new method "Fitting with Spectral Components", FSC, based on NASVD, was tested with some success. Yet, the method still needs a lot of improvement.

In Finland a database “LINSSI” has been developed for spectrum data. In CGS search mode a "peak hypothesis test" is applied to the measured spectra. This system was tested during the Helsinki 2005 Athletics World Championship and it provides fast and accurate automated alarms for intermediate and high level signals, but optimisation of detecting small signals is needed.

In Sweden mobile detector systems are used for border controls and problems are encountered when making measurement in harbour, container areas.

The aim of this project is to improve the methods handling data and for interpretation of urban gamma spectrometry measurements. The Finnish and Danish methods will be compared and tested on the same data sets from Copenhagen and Helsinki and, if available, SSI customs measurements with a possible combination of the two methods in mind. Data sets with and without source signals will be examined, with special emphasis on difficult background signals.

3 DANISH CGS MEASUREMENTS

3.1 The Danish CGS Systems

The Danish CGS system is equipped with a 4L NaI(Tl) of dimensions 16"×4"×4"(40.64 cm×10.16 cm×10.16cm) and a GR-320 spectrometer. The system runs with the software 660Rover. The hardware and the software both originate from SAIC (Exploranium).

The detector is positioned on the roof top of the car at a height of 2.2 m to the passenger's site, i.e. closest to the roadside (DK: right side of the road).
The detector encapsulation is stainless steel of thickness 0.25 mm. The detector box itself is made of aluminium with thickness approximately 1.5 mm. Inside the detector box is a layer of 2 cm polyurethane foam. In 2004 the detector box was given an additional cover in the form a "box for skiing equipment" to protect the system (smelting water in winter, slower temperature changes). Figure 3.1.1 shows the detector position relative to the car.

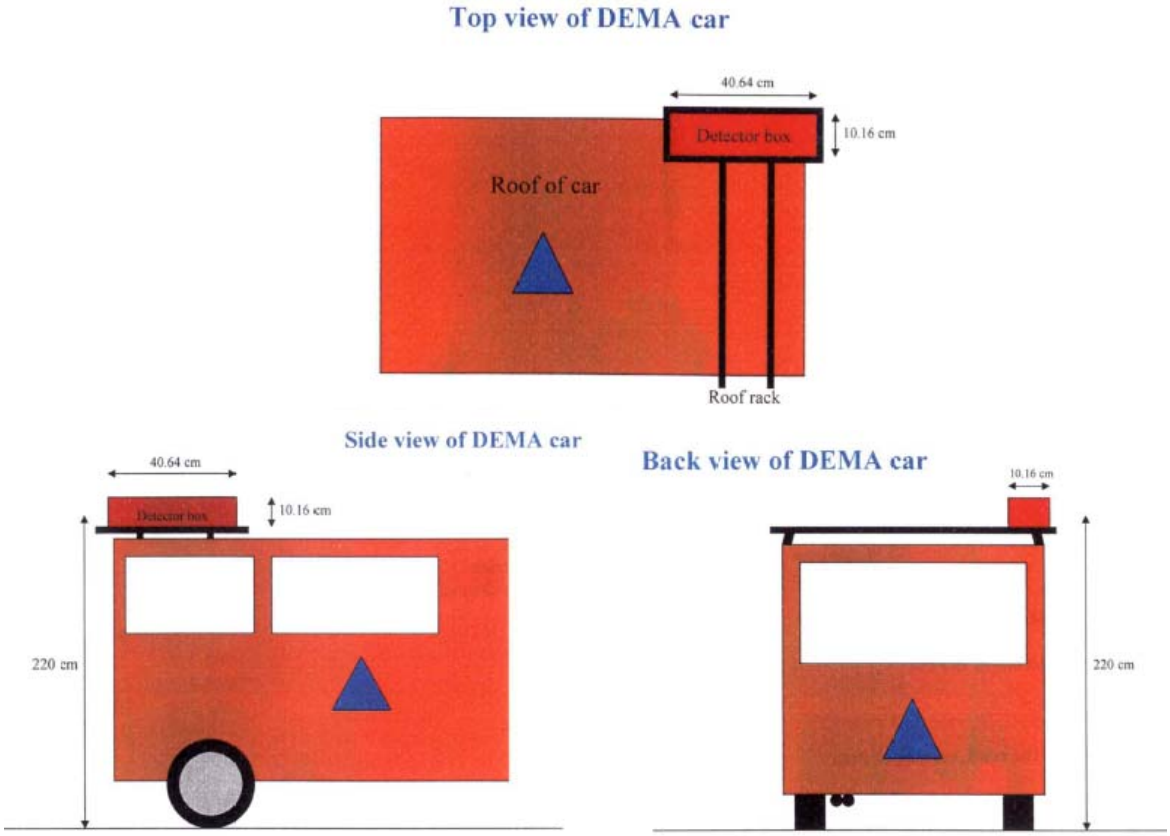

Figure 3.1.1. Danish CGS system. Top, side and back view. (Ref. 1)

The system is stabilised on a Th-calibration source for normal operation (2614 keV in channel 418), but the possibility of stabilising using a ^{137}Cs source exists for measurements in contaminated areas. All spectra are stored as binary data including GPS positions.

The standard spectrometer mode is the MCA mode with 512-channels spectra with a sampling frequency of approximately 2-s real time. The measurement time can be changed. CGS measurements from the early years, however, only include 1-s real time 256-channels spectra.

The software includes the features of on-line (slightly delayed) count rates, stripped count rates and dose rates. The XY track lines can also be verified during operation. The data are present on screen either as a moving vertical bar showing count rate fluctuations or as a rainbow plot with colour coded pixels representing either high or low count rates. Upon request, a single spectrum can be shown separately for a further evaluation and compared with another (chosen prior to the comparisons) spectrum.

The system alarm level can be chosen manually and changed during operation. If a window count rate or a total dose rate, for example, exceeds the level, the alarm will be displayed. One of the newer features is temperature logging at the detector crystal to check for non-temperature stabilisation that could possibly introduce spectrum drift in the measurements.

There are two functional Danish CGS systems, B11 and B12, and a replacement system. The data used in this report were made with system B12.

3.1.1 Standard Windows and Energy Calibration

The 512-channels Danish CGS systems have approximately the same energy calibration based on the full energy peak from ^{137}Cs in channel 110 (662 keV) and the full energy peak from ^{208}Tl in channel 418 (2615 keV).

The average energy calibration for the systems is:

$E\gamma = 0.00057 \cdot (chn)^2 + 6.05451 \cdot (chn) - 13.53113$ keV

All energies refer to the centre of a channel and first channel is channel 0.

Table 3.1.1.1. Standard radionuclide window.

Radionuclide	LL (chn)	LL(keV)	UL(chn)	UL(keV)
Cs	100	598	120	721
K	222	1359	253	1555
U	267	1644	299	1848
Th	386	2408	449	2820

Table 3.1.1.2. Background count rates and sensitivities.

Radionuclide	Background (cps)	Sensitivity	Sensitivity unit
Cs	4.73	20.30	kBq/m^2 (ESC)*
K	2.43	28.25	cps / %
U	1.32	3.804	cps / ppm eU
Th	0.89	1.771	cps / ppm eTh

*Equivalent Surface Concentration.

Table 3.1.1.3. Standard windows stripping factors.

a	b	g	α	β	γ	δ	ε	ζ
0.0537	0	0	0.336	0.442	0.833	2.072	2.776	0.341

The following windows are used with FSC calculations and ASSS calculations (Ref. 2).

Table 3.1.1.4. Δ^2-windows for the FSC and ASSS method.

No	LL (chn.)	UL (chn.)	LL (keV)	UL (keV)	
0	User's choice	User's choice	-	-	-
1	20	40	107	230	^{199}Tcm
2	48	65	278	382	Scatter
3	50	70	291	413	Scatter
4	55	72	321	425	^{131}I
5	100	120	598	721	^{137}Cs
6	180	220	1095	1346	^{60}Co
7	222	253	1359	1555	K
8	267	299	1644	1848	U
9	386	449	2408	2820	Th
10	20	240	107	1472	Total_1
11	20	435	107	2728	Total_2

Window 10 ends at the ^{40}K centroid and window 11 ends after the Th-peak.

3.1.2 File Layout

The following Exploranium data layout (layout 3), ref. 17 June 2003 GR660 version 6.0, is valid for the Danish CGS files:

Header 547 bytes
Struct 1152 bytes:
unsigned long Record_number;
unsigned long Line_number;
double UTC_time;
double X;
double Y;
double Z;
double Northing;
double Easting;
float PDOP;
long DGPS;
float ralt;
float Live_time;
float roi[10];
short gain
short peak
int clock time
char spare[8];
unsigned int SPC[512];

X, Y, Z are GPS ECEF-co-ordinates.
UTC time is seconds since 1. January 1970, PC time dependent.

3.2 CGS Data Treatment Tools

3.2.1 Standard Software

The standard software tool for post-processing of Danish CGS data is the program NUCSpec developed in corporation between the Danish Emergency Management Agency and Prolog Development Centre (Copyright PDC).

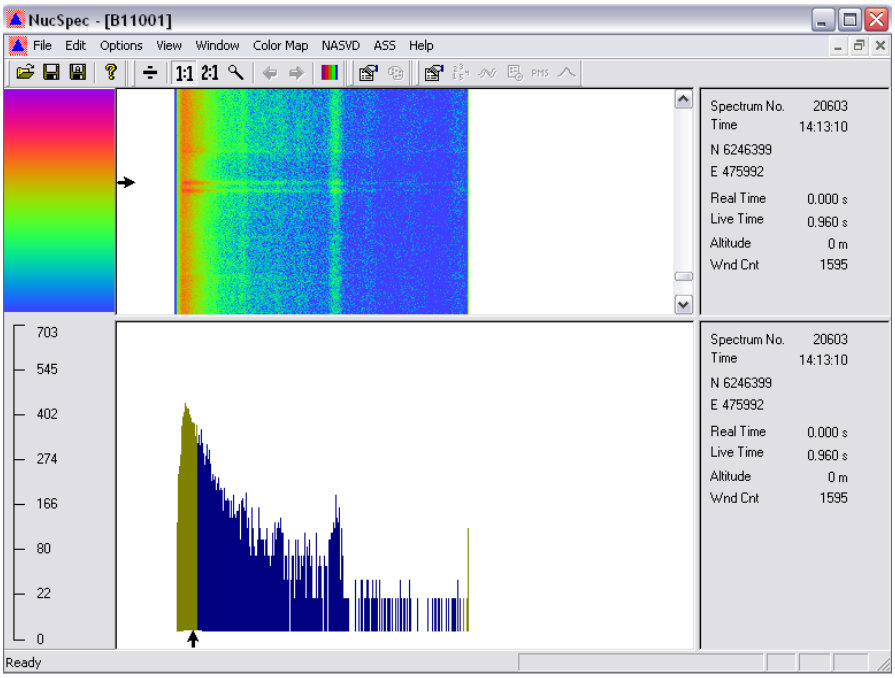

Figure 3.2.1.1. NUCSpec screen dump.

The earliest version only allowed for AGS (Airborne Gamma Spectrometry) measurements but the newer versions are for AGS and CGS both. A few years ago the NASVD (Noise Adjusted Single Value Decomposition) method invented by Dr. Jens Hovgaard was supplied upon request as a special NUCSpec feature. The latest version of NUCSpec also includes the method of ASSS (Area Specific Spectrum Stripping). NASVD and ASSS are not necessary in order to run NUCSpec but are separate dll files. This report will include a short discussion of measurements investigated by the ASSS method.

Table 3.2.1. The NUCSpec program structure.

File	Description
NUCSpec.exe	The main program – always needed
Nasvddlll.dll	A DLL for running the NASVD program
Mapdll.dll	A DLL for running the MAP program
Projections.def	A text file defining the projections available in NUCSpec
Positions.def	A tects file defining the geographical positions of the PMS stations
Default.xml	A default setup file
DefaultASS.xml	A default area specific stripping setup file

The basic program facilities are the standard 4-windows-stripping method for Th, U, K and ^{137}Cs concentrations, calculation of air kerma rates based on SDI-values, plotting of track lines and creation of colour maps for direct export to MapInfo.

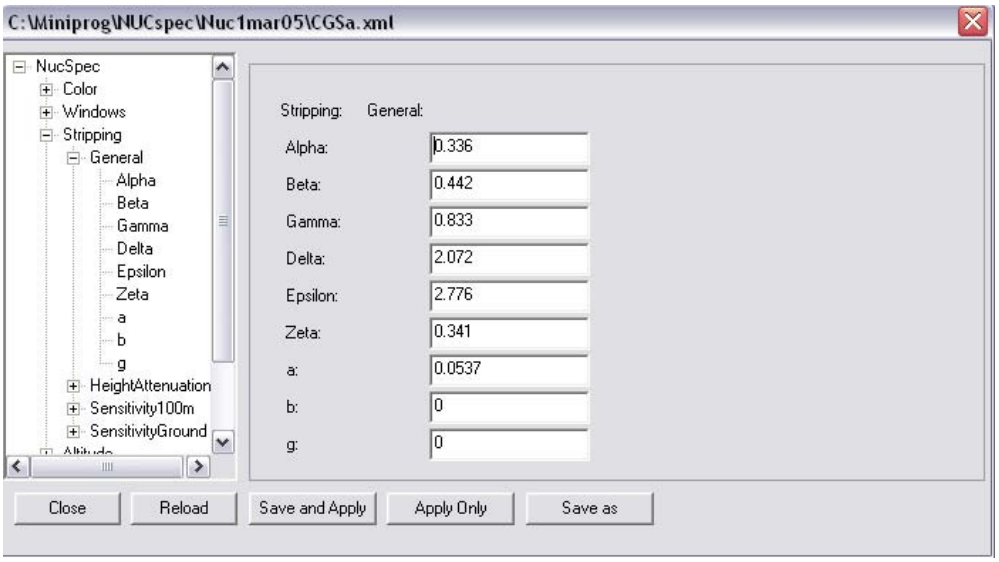

Figure 3.2.1.2. NUCSpec CGS stripping factors.

Destroyed spectra can be deleted from the data files and selections of data saved as new data files. It is also possible to extract single spectra in text file layout. NASVD treatment of data before the calculations take place will eliminate "noise" to a large extent: groups of spectra are divided into a number of spectral shapes and the shapes are then recombined according to the users' choice, e.g. the mean spectrum can be subtracted from all spectra. The relatively new ASSS feature (Ref. 3, 4) provides the possibility for extracting stripping factors for any radionuclide window directly from a set of measured data instead of using pre-calculated values.

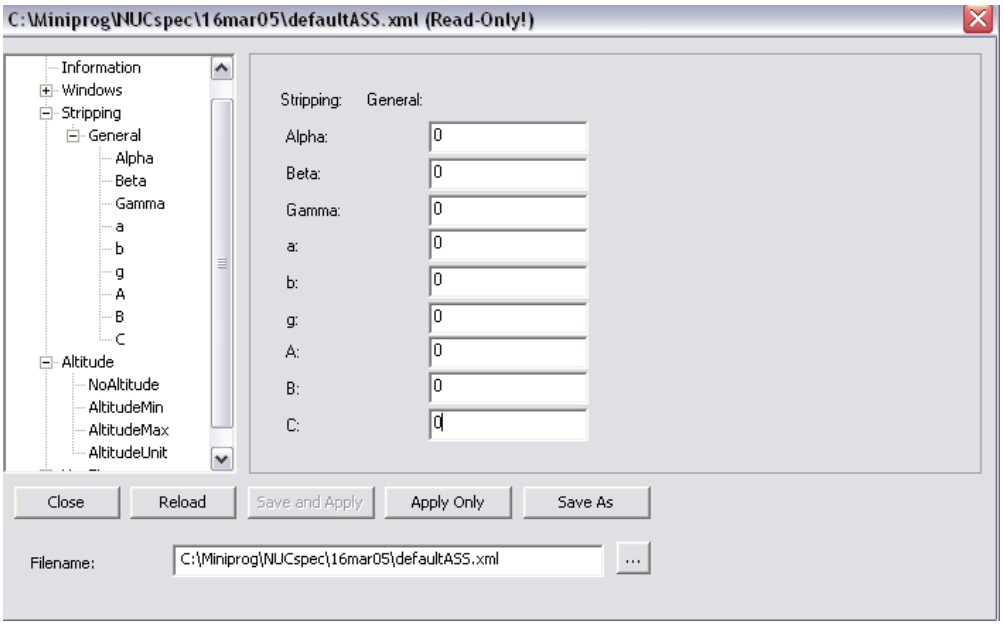

Figure 3.2.1.3. NUCSpec Area Specific Stripping.

3.2.2 Non-standard Tools: Fitting with Spectral Components, FSC

This method is not a part of the standard processing tool pack NUCSpec, but may be included in the future. The Danish Permanent Monitoring Stations, PMS, are equipped with a slightly similar fitting procedure, but fitting with two or three components only.
The FSC method has been tested with stationary measurements from the PMS station at DTU (research station only) with very good results (Ref. 5). Recently the method was tried on a very small selection of spectra measured in the central part of Copenhagen (Ref. 6). The results were promising, but more work needs to be done to perform an evaluation of the method in an environment where the spectrum shapes changes constantly.

The FSC method consists of a series of small programs written in Microsoft Visual Studio C^{++} NET 2003 (Microsoft Development Environment Version 7.1.3088). Dr. Jens Hovgaard (Radiation Solutions Inc.) kindly supplied the matrix inversion procedure in the program FSC_2006.

The programs are:

CGSdif — Creates a difference spectrum for two CGS measurements. The outputs are a binary file containing a 512-channels spectrum (1024 bytes, short integers) and txt file containing the two chosen spectra and their difference. The program is for 512-channels CGS data.

SpecAdd — Adds a binary 512-channels spectrum without header (1024 bytes, short integers) to a spectrum in a 512-channels CGS data file. The spectrum can be added several times to different spectrum numbers. A multiplication factor of 0 will result in no addition. Data are saved in CGS layout 3 (header 547 bytes and spectrum struct 1152 bytes).

Txt2Bin — Translates a 512-channels spectrum text file to a 512-channels binary spectrum file that can be used with SpecAdd.

FSC_2006 — Main fitting program
In order to run the program the following files must be available:

- A file containing up to a maximum of 10 spectral components. The first column contains the mean spectrum, $\mathbf{s}_0$.
- A file with the measured data. The data format should be Danish CGS layout.

The outputs from the main fitting programs are:

Fitting file — Number of runs, lower channel for fitting, upper channel for fitting, fitting constants, Δ^2-values, co-ordinates, UTC time and live time. The Δ^2-windows are based on the windows used in the Barents Rescue Exercise, Boden, Sweden, 2001 and cannot be changed. One additional voluntary window is possible.

Spectra file — Spectrum number, the measured spectrum, the weight factor, the reproduced spectrum, the difference spectrum and the live time in seconds.

3.3 Data Processing Methods

3.3.1 NASVD Noise Adjusted Singular Value Decomposition

The method was introduced by J. Hovgaard in 1997 and information on the basic properties and the applications of the NASVD technique can be studied in Ref 7, 8 and 9.

The measured spectra are decomposed into a set of spectral components. The first spectral component $\mathbf{s}_0$ is the mean spectrum containing the background. For each measured spectrum is determined the amount – the amplitude $b_{i,j}$ – of each spectral components $\mathbf{s}_i$ that should be included in a best fit of the measured spectrum.
For most natural data sets all spectra can be reconstructed by using only the mean spectrum $\mathbf{s}_0$ and five additional spectral components i.e. there is no important information in $\mathbf{s}_6$, $\mathbf{s}_7$ etc. The reconstructed spectrum number i - $\mathbf{r}_i$ – is therefore calculated as:

$$\mathbf{r}_i = \mathbf{s}_0 + (b_{i,1}\mathbf{s}_1 + b_{i,2}\mathbf{s}_2 + b_{i,3}\mathbf{s}_3 + b_{i,4}\mathbf{s}_4 + b_{i,5}\mathbf{s}_5)/LT_i \qquad (3.3.1.1.)$$

$b_{i,j}$ is the amplitude (amount) of spectral component No. j to be included in the reconstruction and LT_i is the live time for measurement No. i.

3.3.2 ASSS Area Specific Spectrum Stripping

Consider a large number of CGS spectra that have been measured in an environment with varying concentrations of Th, U, and K. Significant measuring parameters as energy calibration is assumed constant during the measurements. Furthermore it is assumed that variations in air radon concentrations are few. Then by having three primary parameters - i.e. the concentrations of Th, U, and K - the count rate of any energy window of a spectrum can be described as a linear combination of the concentrations of Th, U, and K, i.e.:

$$r_{l,i} = \alpha c_{Th,i} + \beta c_{U,i} + \gamma c_{K,i} + \delta_i \qquad (3.3.2.1)$$

Where $r_{l,i}$ is the count rate of a low energy window for spectrum number i after subtraction of the background count rate. $c_{Th,i}$ is the concentration of thorium in the surroundings corresponding to spectrum number i. $c_{U,i}$ and $c_{K,i}$ have similar meanings. δ_i is the statistical error for Equation (3.3.2.1) caused by the Poisson statistics of the window counts.

The concentrations of Th, U, and K corresponding to spectrum number i can be determined from window count rates for the full energy peaks of Th (2615 keV), U (1764 keV) and K (1461 keV) and there are linear relations between those count rates and the concentrations (as used for the normal three-window method). Therefore the count rate of the low energy window also can be described as:

$$r_{l,i} = a \cdot r_{Th,i} + b \cdot r_{U,i} + c \cdot r_{K,i} + \Delta_i \qquad (3.3.2.2)$$

where $r_{Th,i}$, $r_{U,i}$ and $r_{K,i}$ are the count rates of the "standard" windows for Th, U, and K respectively. Δ_i is the statistical error for the equation caused by having statistical fluctuations for all four window count rates of Equation (3.3.2.2). The parameters a, b, and c are constants for a specific set of windows and, therefore, Equation (3.3.2.2) tells that the count rate of a low energy window can be described as a linear combination of the count rates of the other windows.

The parameters a, b and c depend on the detector and its position in/on a car, on the energy calibration and on the channel numbers included in each window.

For a specific detector mounted in a specific way on/in a specific car etc. one will be able to extract the best parameters a, b and c from a large set of data by investigating the "error" F defined by:

$$F = \Sigma\Delta_i^2 = \Sigma(r_{l,i} - a\cdot r_{Th,i} - b\cdot r_{U,i} - c\cdot r_{K,i})^2 \qquad (3.3.2.3)$$

The task now is to find the a, b, and c values that gives the smallest value of F.
One may include a weight factor - w_i - as for example:

$$F = \Sigma\Delta_i^2\cdot w_i = \Sigma w_i\cdot(r_{l,i} - a\cdot r_{Th,i} - b\cdot r_{U,i} - c\cdot r_{K,i})^2 \qquad (3.3.2.3a)$$

Here w_i is a weight factor that takes into account that Δ_i^2 varies from measurement to measurement (from spectrum to spectrum). Usually one uses a weight factor w_i that is inversely proportional to the variance of measurement No. i, i.e. one will have:

$$F = \Sigma\Delta_i^2/var_i = \Sigma(r_{l,i} - a\cdot r_{Th,i} - b\cdot r_{U,i} - c\cdot r_{K,i})^2 /var_i \qquad (3.3.2.3b)$$

A weight factor w_i is not included in the calculations described below. The reason is that for measurements in a normal environment the count rates will not vary much more that a factor 2. However, an inclusion of a weight factor is a simple matter. One at first finds some preliminary values of a, b, and c without using a weight factor. Then by using the preliminary values one calculates the variance for $(r_{l,i} - a\cdot r_{Th,i} - b\cdot r_{U,i} - c\cdot r_{K,i})$ and includes it into Equation (3.3.3.2b) and then calculates new values for a, b, and c.

[By not including a weight factor in the calculations the spectra with high count rates will get a somewhat too large influence on the results. If the measuring geometry is the same for all spectra - and only the concentrations vary - this is without influence. However, if varying concentrations are correlated to varying measuring geometry a minor error may come up. But practical experiences with strongly varying geometry and concentrations indicate that the error is in the order of 1%.]

Now by using the Equation (3.3.2.3) for minimising F by varying the values of a, b, and c one gets:

$$dF/da = 2\cdot\Sigma(-r_{Th,i})\cdot(r_{l,i} - a\cdot r_{Th,i} - b\cdot r_{U,i} - c\cdot r_{K,i}) = 0 \qquad (3.3.2.4a)$$
$$dF/db = 2\cdot\Sigma(-r_{U,i})\cdot(r_{l,i} - a\cdot r_{Th,i} - b\cdot r_{U,i} - c\cdot r_{K,i}) = 0 \qquad (3.3.2.4b)$$
$$dF/dc = 2\cdot\Sigma(-r_{K,i})\cdot(r_{l,i} - a\cdot r_{Th,i} - b\cdot r_{U,i} - c\cdot r_{K,i}) = 0 \qquad (3.3.2.4c)$$

The equations can now be rewritten to:

$$a\cdot\Sigma r_{Th,i}^2 + b\cdot\Sigma r_{Th,i}\cdot r_{U,i} + c\cdot\Sigma r_{Th,i}\cdot r_{K,i} = \Sigma r_{l,i}\cdot r_{Th,i} \qquad (3.3.2.5a)$$
$$a\cdot\Sigma r_{Th,i}\cdot r_{U,i} + b\cdot\Sigma r_{U,i}^2 + c\cdot\Sigma r_{U,i}\cdot r_{K,i} = \Sigma r_{l,i}\cdot r_{U,i} \qquad (3.3.2.5b)$$
$$a\cdot\Sigma r_{Th,i}\cdot r_{K,i} + b\cdot\Sigma r_{U,i}\cdot r_{K,i} + c\cdot\Sigma r_{K,i}^2 = \Sigma r_{l,i}\cdot r_{K,i} \qquad (3.3.2.5c)$$

The practical way of solving the equations by a computer program is to calculate a set of new parameters, namely:

$$\begin{array}{lll} TT = \Sigma r_{Th,i}^2 & UU = \Sigma r_{U,i}^2 & KK = \Sigma r_{K,i}^2 \\ TU = \Sigma r_{Th,i} \cdot r_{U,i} & TK = \Sigma r_{Th,i} \cdot r_{K,i} & UK = \Sigma r_{U,i} \cdot r_{K,i} \\ LT = \Sigma r_{l,i} \cdot r_{Th,i} & LU = \Sigma r_{l,i} \cdot r_{U,i} & LK = \Sigma r_{l,i} \cdot r_{K,i} \end{array} \qquad (3.3.2.6)$$

Finally one may define a matrix **H** and the column vectors **v** and **w** by:

$$\mathbf{H} = \begin{array}{ccc} TT & TU & TK \\ TU & UU & UK \\ TK & UK & KK \end{array} \qquad \mathbf{v} = \begin{array}{c} a \\ b \\ c \end{array} \qquad \mathbf{w} = \begin{array}{c} LT \\ LU \\ LK \end{array} \qquad (3.3.2.7)$$

Now (3.3.2.5) can be written as:

$\mathbf{H}\,\mathbf{v} = \mathbf{w}$ or $\mathbf{v} = \mathbf{H}^{-1}\mathbf{w}$, from where a, b, and c can be determined.

Next assume that a, b, and c has been determined for a large set of spectra. One now investigates the original formula:

$$r_{l,i} = a \cdot r_{Th,i} + b \cdot r_{U,i} + c \cdot r_{K,i} + \Delta_i \qquad (3.3.2.1)$$

rewritten to:

$$\Delta_i = r_{l,i} - a \cdot r_{Th,i} - b \cdot r_{U,i} - c \cdot r_{K,i} \qquad (3.3.2.8)$$

For a normal environment - and perfect equipment - the Δ_i values will scatter around zero when going from one spectrum to the next. For a real world situation one may have spectrum drift causing Δ_i having somewhere mostly positive values and somewhere mostly negative values. Changes in measuring geometry also influence the result (slightly). If, however, a low energy emitter has added a signal to a sequence of spectra - for example when bypassing a point source with a low energy gamma emitter - then the Δ_i values will - when plotted spectrum by spectrum - exhibit a short peak above the general level.

One may include all spectra in the calculations - also spectra that are "suspected for carrying a signal from a low energy emitter. One then obtains "erroneous" a, b, and c values and a plot of Δ_i from Equation (3.3.3.8) will have a shift in level. However, the low energy emitter will yet show up with a peak.
In a search for unusual gamma radiation one may calculate sets of a, b, and c values for a number of low energy windows and investigate the corresponding Δ_i values.

3.3.3 FSC Fitting with Spectral Components

Least squares fitting of (city) CGS spectra with NASVD spectral components.

It is assumed that a set of CGS spectra has been decomposed into a number of spectral components by the NASVD technique.

For city CGS spectra the components will have to adjust for the intensity of radiation from Th + U and from K independently, and some spectrum drift usually also influences the spectrum shape. Therefore at least three spectral components are needed for reconstructions. In addition the "concentration" of Th and U may vary relative to each other whereby an additional spectral component is needed for the reconstructions. Finally the "geometry effect" in a city area will influence the spectrum shape - mostly at the lower energies. Therefore, in all at least five spectral components (+ $\mathbf{s}_0$) will normally be needed for reconstruction of city CGS spectra.

It is now assumed that a new set of CGS spectra has been recorded in the same or a similar area with the same equipment. The new set of spectra therefore has to include the same spectrum shapes as the "old" set of spectra. Therefore each of the new spectra also can be fitted from suitable combinations of spectral components from the old set of spectra i.e. it is assumed that one may write:

$$\mathbf{n}_i = \mathbf{s}_0 \cdot LT_i + c_{i,1} \cdot \mathbf{s}_1 + c_{i,2} \cdot \mathbf{s}_2 + c_{i,3} \cdot \mathbf{s}_3 + c_{i,4} \cdot \mathbf{s}_4 + c_{i,5} \cdot \mathbf{s}_5 + \boldsymbol{\delta}_i \qquad (3.3.3.1)$$

$\mathbf{n}_i$ is the measured "count spectrum" ($\mathbf{n}_i = \mathbf{r}_i \cdot LT_i$). $\boldsymbol{\delta}_i$ is the "errors" caused by statistical fluctuations. For convenience the term $\mathbf{s}_0 \cdot LT_i$ will be substituted by $\mathbf{n}_0$ in the following text. For the Danish CGS systems the count period is 2 s including a "dead time" of approximately 0.07 s. Therefore, Eq. 3.3.3.1 refers to the counts for one standard Live Time period of approximately 1.9 s. The product $\mathbf{s}_0 \cdot LT_i$ should include the actual live time whereas the live time is without influence on the remaining part of the equation. The indices "i" tells that each new spectrum should have its own set of parameters c_1, c_2, c_3, c_4, and c_5 those parameters automatically take the live time into account.

One may also write that:

$$\boldsymbol{\delta}_i = \mathbf{n}_i - \mathbf{n}_0 - c_{i,1} \cdot \mathbf{s}_1 - c_{i,2} \cdot \mathbf{s}_2 - c_{i,3} \cdot \mathbf{s}_3 - c_{i,4} \cdot \mathbf{s}_4 - c_{i,5} \cdot \mathbf{s}_5 \qquad (3.3.3.2)$$

As with the ASSS method a weight factor, w_i, can be applied.
The task now is to find the combination of c_1-, c_2-, c_3-, c_4- and c_5-values that produces the best fit. The "best" fit is determined by the standard least squares fit i.e. by demanding that Δ^2 - Δ^2 is defined as $\Sigma\delta_i^2 \cdot w_i$ has its minimum value:

$$\Delta^2_i = \Sigma \left(n_{i,j} - n_{0,j} - c_1 \cdot s_{1,j} - c_2 \cdot s_{2,j} - c_3 \cdot s_{3,j} - c_4 \cdot s_{4,j} - c_5 \cdot s_{5,j}\right)^2 \cdot w_{i,j} \qquad (3.3.3.3)$$

The summation (over j) covers all channels of interest. (For a 511 channels spectrum the summation may go from j = 20 to j = 480.)
$w_{i,j}$ is a weight factor that should be assigned to element number j in the summation i.e. each channel counts. According to standard theory the weight factor should be inverse proportional to the variance - $Var(n_{i,j})$ - of the element $n_{i,j}$ (Ref. 10). $\mathbf{s}_0$, $\mathbf{s}_1$, $\mathbf{s}_2$, $\mathbf{s}_3$, $\mathbf{s}_4$ and $\mathbf{s}_5$ are assumed to be without uncertainty.

For a Poisson distribution the $Var(n_{i,j})$ is equal to the "expected" value of $n_{i,j}$. However, for simplicity the mean value for the set of "base" spectra - $\mathbf{s}_0 \cdot LT_i$ - is used instead. This introduces an error that is neglected here. (A reason for not using the measured spectrum for the weight, i.e. $w_{i,j} = 1/n_{i,j}$ is that the number of measured counts - $n_{i,j}$ - may be zero.)

Eq. 3.3.3.3 is therefore replaced by:

$$\Delta^2_i = \Sigma\,(n_{i,j} - n_{0,j} - c_1 \cdot s_{1,j} - c_2 \cdot s_{2,j} - c_3 \cdot s_{3j} - c_4 \cdot s_{4j} - c_5 \cdot s_{5j})^2 / n_{0,j} \qquad (3.3.3.4)$$

The task therefore is to minimise Δ^2_i by varying c_1, c_2, c_3, c_4, and c_5 i.e. one has to demand that:

$$d(\Delta^2)/dc_1 = 0;\ d(\Delta^2)/dc_2 = 0;\ d(\Delta^2)/dc_3 = 0;\ d(\Delta^2)/dc_4 = 0 \text{ and } d(\Delta^2)/dc_5 = 0 \qquad (3.3.3.5)$$

(The summation covers all channel numbers "j" of interest)

$$d(\Delta^2)/dc_1 = d\{\Sigma\,(n_{i,j} - n_{0,j} - c_1 \cdot s_{1,j} - c_2 \cdot s_{2,j} - c_3 \cdot s_{3,j} - c_4 \cdot s_{4,j} - c_5 \cdot s_{5,j})^2 / n_{0,j}\}/dc_1 \qquad (3.3.3.6)$$

$$= d\{\Sigma\,[(n_{i,j} - n_{0,j} - c_2 \cdot s_{2,j} - c_3 \cdot s_{3,j} - c_4 \cdot s_{4,j} - c_5 \cdot s_{5,j})^2$$
$$- 2c_1 \cdot s_{1,j} \cdot (n_{i,j} - n_{0,j} - c_2 \cdot s_{2,j} - c_3 \cdot s_{3,j} - c_4 \cdot s_{4,j} - c_5 \cdot s_{5,j}) + c_1^2 \cdot s_{1,j}^2]/n_{0,j}\}/dc_1$$
$$= \Sigma\,[0^2 - 2 \cdot s_{1,j} \cdot (n_{i,j} - n_{0,j} - c_2 \cdot s_{2,j} - c_3 \cdot s_{3,j} - c_4 \cdot s_{4,j} - c_5 \cdot s_{5,j}) + 2c_1 \cdot s_{1,j}^2]/n_{0,j}$$

Therefore:

$$d(\Delta^2)/dc_1 = [-\Sigma\,2 \cdot s_{1,j} \cdot (n_{i,j} - n_{0,j}) + 2c_2 \cdot \Sigma s_{1,j} \cdot s_{2,j} + 2c_3 \cdot \Sigma s_{1,j} \cdot s_{3,j} + 2c_4 \cdot \Sigma s_{1,j} \cdot s_{4,j}$$
$$+ 2c_5 \cdot \Sigma s_{1,j} \cdot s_{5,j} + 2c_1 \cdot \Sigma s_{1,j}^2]/n_{0,j} = 0$$

$$= -\Sigma\,2 \cdot s_{1,j} \cdot (n_{i,j} - n_{0,j})/n_{0,j} + 2c_2 \cdot \Sigma s_{1,j} \cdot s_{2,j}/n_{0,j} + 2c_3 \cdot \Sigma s_{1,j} \cdot s_{3,j}/n_{0,j}$$
$$+ 2c_4 \cdot \Sigma s_{1,j} \cdot s_{4,j}/n_{0j} + 2c_5 \cdot \Sigma s_{1,j} \cdot s_{5,j}/n_{0j} + 2c_1 \cdot \Sigma s_{1,j}^2/n_{0,j} = 0$$

or

$$c_2 \cdot \Sigma s_{1,j} \cdot s_{2,j}/n_{0,j} + c_3 \cdot \Sigma s_{1,j} \cdot s_{3,j}/n_{0,j} + c_4 \cdot \Sigma s_{1,j} \cdot s_{4,j}/n_{0j} + c_5 \cdot \Sigma s_{1,j} \cdot s_{5,j}/n_{0j} + c_1 \cdot \Sigma s_{1,j}^2/n_{0,j}$$
$$= \Sigma s_{1,j} \cdot (n_{i,j} - n_{0,j})/n_{0,j} \qquad (3.3.3.7)$$

$d(\Delta^2)/dc_2 \Rightarrow$

$$a \cdot \Sigma s_{2,j} \cdot s_{1,j}/n_{0,j} + c_3 \cdot \Sigma s_{2,j} \cdot s_{3,j}/n_{0,j} + c_4 \cdot \Sigma s_{2,j} \cdot s_{4j}/n_{0j} + c_5 \cdot \Sigma s_{2,j} \cdot s_{5,j}/n_{0j} + c_2 \cdot \Sigma s_{2,,j}^2/n_{0,j}$$
$$= \Sigma s_{2,j} \cdot (n_{i,j} - sn_{0,j})/n_{0,j} \qquad (3.3.3.8)$$

$d(\Delta^2)/dc_3 \Rightarrow$

$$c_2 \cdot \Sigma s_{3,j} \cdot s_{2,j}/n_{0,j} + c_1 \cdot \Sigma s_{3,j} \cdot s_{1,j}/n_{0,j} + c_4 \cdot \Sigma s_{3,j} \cdot s_{4,j}/n_{0j} + c_5 \cdot \Sigma s_{3,j} \cdot s_{5,j}/n_{0j} + c_3 \cdot \Sigma s_{3,,j}^2/n_{0,j}$$
$$= \Sigma s_{3,j} \cdot (n_{i,j} - n_{0,j})/n_{0,j} \qquad (3.3.3.9)$$

$d(\Delta^2)/dc_4 \Rightarrow$

$$c_2 \cdot \Sigma s_{4,j} \cdot s_{2,j}/n_{0,j} + c_3 \cdot \Sigma s_{4,j} \cdot s_{3,j}/n_{0,j} + c_1 \cdot \Sigma s_{4,j} \cdot s_{1j}/n_{0j} + c_5 \cdot \Sigma s_{4,j}\ s_{5,j}/n_{0,j} + c_4 \cdot \Sigma s_{4,j}^2/n_{0,j}$$
$$= \Sigma s_{4,j} \cdot (n_{i,j} - n_{0,j})/n_{0,j} \qquad (3.3.3.10)$$

$d(\Delta^2)/dc_5 \Rightarrow$

$$c_2 \cdot \Sigma s_{5,j} \cdot s_{2,j}/n_{0,j} + c_3 \cdot \Sigma s_{5,j} \cdot s_{3,j}/n_{0,j} + c_1 \cdot \Sigma s_{5,j} \cdot s_{1,j}/n_{0j} + c_4 \cdot \Sigma s_{4,j} \cdot s_{5,j}/n_{0j} + c_5 \cdot \Sigma s_{5,j}^2/n_{0,j}$$
$$= \Sigma s_{5,j} \cdot (n_{i,j} - n_{0,j})/n_{0,j} \qquad (3.3.3.11)$$

From the equations (3.3.3.7) to (3.3.3.11) one then gets the best fit for the new measured spectrum number "i" by using the calculated c_1, c_2, c_3, c_4, and c_5 values.

$$\mathbf{n}_i = \mathbf{n}_0 + c_{i,1} \cdot \mathbf{s}_1 + c_{i,2} \cdot \mathbf{s}_2 + c_{i,3} \cdot \mathbf{s}_3 + c_{i,4} \cdot \mathbf{s}_4 + c_{i,5} \cdot \mathbf{s}_5 + \boldsymbol{\delta}_i \qquad (3.3.3.1 \text{ repeated})$$

The equations (3.3.3.7) to (3.3.3.11) can be written as:

$$AA_{i,1}\cdot c_{i,1} + BB_{i,1}\cdot c_{i,2} + CC_{i,1}\cdot c_{i,3} + GG_{i,1}\cdot c_{i,4} + HH_{i,1}\cdot c_{i,5} = EE_{i,1} \quad (3.3.3.12a)$$
$$AA_{i,2}\cdot c_{i,1} + BB_{i,2}\cdot c_{i,2} + CC_{i,2}\cdot c_{i,3} + GG_{i,2}\cdot c_{i,4} + HH_{i,2}\cdot c_{i,5} = EE_{i,2} \quad (3.3.3.12b)$$
$$AA_{i,3}\cdot c_{i,1} + BB_{i,3}\cdot c_{i,2} + CC_{i,3}\cdot c_{i,3} + GG_{i,3}\cdot c_{i,4} + HH_{i,3}\cdot c_{i,5} = EE_{i,3} \quad (3.3.3.12c)$$
$$AA_{i,4}\cdot c_{i,1} + BB_{i,4}\cdot c_{i,2} + CC_{i,4}\cdot c_{i,3} + GG_{i,4}\cdot c_{i,4} + HH_{i,4}\cdot c_{i,5} = EE_{i,4} \quad (3.3.3.12d)$$
$$AA_{i,5}\cdot c_{i,1} + BB_{i,5}\cdot c_{i,2} + CC_{i,5}\cdot 7c_{i,3} + GG_{i,5}\cdot c_{i,4} + HH_{i,5}\cdot c_{i,5} = EE_{i,5} \quad (3.3.3.12e)$$

The indices "i" refer to the fact that each new spectrum should have its own calculations.
The constants $AA_{x,y}$ to $HH_{x,y}$ are the same for all calculations; only the $EE_{x,y}$ vary from spectrum to spectrum.

$$AA_{i,1} = \Sigma s_{1,j}^2/n_{0,j} \quad BB_{i,1} = \Sigma s_{1,j}\cdot s_{2,j}/n_{0,j} \quad CC_{i,1} = \Sigma s_{1,j}\cdot s_{3,j}/n_{0,j} \quad GG_{i,1} = \Sigma s_{1,j}\cdot s_{4,j}/n_{0,j}$$
$$HH_{i,1} = \Sigma s_{1,j}\cdot s_{5\,j}/n_{0,j} \quad EE_{i,1} = \Sigma s_{1,j}\cdot(n_{i,j} - n_{0,j})/n_{0,j} \quad (3.3.3.13a)$$

$$AA_{i,2} = \Sigma s_{2,j}\cdot s_{1,j}/n_{0,j} \quad BB_{i,2} = \Sigma s_{2,j}^2/n_{0,j} \quad CC_{i,2} = \Sigma s_{2,j}\cdot s_{3,j}/n_{0,j} \quad GG_{i,2} = \Sigma s_{2,j}\cdot s_{4,j}/n_{0,j}$$
$$HH_{i,2} = \Sigma s_{2,j}\cdot s_{5,j}/n_{0,j} \quad EE_{i,2} = \Sigma s_{2,j}\cdot(n_{i,j} - n_{0,j})/n_0 \quad (3.3.3.13b)$$

$$AA_{i,3} = \Sigma s_{3,j}\cdot s_{1,j}/n_{0,j} \quad BB_{i,3} = \Sigma s_{3,j}\cdot s_{2,j}/n_{0,j} \quad CC_{i,3} = \Sigma s_{3,j}^2/n_{0,j} \quad GG_{i,3} = \Sigma s_{3,j}\cdot s_{4,j}/n_{0j,}$$
$$HH_{i,3} = \Sigma s_{3,j}\cdot s_{5,j}/n_{0,j} \quad EE_{i,3} = \Sigma s_{3,j}\cdot(n_{i,j} - n_{0,j})/n_{0,j} \quad (3.3.3.13c)$$

$$AA_{i,4} = \Sigma s_{4,j}\cdot s_{1\,j}/n_{0,j} \quad BB_{i,4} = \Sigma s_{4,j}\cdot s_{2,j}/n_{0,j} \quad CC_{i,4} = \Sigma s_{4,j}\cdot s_{3,j}/n_{0,j} \quad GG_{i,4} = \Sigma s_{4,j}^2/n_{0j}$$
$$HH_{i,5} = \Sigma s_{4,j}\cdot s_{5,j}/n_{0,j} \quad EE_{i,4} = \Sigma s_{4,j}\cdot(n_{i,j} - n_{0,j})/n_{0,j} \quad (3.3.3.13d)$$

$$AA_{i,5} = \Sigma s_{5,j}\cdot s_{1,j}/n_{0,j} \quad BB_{i,5} = \Sigma s_{5,j}\cdot s_{2,j}/n_{0,j} \quad CC_{i,5} = \Sigma s_{5,j}\cdot s_{3,j}/n_{0,j} \quad GG_{i,4} = \Sigma s_{5,j}\cdot s_{4,j}/n_{0j}$$
$$HH_{i,5} = \Sigma s_{5,j}^2/n_{0,j} \quad EE_{i,5} = \Sigma s_{5,j}\cdot(n_{i,j} - n_{0,j})/n_{0,j} \quad (3.3.3.13e)$$

Then after having the values $c_{i,1}$ to $c_{i,5}$ for all spectra each spectrum could be reproduced according to Formula 3.3.3.1 i.e.:

$$\mathbf{n}_i = \mathbf{n}_0 + c_{i,1}\cdot\mathbf{s}_1 + c_{i,2}\cdot\mathbf{s}_2 + c_{i,3}\cdot\mathbf{s}_3 + c_{i,4}\cdot\mathbf{s}_4 + c_{i,5}\cdot\mathbf{s}_5 + \boldsymbol{\delta}_i \quad (3.3.3.1 \text{ repeated})$$

In order to test the quality of the fit $\boldsymbol{\delta}_i$ should be evaluated.

$$\boldsymbol{\delta}_i = \mathbf{n}_i - \mathbf{n}_0 - c_{i,1}\cdot\mathbf{s}_1 - c_{i,2}\cdot\mathbf{s}_2 - c_{i,3}\cdot\mathbf{s}_3 - c_{i,4}\cdot\mathbf{s}_4 - c_{i,5}\cdot\mathbf{s}_5 \quad (3.3.3.2 \text{ repeaeted})$$

The δ_i values could be shown as an error spectrum and possibly one may discover if anomalous radiation is present. In order to get just one number expressing the quality of the fit one should calculate the sum of squared errors:

$$\Delta^2 = \Sigma\, \delta_{i,j}^2 \cdot w_{i,j} = \Sigma\,(n_i - n_0 - c_{i,1}\cdot s_1 - c_{i,2}\cdot s_2 - c_{i,3}\cdot s_3 - c_{i,4}\cdot s_4 - c_{i,5}\cdot s_5)^2\cdot w_{i,j} \quad (3.3.3.19)$$

If Δ^2 exceeds a certain value - found from experiences - the fit is of insufficient quality and the new measured spectrum contains unusual information.

The weight factor $w_{i,j}$ should represent the uncertainty of each element of the summation. Therefore, $w_{i,j}$ is selected as $1/\mathrm{var}(n_{i,j}) = 1/(n_{0,j} + a_i\cdot s_{1,j} + b_i\cdot s_{2,j} + c_i\cdot s_{3,j} + g_i\cdot s_{4,j} + h_i\cdot s_{5,j})$

The distribution of the results - the Δ^2 values - could be compared to a χ^2 distribution. If 461 channels are included in the fitting the degrees of freedom is 457 as five degrees have "been lost" by calculation of c_1, c_2, c_3, c_4, and c_5.

3.4 Danish Data Files and Quality

The following files contain 512-channels measurements from the Copenhagen area (UTM Zone 32, WGS84) and suburbs:

Area017.spc	January	System B12	Spectrum drift (temperature problems)
Area17cl.spc	(=Area017.spc excl. the first 200 spc.)		Might include ^{81}Kr and ^{41}Ar signals.
Area051.spc		System B12	Good data quality.
Area052.spc		System B12	Good data quality.

3.4.1 Area017.spc

The measurements were begun during heavy snowfall with the additional consequence of slow-moving traffic (including minor traffic jams) and ended in bright weather. The survey includes a drive around a hospital.

0-172	parked, back door of building 327 (Ørsted-DTU)
172-196	driving to front end of build. 327
215	department Elektrofysik 322 to the right
236-265	driving along Akademivej
265	right turn to Toftegårdsvej
290	Statoil gasoline station to the right
299	road crossing at Klampenborgvej
307	onto motorway
353	road crossing at motorway/Jægersborgvej
360	left turn
383	stop for red at Jægersborg Alle
399	Smakkegårdsvej
433	crossing Ermelundsvej
4521	Smakkedal
466	Gentoftegade to the right
492	sideroad to the left
510	crossing Adolphsvej, Tranegårdsvej
530	road crossing at Bernstorffsvej
553	Bernstorffsvej station to the right
561	Ingeborgvej to the left
570	Charlottenlundvej to the left
576	Taffelbays Alle to the right
584	stop for red at Gersonsvej
616	Ørehøj
627	Øregårdsparken to the left
639-648	at road crossing Strandvejen/Tranegårdsvej
648-885	Strandvejen, alongside Øregårdsparken
667	Hellerup Park Hotel to the right
688	Duntzfeldts Alle to the right
721	Margrethevej to the right
740	Jomsborgvej to the left
748	Hellerupvej to the right
757	Sankt Pedersvej to the right
764	Callisensvej to the right
770	gasoline station to the left
779	stop for red at Tuborgvej
800	Tuborg flask building to the left
814	road crossing, Gl. Vartovvej to the right
830	Strandøre to the left
851	Østerled to the right
859-894	stop for red at road crossing, Jagtvejen
905-909	Svanemøllen station, bus station to the left
917	Kildevældsgade to the right
926	Carl Nielsensvej to the left
940	Hjortøgade to the right
950-958	stop for red at Strandboulevarden
976	Århusgade to the left
988	stop for red at Gunnar Nu Hansens Plads
1001	Sct. Jacobs church to the right
1020	behind parked car
1039	stop for red at Trianglen
1058	Øster Alle to the right
1070	Red Cross building
1088	Rigshospitalet to the right
1099	turn toward Rigshospitalet, Tagensvej
1120	main entrance to Rigshospitalet
1148	left turn towards cyclotron
1155	above cyclotron western direction
1183	turning around
1199	turned around
1203	exit from Finsen Institute to the right
1222	turning
1250	exit from Rigshospitalet
1270	right turn to Blegdamsvej, stop for red
1277	Juliane Mariesvej to the right
1283-1319	stop for red, road crossing Fredensgade/Tagensvej
1322-1334	Panum-instituttet to the right
1340	Skt. Johannes Church to the right
1348-1365	Stop for red at Sankt Hanstorv
1370	Sankt Hans torv
1390-1410	stop for red at Fælledvej/Nørrebrogade left turn to Nørrebrogade
1424	stop for red right before Dr. Louises bro (bridge)
1438-1463	on Dr. Louises bro (bridge)
1467-1507	stop for red at Søtorvet
1507	right turn to Nørre Søgade
1507-1568	along lakes (right side)
1523-1529	Traffic jam **SPECTRUM DISPLACEMENT**
1575-1632	Gyldenløvsgade, stop for red at Søpavillonen
1623-1662	Traffic jam
1666-	Traffic jam, waits in line at Gyldensløsvsgade
1842-1879	Vester Farimagsgade to the right Jarmers Plads to the left
1949	on bridge above railway
1985-2004	left turn
2013	right turn to Vester Voldgade
2030	crossing Studiestræde?
2041	Politiken (newspaper domicil) to the left
2048	central bus terminal to the right
2054	Rådhuspladsen (main city square)
2069	brick buildings
2076-2083	right turn at road crossing Stormgade
2110	right turn to H.C. Andersens Boulevard
2122	Rådhuspladsen to the right
2130-2148	parked at Rådhuspladesen

2149	central bus terminal to the right
2157	crosing Studiestræde
2186	”lions” (statues) at Jarmers Plads
2194	road crossing at Nørre/Vester Farimagsgade
2207	left turn to Vester Farimagsgade
2217	tall brick walls
2223-2246	stop for red at Kampmannsgade
2247	railway at Vesterport station to the left
2259-2281	parked at road crossing, Vesterport station
2287	Trommesalsbuen GPS error
2303-2310	crossing Vesterbrogade, GPS error
2319	Central railway staion West
2325	right turn to Istedgade
2340	crossing Helgolandsgade
2350	crossing Abel Cathrinesgade
2369	road crossing at Gasværksvej
2380	left turn to Gasværksvej, GPS error
2397	right turn to Halmtorvet
2420	road crossing at Skelbækgade
2428	left turn to Skelbækgade
2455	roundabout at Fisketorvet, Dybbølsbro
2460	left turn to Ingerslevsgade
-2503	driving along railway (right dside)
2503	Tietgensbroen (bridge)
2508	right turn to Tietgensgade
2508-2515	alongside the central railway staion
2521-2546	stop for red at Bernstorffsgade
2561	right turn to Ved Glyptoteket
2573	Stoltenbergsgade to the right
2580	crossing Niels Brocksgade,
	driving along Otto Mønstedsgade, GPS error
2600	right turn to Hambrosgade
2612	right turn to Mitchellsgade, Polititorvet
2618	right turn to Niels Brocksgade
2632	right turn to Otto Mønstedsgade
	”marble”- building to the right
2650	right turn to Hambrosgade, GPS error
2673	left turn to Bernstorrfgade
2681	cargo railroad to the right
2691	right turn to Kalvebod Brygge
2700	Ingeniørhuset (engineer domicil) to the left
2721	right turn to “rame” towards Dybbølsbro
2740	road crossing at Dybbølsbro staion
2756-2770	Dybbølsbro, driving on bridge above railway
2772	roundabout at Dybbølsbro
2776	right turn to Ingerslevgade
	railroad to the right højre
2826-2830	Tietgensbroen (bridge)
2855-2865	stop for red at Bernstorffsgade
2893	crossing H.C. Andersens Boulevard, turn to
Stormgade	
2920	National Museum to the right, close to pillars
	crossing (water) Frederiksholms Kanal
2948	Thorvaldsens Museum to the right
2955	parked
2973	right turn to Christiansborg Slotsplads
2980	driving past main entrance
2998	driving through gate
3010	driving through gate, tall stone walls
3027-3029	turn to Frederiksholm Kanal
3040-3050	right turn to Marmorbroen (”marble bridge”)
3060	southern end of Ridebanen
3078	between parked cars
3084	statue to the left
3093	eastern end
3103	northern side
3125	exit from Ridebanen
3140	Ny Vestergade, GPS error
3167	left turn to Vester Voldgade
3190	GPS error
3194	left turn to Frederiksholms Kanal
3212	construction debris
3220	right turn to Bryghusgade
3235	left trun to Vester Voldgade
3254	water to the right
3266	under viaduct
3286	under Knippelsbro (bridge)
3294	water to the right
3320	driving along Niels Juelsgade
3364-	Magasin (department store) to the left, parked
3387-3389	Royal Theatre to the right
3406	road crossing
3420	turn to Bredgade, GPS error
3436	right turn to Sankt Annæs Plads
3449	crossing Lille Strandstræde
3466	Toldbodsgade to the right
3486	ferry to left,”harbour area”
	Kvæsthusbroen
3496	water to the right
3504-3512	lorry turns in front of ”measurement car”
3519-3528	turnaround, close to waterfront
3553	”Harbour b ridge”, ships
3566	road crossing at Toldbodgade
3583	right turn to Toldbodgade
3601-3608	in front of Admiral Hotel
	Amaliehaven to the right
3623	left turn to Amalienborg (castle)
3641	Amaliegade to the right side
3648	Western side
3650	Frederiksgade to the right
3661	exit
3670	exit, Toldbodgade
3680	left turn to Toldbodgade
3703	curve on Toldbodgade
3712	right turn to Amaliegade
3728-3736	road crossing at Esplanaden
3739	left turn to Esplanaden
3760	right turn to Grønningen
3784-4300	parked at Folke Bernadottes Alle
4300	exit from parking area
4314	left turn to Sølvgade
4325	Nyboderhuse to the left
4355-4380	stop for red, right turn
4406	left turn to Webersgade
4418	crossing Øster Søgade
4426	driving on Fredensbro (bridge)
4442	crossing Blegdamsvej
	tall brick walls, Panum Institute to the left
4464-4468	right turn to Nørre Alle, very wide road
4501	street crossing at Universitetsparken
4527	crossing Jagtvej, driving along Lyngbyvej
4548	crossing Sejrøgade/Haraldsgae
4556	Omøgade to the right
4564-4570	parked at Hans Knudsens plads
4579-4582	under railway (viaduct), Ryparken, motorwayj
4592	viaduct (road)
4618	viaduct (road)
4647	"motorway shields to left and right"
4653	viaduct (road)
4671	viaduct (road)
	Gentofte sø (lake) to the right
4705	exit E47 to Lyngby
4723	under bridge
4732	over bridge
4740-4750	over bridge
4751	roundabout
	turn to Lyngby Hovedgade
4764	Vintappervej to the right
4783-4800	on bridge above railway
4808	left turn to Lyngby Hovedgade
4532	paving stones
4548	Jernbanevej to the left
4860-4878	stop for red, Magasin (warehouse) to the right
4878	crossing Klampenborgvej
4898	Toftebæksvej to the right
4915	roundabout
4932	Stades Krog to the right
4935	Lyngby church to the right
4941	right turn to Gammel Lundtoftevej
4953	ILVA (warehouse) to the left
4959	driving between stone walls
4967	right turn to Høstvej
4974	Peter Lunds vej
4989	left turn to Toftebæksvej
5010-5019	stop for red, street crossing at Sorgenfrigårdsvej
5033	Lyngvej to the right
5039	Akademivej (DTU) to the right
5051	right turn to Elektrovej (DTU)

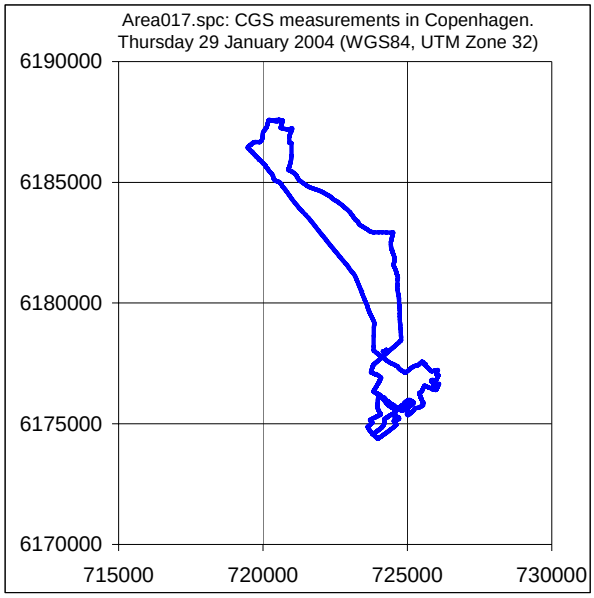

Figure 3.4.1.1. Track lines for Area017.spc.

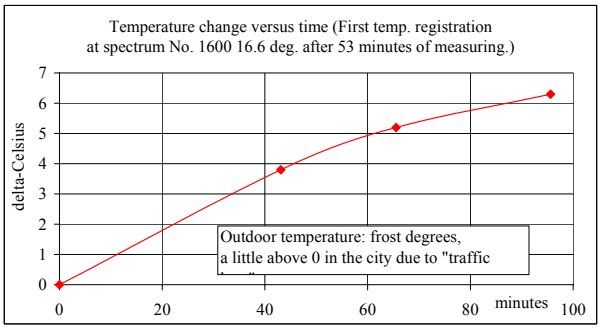

Figure 3.4.1.2. Detector temperature.

3.4.2 Area051.spc

31	Start building 327, DTU
53	paving stones
74	right turn to Asmussens vej
97	left turn to Akademivej
120	right turn to Toftegårdsvej
153	Statoil tank to the right
160	onto motorway ramp
174	on motorway
201	motorway exit
219	left turn to Jægersborgvej
237	Ibstrupvænget to the right
241	road crossing at Smakkegårdsvej
276	Søndersøvej to the left
285	road crossing
311	Vældegårdsvej to the left
318	Gentoftegade to the right
341	Maltegårdsvej to the left
358	Adolphsvej to the right
371	Statoil tank to the left
374-380	stop f or red at Bernstorffsvej
392	Bernstorffsvej Station to the left
399	Ingeborgvej tot he right
403	crossing railway
415	on railway bridge
422-438	stop for red at Cersonsvej
453	Vinager Alle to the left
465	right turn to Strandvejen
486-488	road crossing
500	Margrethevej to the right
517	Hellerupvej to the right
528	Callisensvej to the right
550	Tuborg North to the left
566	Gammel Vartov Vej
602	road crossing at Svanemøllen
	Station
627	Kildevældsgade to the right
639	Nygaardsvej to the right
652-671	stop for red at Strandboulevarden
690-692	roadworks
700-713	stop for red at Gunner Nu Hansens Plads
720	church to the right
727	roadworks
763-771	stop for red at Trianglen
780	to the right at Trianglen
792	Øster Alle to the right
802	Red Cross building to the right
821	hospital to the right
829	turn to Rigshospitalet crosing paving stones
847	main entrance at Rigshospitalet
857-867	waits in line
870	turning around
895	left turn
901	entrance 39, cyclotron
923	paving stones
935-947	turning around
955	road bump
972	road bump
1005	turn around
1050	parked
1067	turning around
1083	parked
1134	turn to the right
1154-1156	exit, right turn to Blegdamsvej
1194	road crossing Fredensgade/ Tagensvej
1200	Panum Institute to the right

1204	church to the right
1220	stop for red at Skt. Hans Torv
1235	Skt. Hans Torv to ther ight
1247	Fælledgade/Nørrebrogade
1265	left turn to Nørrebrogade
1284-1295	Dr. Louises Bridge
1320	right turn to Nørre Søgade
1356	stop for red at Gyldenløwsgade
1381	left turn to Gyldenløwsgade
1415	Jarmers Plads
1436	waits in line (buses)
1357	right turn to Studiestræde
1467-1472	Palads to the left
1494	right turn, along railroad
1535	crossing Jarmers Plads
1565	right turn to Vester Voldgade
1587	HT busterminal to the right
1625	right turn to Stormgade
	right turn to H. C. Andersens Boulevard
1671	Rådhuspladsen to the right
1690-1698	behind large lorry
1706	stop for red at Rådhuspladsen
1740	Jarmers plads
1759	left turn to Vester Farimagsgade
1804	Trommesalen, GPS error
1826	crossing Vesterbrogade
1846	Right turn to Istedgade
1864	Helgolandsgade
1869	Abel Cathrinesgade
1881	Victoriagade to the left
1903	left turn to Gasværksvej
1915	right turn to Halmtorvet
1926	paving stones
1932	left turn to Skelbækgade
1954	stop for red
2000	turning at Fisketorvet
2016	crossing railway
2045-2053	above railway
2081	right turn to Ingerslevsgade (new asphalt)
2112-2255	pausing at Ingerslevsgade
2273	right turn across railway bridge
2287	crossing Bernstorffsgade
2303	right turn to Ved Glyptoteket
2316	crossing Niels Brocksgade
	Police station
2332	right turn
2344	right turn
2364	right turn to Otto Mønstedsgade
2375	right turn to Hambrosgade
	stop for red
2402	left turn to Bernstorffsgade
2406	roadwork
2428	right turn to Kalvebod Brygge
2449	stop for red
2460	ramp to Dybbølsbro Station
	pausing
2674	top of ramp
2687	right turn across railway
2702	right turn to Ingerslevsgade
2744	Central Railway Station to the right
2760	stof for red at Bernstorffsgade
2787	stop for red at H. C. Andersens Boulevard
2807	crossing H. C. Andersens Boulevard
2822	National Museum to the right
2834	stop for red
2844-2851	crossing Frederiksholm Kanal
2860	Thorvaldsens Museum to the right
	paving stones
2873	Christiansborg ato the right
2879	statue to the right
2884	right turn, under gate
2895	right turn under gate
2909	under gate, tall stone walls
2921	paving stones to the right
2928	right turn to Frederiksholm Kanal
	paving stones
	parked
	circling at Ridebanen
3083	at Frederiksholm Kanal
3089	at Ny Vestergade
3108	left turn to Vester Voldgade
3161	turning at waterfront
3202	crossing Christians Brygge
	brick buildings
3227	road crossing at Ny Kongensgade
3245	circling at Ridebanen
3383	at Ny Vestergade
3401	stop for red
3410	left turn to Vester Voldgade
3438	left turn to Ny Kongensgade
3453	right turn to Frederiksholm Kanal
3481	right turn to Bryghusgade
3564	left turn to Vester Voldgade
3511	left turn to Christians Brygge
	water to the right
3530	under viaduct, ”glass” buildings
3560	under Knippelsbro
3569	crossing at Havnegade
	on Niels Juulsgade
3593	at Holmens Kanal
3620	Magasin to the left
3643	Royal Theatre to the right
3649	roundabout at Kgs. Nytorv
3663-3677	stop for red
3680	at Bredgade
3708	right turn to Skt. Annæ Plads
3729	stop for red
	left turn to Toldbodgade
3760	Amaliehaven to the right
	at Toldbodgade
3810	right turn to Amaliegade
3824	right turn
	at waterfront, Esplanaden
3862	stop for calibration check.

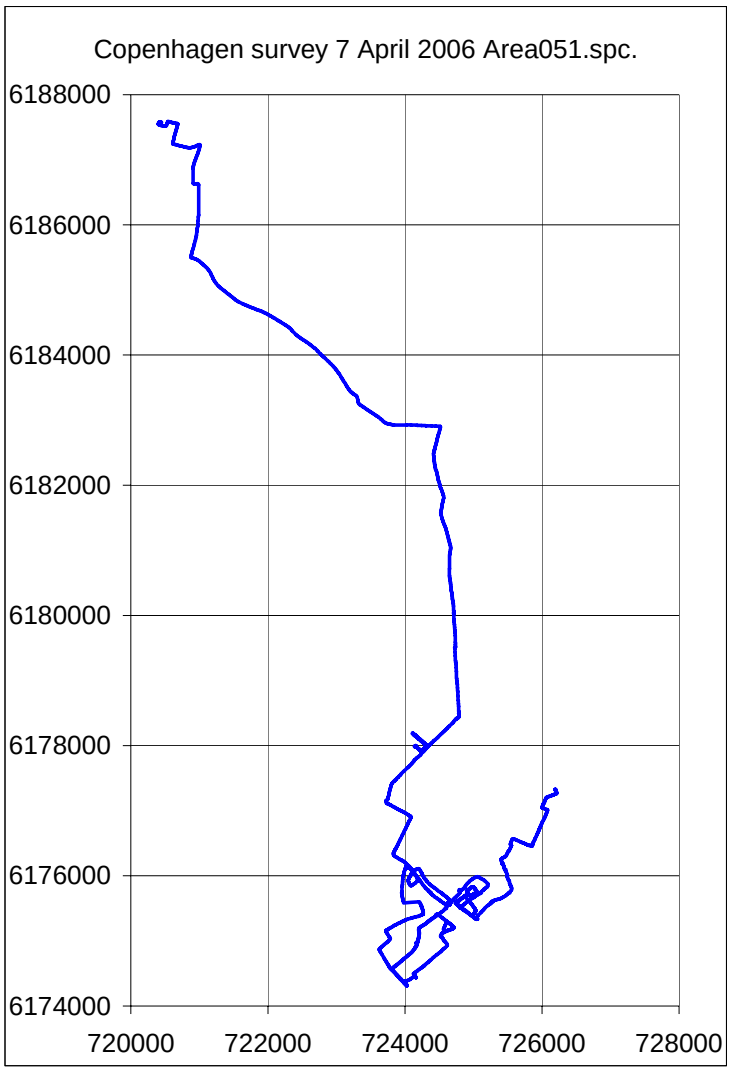

Figure 3.4.2.1. Track lines for file Area051.spc.

3.4.3 Area052.spc

	turning at Nordre Toldbod
62	crossing at Churchillparken
66	Kongeporten to the right
100	right turn to Grønningen
139-150	left turn to Øster Voldgade
158	Nyboder to the left
189-221	stop for red Georg Brandes Plads
246	stop for red at Nørre Voldgade
262	Nørreport Station, stop for red
286	at Nørre Voldgade, along park Jarmers Plads
321	at Hammerichsgade
334	left turn to Vesterbrogade
395-404	stop for red at Vesterbrogade
416	stop for red at Rådhuspladsen
440	right turn to H. C. Andersens Boulevard
454	Tivoli to the right, stop for red at Stormgade
479	crossing road
485	on Langebro
489-496	on Langebro above water
	on Amager Boulevard
540	right turn to Artillerivej
555-1079	pause at Q8-gasoline station
1114	crossing Halfdansgade
1147	Axel Heidesgade to the right
1172	Dreschersgade to the right
1190	left turn to Lossepladsvej
1225	Hekla Park
1279	left turn to Vejlands Alle
1321	stop for red at Center Boulevard
1356	viaduct under metro
1363	crossing Fælleddiget
1403	right turn to Englandsvej
1425	Kålagervej to the right
1454	roundabout at Vandtårnet
1474	stop for red at Sneserevej
1509	left turn to motorway
1513	under viaduct, GPS error 18 s

1540	under bridge
1562	right turn to motorway exit
1615	Terminal 1, Kastrup Airport
1652	At Englandsvej
1668	Amager Landevej
1697	Merkur Alle to the right
1709	Løjtegårdsvej to the right
1727	Christen Kolds Alle to the right
1753	right turn to Tømmerupvej
1784	Kirstinevej to the right
1811	left turn to Englandsvej
	”garden market”
1841	under the lanes, GPS error 25 s
1892	St. Magleby
1912	at Kirkevej
	bare fields
1967	small gardens to the right
1978	stop for red at Hartkornsvej
1998	Jægervej to the right
2026	right turn to Vestgrønningen
2053	left turn to Drogdensvej
2070	right turn to Færgevej
2077	Rønne Alle to the left
2097-2123	Færgehavn (ferry harbour)
2134	right turn to Strandlinien
2146	on parking area
2168	passing Strandlinien
2173	right turn to Rønne Alle
2190	to the right at Vestgrønningen
2230	stop for red
2254	right turn to Kongevejen, paving
	stones
2276	Neels Torv
	left turn to Strandlinien
2332	right turn to Rønne Alle
2351	left turn to Vestgrønningen
	Søndre Strandvej
2408	Krudttårnsvej to the right
2469	right turn to St. Magleby Strandvej
2500	left turn to Krudtværksvej/
	Bachermindesvej
2544	right turn to Fælledvej
2580	farm, bare fields
2604	right turn to Søndergade
2620	left turn to Møllegade
2634	church to the right
2649	left turn to Englandsvej (E20)
2700	under lanes, GPS error 22 s
2732	”garden market”
2745	stop for red at Tømmerupvej
2771	Ugandavej
2809	Brønderslev Alle to the right
2835	crossing at Løjtegårdsvej
2877	Ved Gærdet to the right
2917	church to the left
2953	Vinkelhuse to the right
2968	roundabout
	Englandsvej
3000	left turn to Vejlands Alle
3025	right turn to Vejlands Alle
3060	Bedfordvej to the right
3089	crossing at Amagerbrogade
3097	left turn to Amagerbrogade
3111	large, brick houses
3166	Sundbyvester Plads
3184	Højdevej to the right
3213	Øresundsvej
3226	Lyongade to the right
3240	stop for red at Frankrigsgade
3288	Brysselsgade to the left
3322	Sverrigsgade to the left
3337	crossing Holmbladsgade
3348	Ved Sønderporten to the right
3374	Markmandsgade to the right
	crossing the water at Torvegade
3417	Prinsessegade to the right
3423	Christian Havns Torv
3440	crossing Strandgade
3463	crossing Knippelsbro
	right turn crossing Børsbroen
3486	right turn to Holmens Kanal
3532	left turn to Holmens Kanal
3556	Royal Theater to the right
	Kgs. Nytorv
3578	right turn to Skt. Annæ Plads
3616	left turn to Toldbodgade
3648	entrance to Amalienborg
	circling at Amalienborg
	parked oputside Amalienborg
3672	Frederiksgade, Amalienborg
3814	left turn to Toldbodgade
3857	right turn to Amaliegade
3873	left turn to Esplanaden
3879	Kongeporten to the left
3901	right turn to Grønningen
3920	Nyboder to the left
3951	left turn to Øster Voldgade
4022	right turn to Sølvgade
	Øster Farimagsgade
4056	left turn to Webersgade
	crossing Fredensbro
	at Fredensgade
	at Tagensvej
4098	Panum Institute to the left
4137	right turn to Nørre Alle
4167	road crossing
4188	crossing Jagtvej
	at Lyngbyvej
4226	crossing Sejrøgade/Haraldsgade
4237	under railway bridge, Ryparken
	Helsingørmotorvejen (19)
4388	exit motorway
4400	under bridge
4423	roundabout at Vintapper Sø
4450	”graveyard stones”
4465	crossing railway bridge
4467	right turn to Lyngby Hovedgade
4488	paving stones, traffic jam
4573	Magasin to the right
4608	crossing Lyngby Torv

4667	roundabout	4768	Sorgenfrigårdsvej to the right
4682	Stades Krog to the right	4784	Akademivej to the right
4690	right turn to Gl. Lundtoftevej	4799	right turn to Elektrovej
4712	right turn to Høstvej	4822	parked at building 327, DTU
4737	left turn to Toftebæksvej		

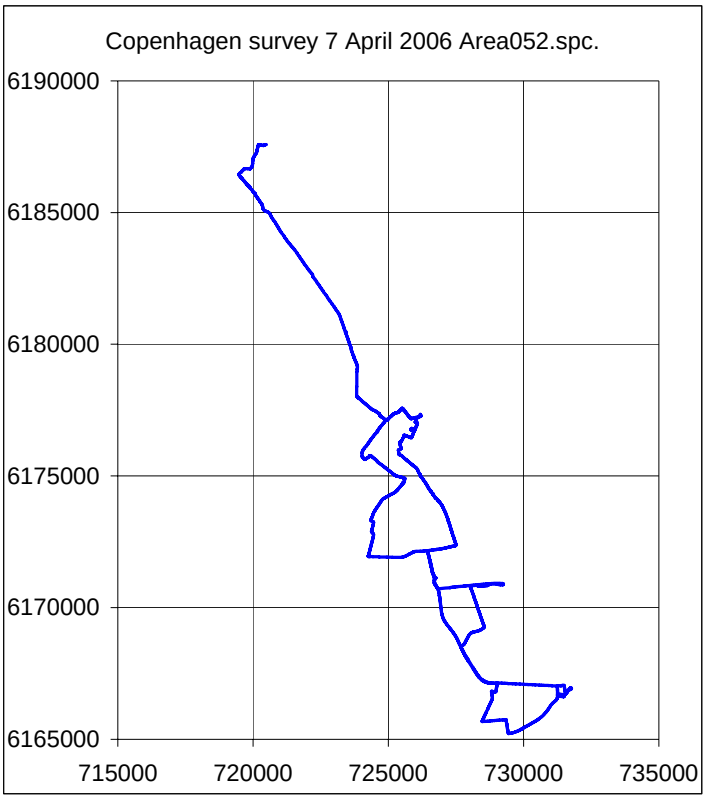

Figure 3.4.3.1. Track lines for file Area052.spc.

3.4.4 Dose Rate Maps for Copenhagen Surveys

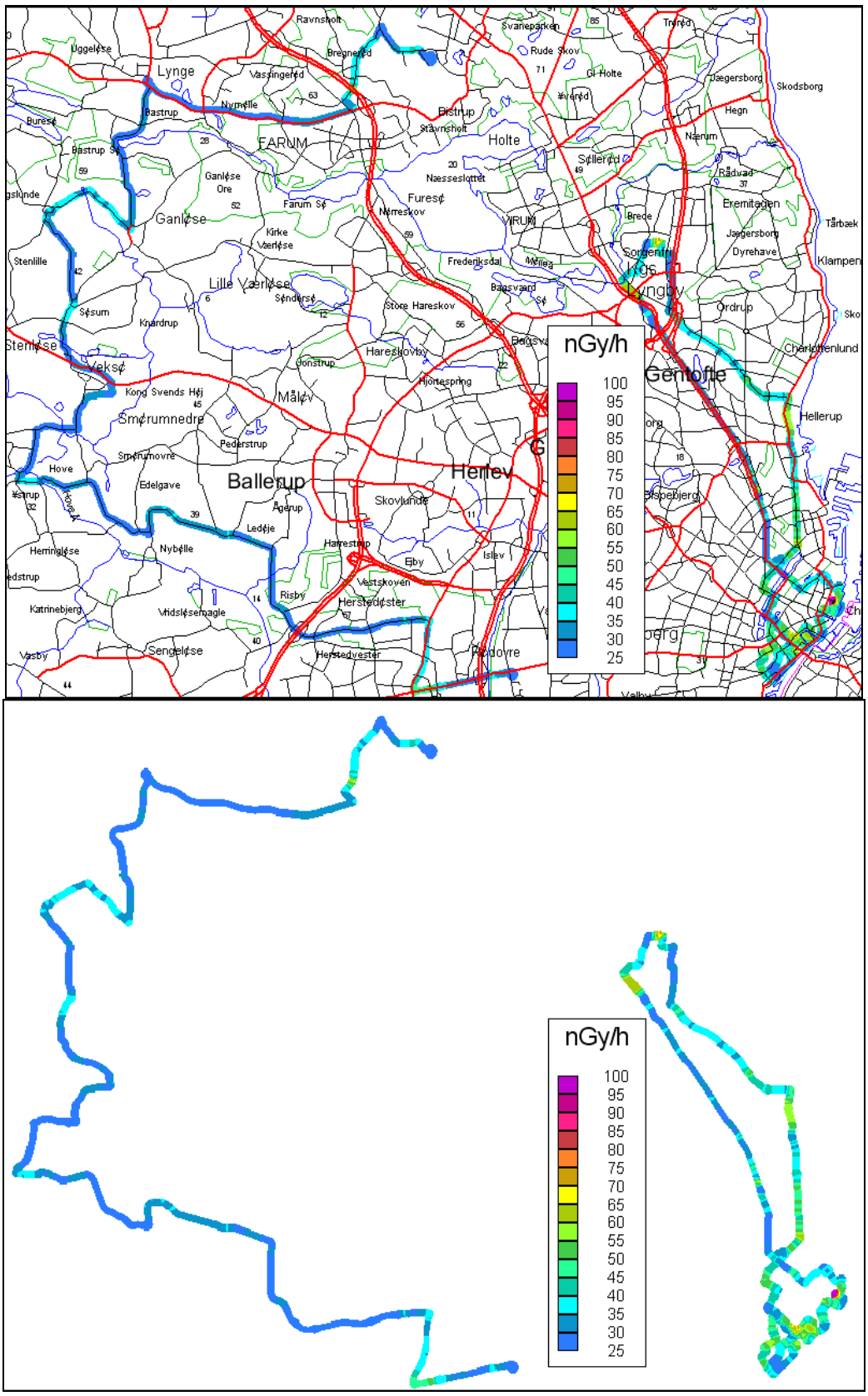

Figure 3.4.4.1. Area015.spc (left) and Area017.spc (right):
Air kerma rate map of Copenhagen roads, January 2004.

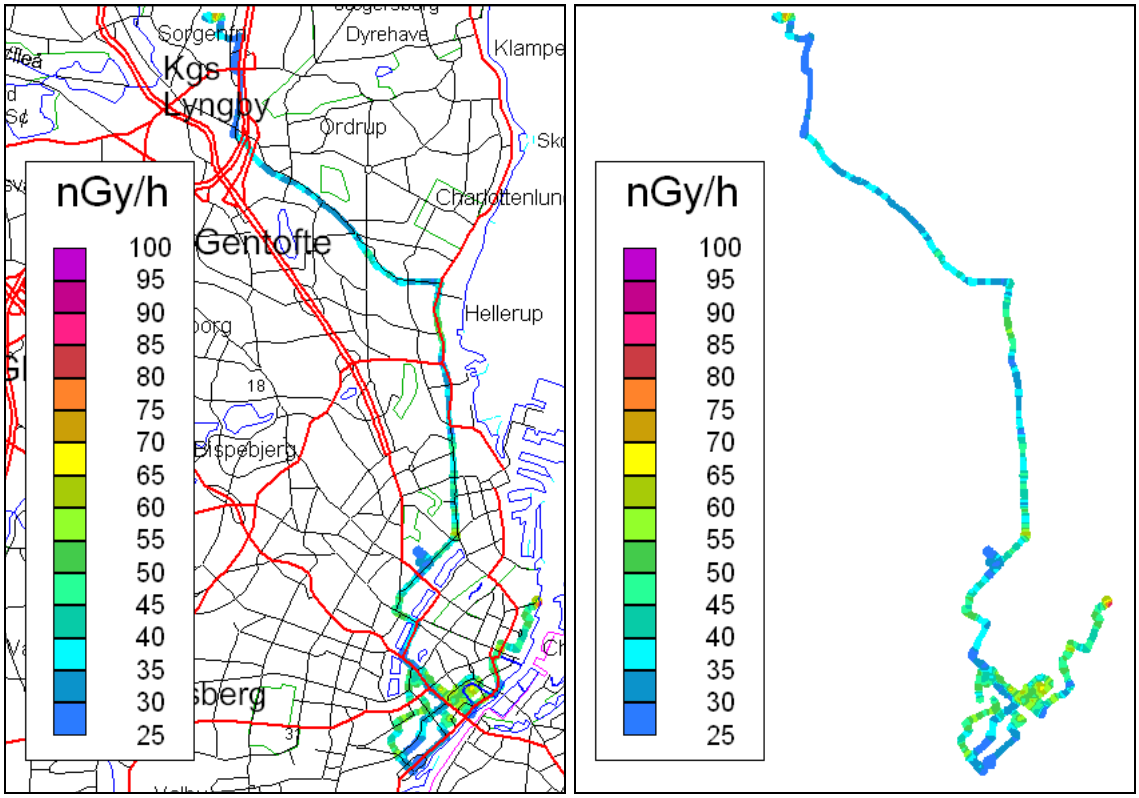

Figure 3.4.4.2. Area051.spc: Air kerma rate map of Copenhagen roads, April 2006.

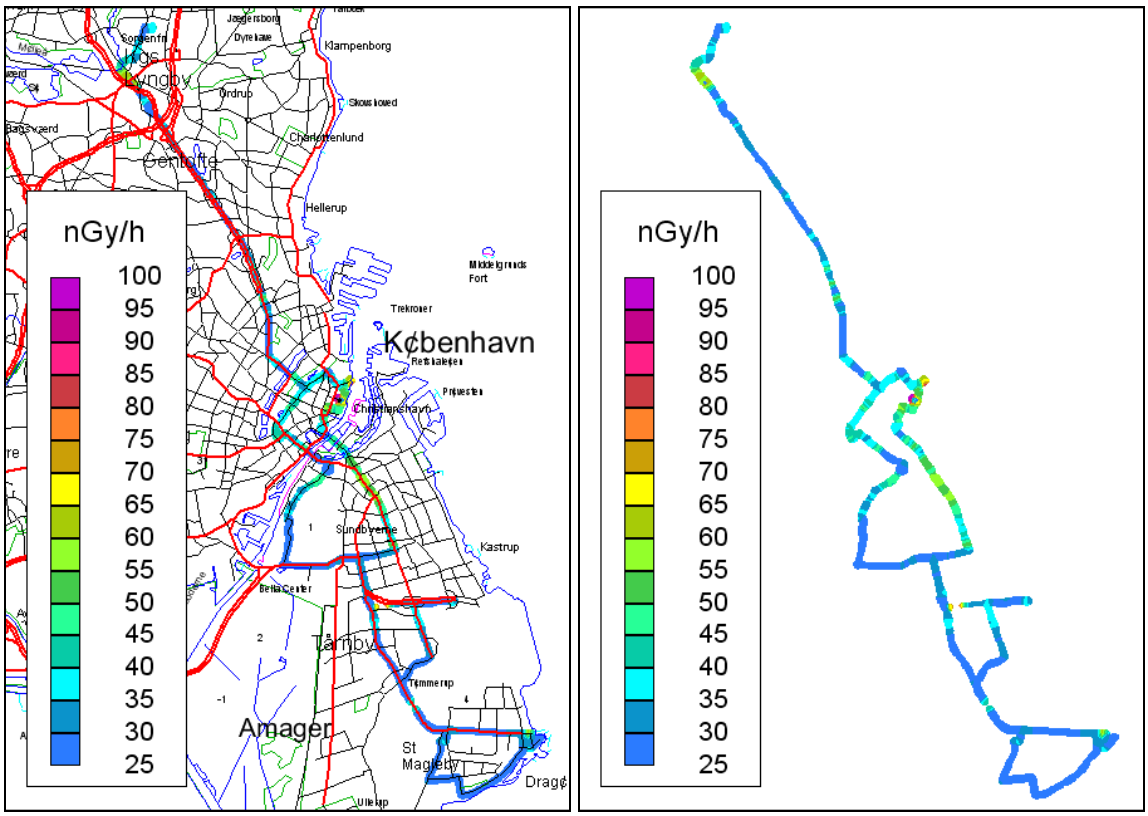

Figure 3.4.4.3. Area052.spc: Air kerma rate map of Copenhagen roads, April 2006.

3.5 Fitting Components

3.5.1 Area17cl.spc

The fitting components for file Area17cl.spc originate from a NASVD processing of the data set from channel 10 to channel 470. The data set contains spectrum drift of significance which shows as a spectrum drift signals as early as in spectral component S2. Only the first five spectral components and the mean spectrum, S0, are shown here. Due to the spectrum drift additional components containing further information on spectrum drift do exist; however, calculations were performed using five spectral components only.
The file name for the fitting constants is Ar17clsc.txt.

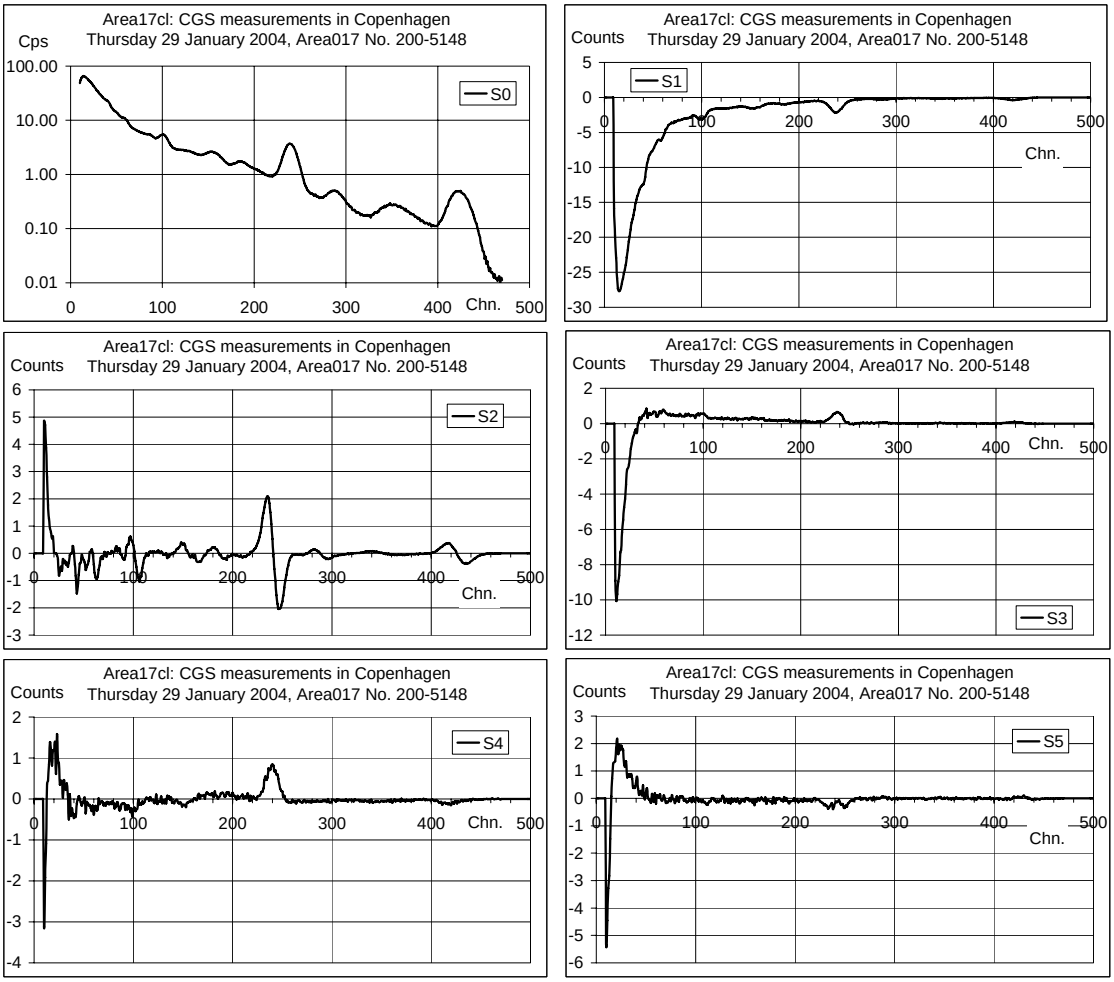

Figure 3.5.1.1. Spectral components for Area17cl.spc. Component file name Ar17clsc.txt.

3.5.2 Area051cl.spc

The fitting components for file Area051.spc originate from a NASVD processing of the data set from channel 10 to channel 470. The data set contains almost no spectrum drift signifying a very stable energy calibration. Only the first five spectral components and the mean spectrum, S0, are shown here. The file name for the fitting constants is Ar51clsc.txt.

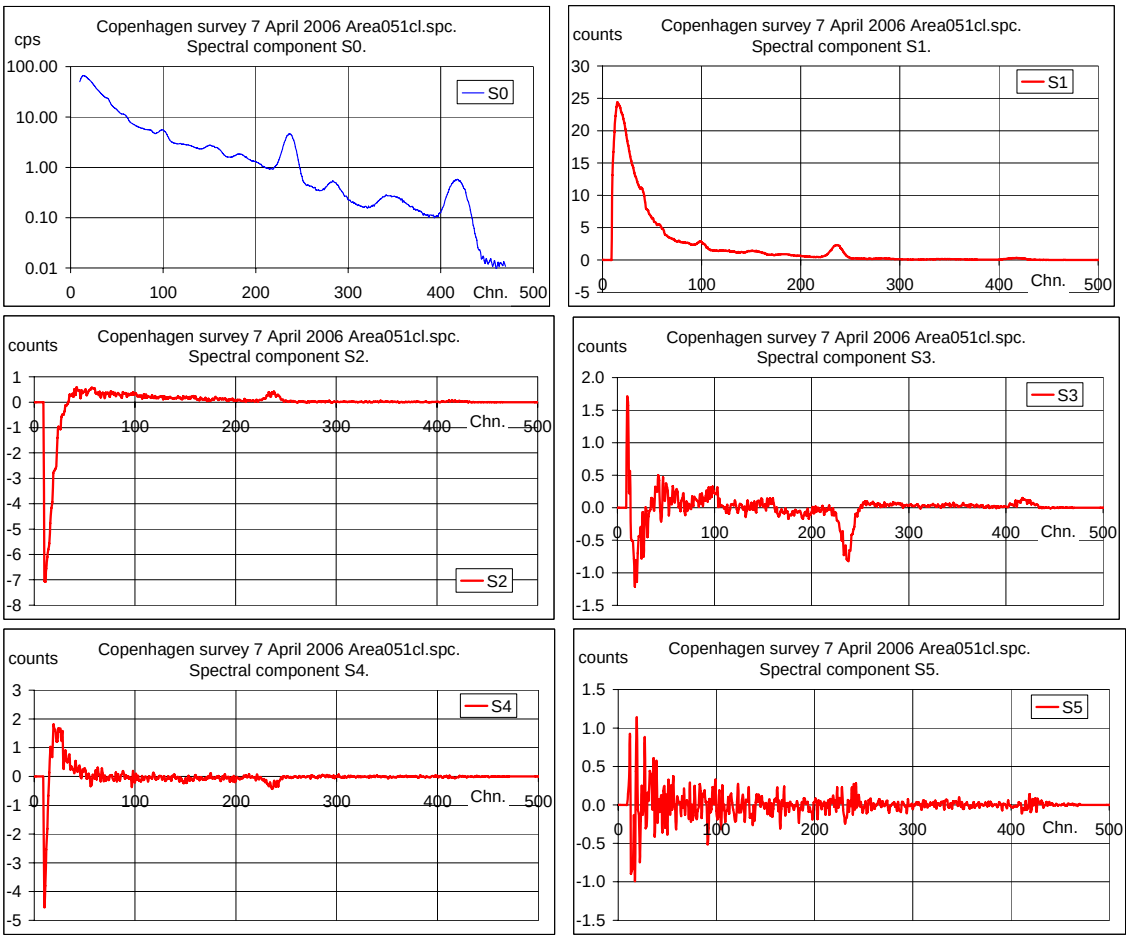

Figure 3.5.2.1. Spectral components for file Area051cl.spc.
Component file name Ar51clsc.txt.

3.5.3 Area052.spc

The fitting components for file Area052.spc originate from a NASVD processing of the data set from channel 10 to channel 470 or from channel 20 to channel 470. The data set contains almost no spectrum drift signifying a very stable energy calibration. Only the first five spectral components and the mean spectrum, S0, are shown here. The file names for the fitting constants are Ar52sc.txt (channel 10 to channel 470) and Ar52sc20.txt (channel 20 to channel 470).

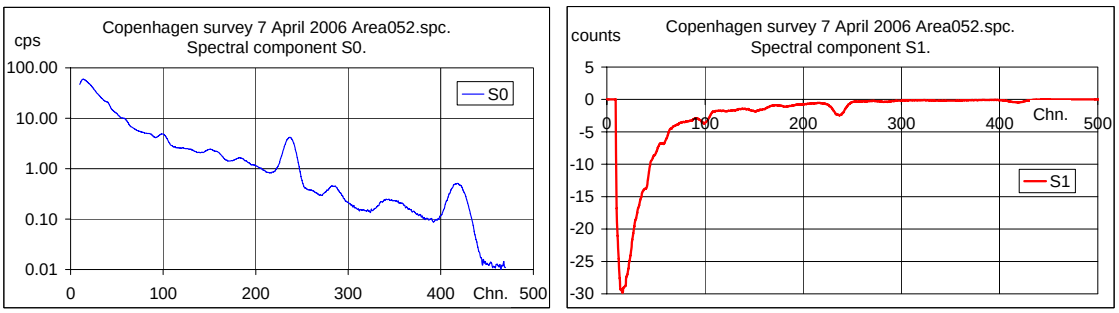

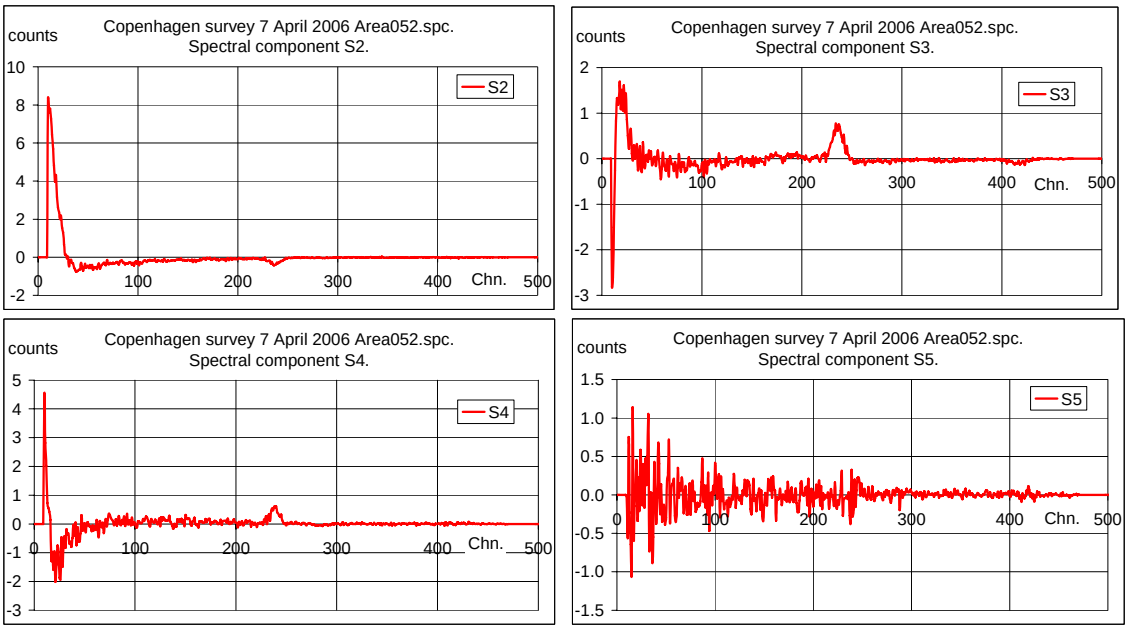

Figure 3.5.3.1. Spectral components for file Area052.spc. Component file name Ar52sc.txt.

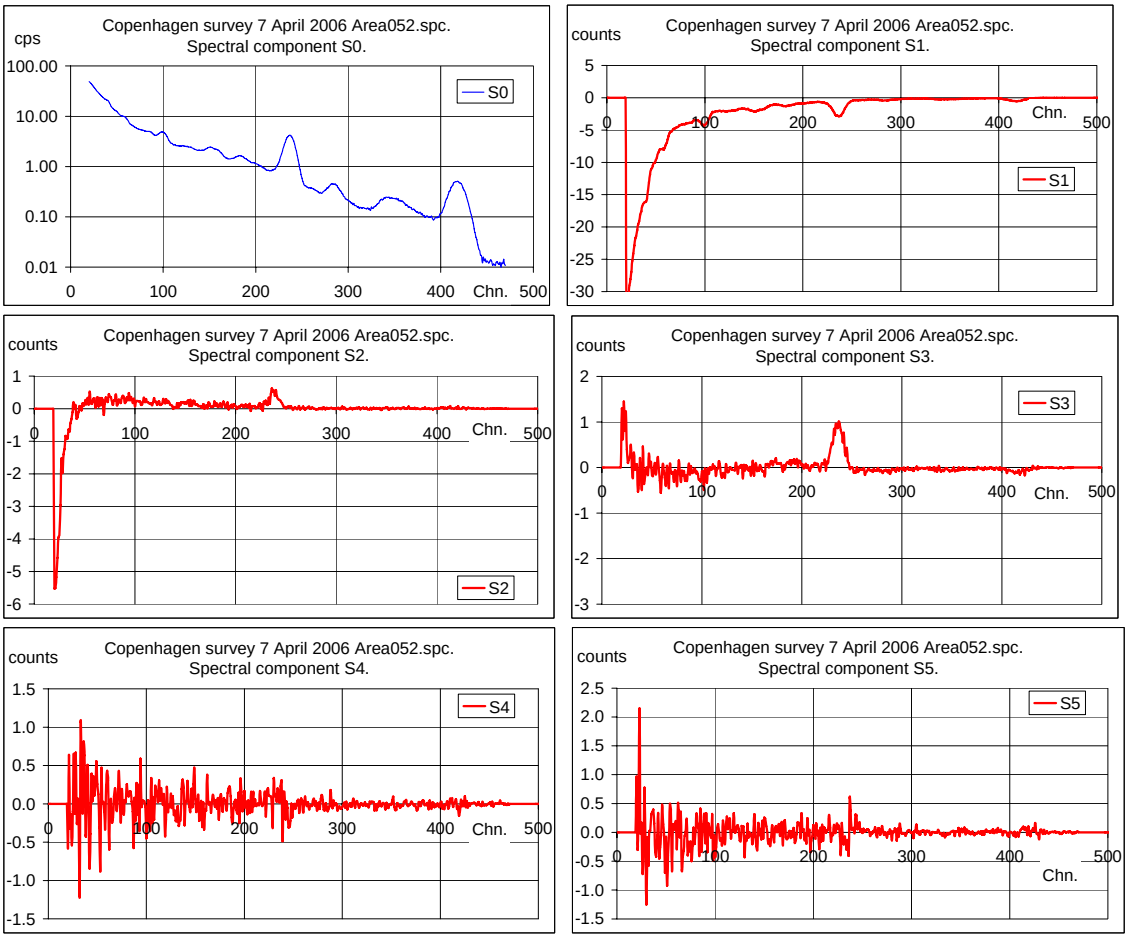

Figure 3.5.3.2. Spectral components for file Area052.spc. Component file name Ar52sc20.txt.

3.6 Spectra for Search for Lost Sources.

The original Danish urban data sets do not contain measurements on sources. To test the ability of the methods to find uncommon signals in a pool of data six different source signal spectra were added to the data sets. The amount of source signal is 62 additional counts. Each of the six spectra was added to specially selected spectra in the files Area052.spc. The spectra were chosen because of their differences in Th/U/K content and amount of scattered photons. Only one source signal were added for each investigation and it was added only once so as not to contribute to the shape of the spectral components or in the calculation of ASSS factors.

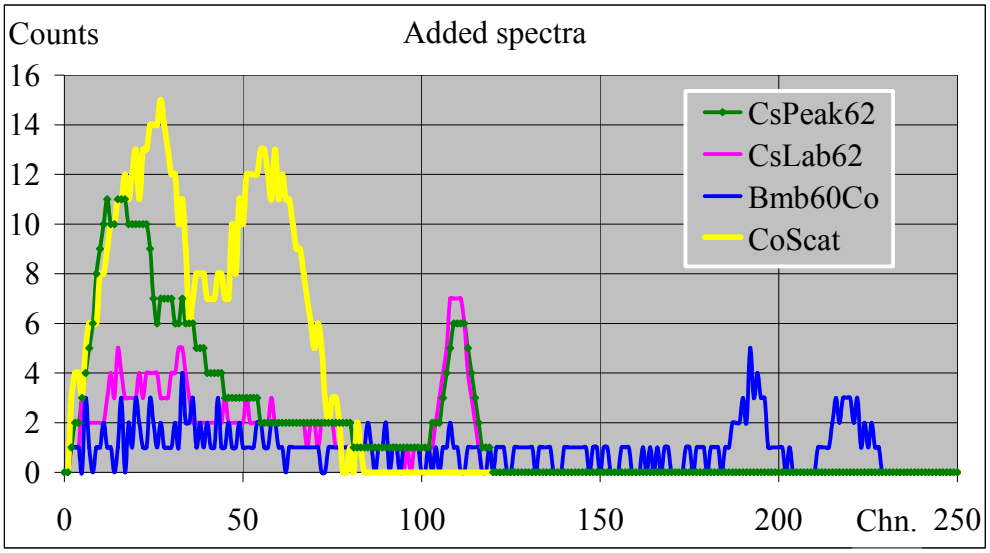

Figure 3.6.1. Spectra recorded with the Danish CGS systems at the Barents Rescue Exercise and in the laboratory (CsLab62).

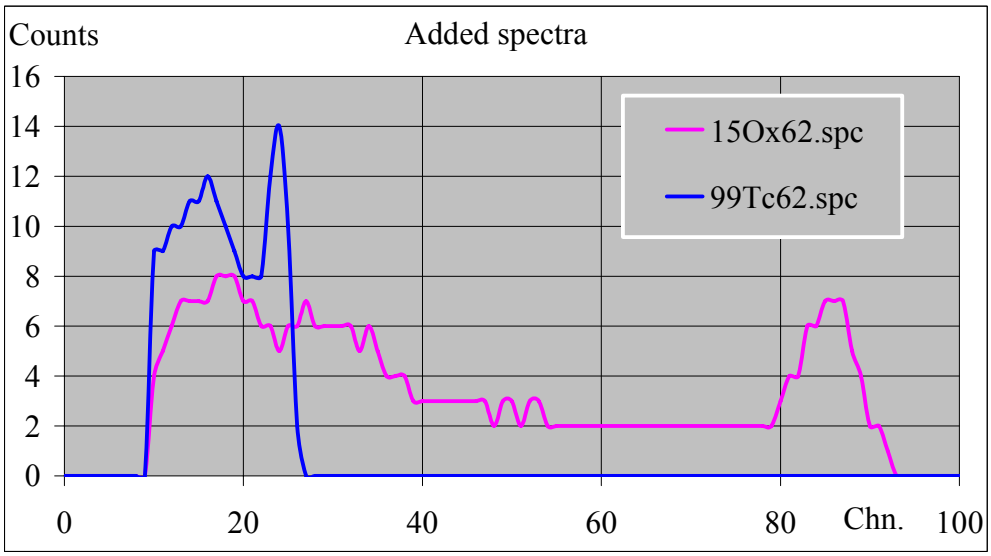

Figure 3.6.2. Spectra recorded with the Danish CGS system at the Finsen Institute April 2006 in cooperation with Chief Physicist Holger J. Jensen.

3.7 Spectra with Added Source Signals

3.7.1 Area052cl.spc: Original Measurements

Figure 3.7.1.1 shows eight measured spectra from file Area052cl.spc. To each of the spectra were added the spectra shown in Figure 3.6.1 and Figure 3.6.2. The spectra were chosen so as to represent different measurement geometries and different contents of natural radionuclides.

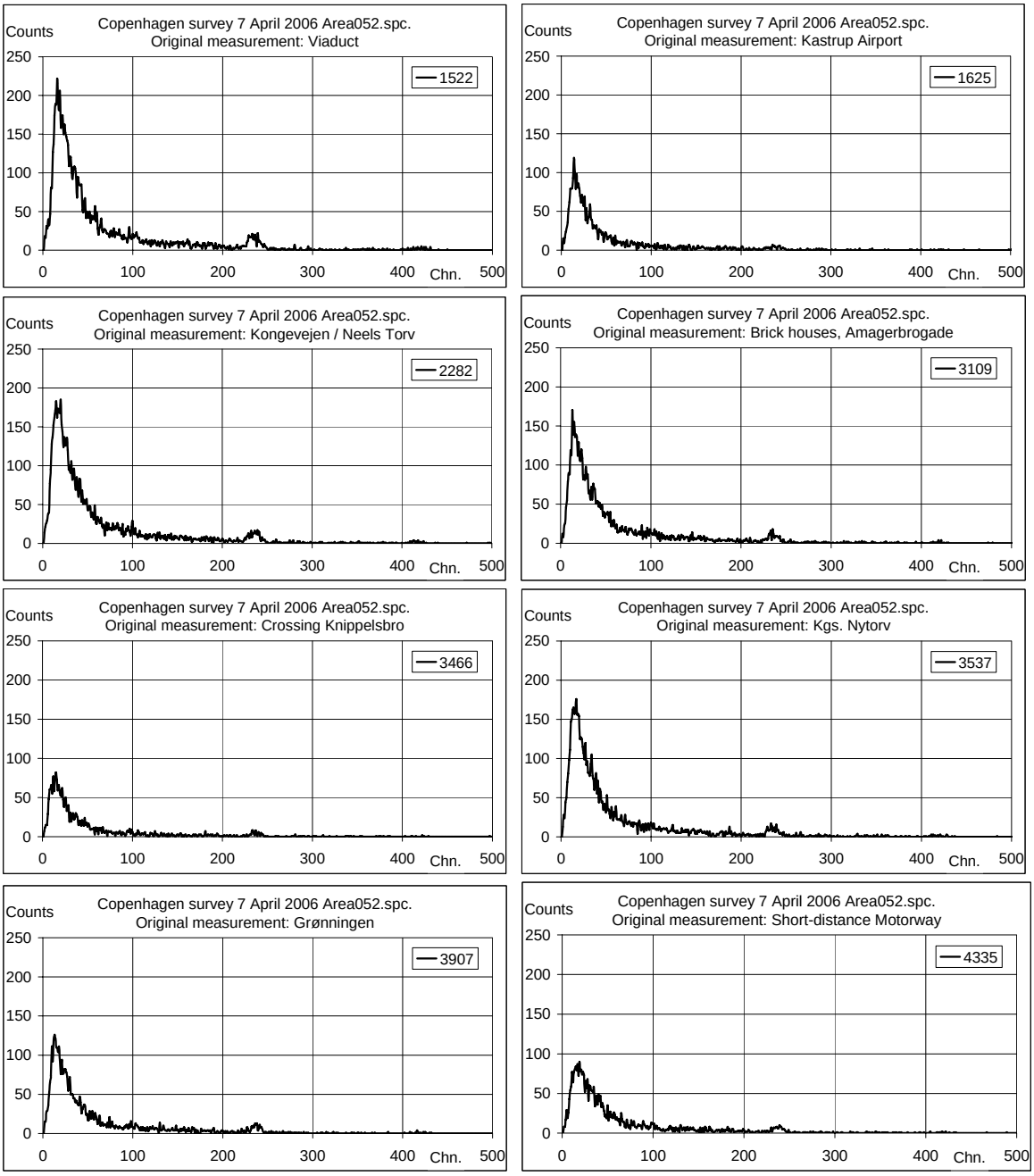

Figure 3.7.1.1. Selected spectra.

3.7.2 Area052cl.spc with Added Source Signals

To limit the size of the report only one spectrum with added source signals is shown here. This spectrum is measurement No. 3466, the spectrum that has the lowest number of total counts of the eight spectra chosen.
Figure 3.7.2.1 shows that the source signal contributes very little to the total spectrum shape. Possibly, though, the signal from CsLab62 could be spotted by a skilled user as a possible source signal.

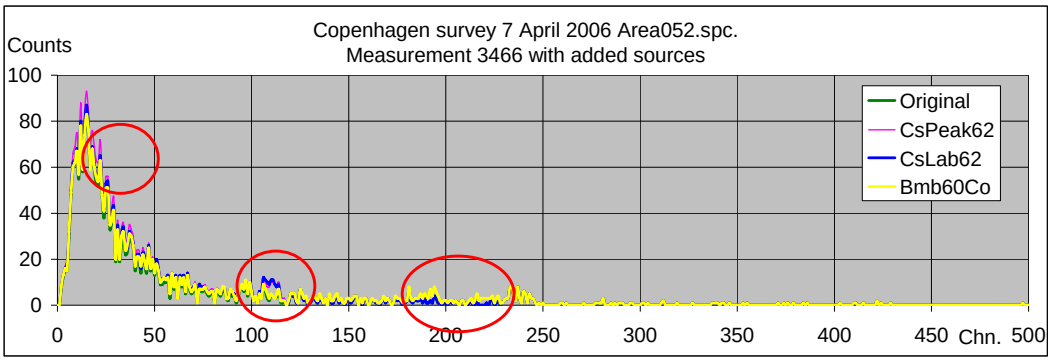

Figure 3.7.2.1. Example of added spectra to measurement No. 3466.

4 DANISH DATA TREATMENT WITH FSC

4.1 FSC Reproduction versus NASVD Reconstruction

In a previous initial test of the method (Ref. 6) showed that for a well stabilised system there is practically no difference between the NASVD fitting and FSC. A reproduced spectrum (FSC) looks exactly like a reconstructed spectrum (NASVD) if the same data set is used for calculation of the spectral components. The fitting constants c_1 to c_x will then be the same as the corresponding amplitudes b_1 to b_x. But what happens for poor calibrated system?

One of the purposes of the FSC method is to limit the amount of calculations and therefore only a few fitting constants are calculated. Under normal circumstances five fitting constants for each spectrum should be quite sufficient. If one includes more than five spectral components in the reconstruction, these additional spectral components are very likely to include source signals if sources were present during the survey. This means that the source signals can be fitted and only normal "error"-values will be calculated. The source can then be missed in the FSC error calculations. However, for a poor stabilised system it might be necessary to include more components as demonstrated in the following.

Area17cl.spc suffers from poor spectrum stabilisation meaning that the centroids "sail up and down" the energy axis during the measurement series. Fitting constants were calculated for this file by NASVD processing the data from channel 10 to channel 470 and using five of the created spectral components in the calculations. Two fitting iterations were made (confer next section).

The magnitudes of the fitting constants were compared to the magnitude of the amplitudes and differences were observed. NASVD calculates in principle as many spectral components as there are measurement channels and the same amount of sets of amplitudes. Additional information exists and can be applied by the user if the reconstruction with e.g. five components is not sufficiently good. FSC calculates only N sets of fitting constants from N spectral components. And no additional information exists. So how much information could one risk to lose? Figure 4.1.1 shows the cross plots of the FSC fitting constants to the amplitudes for Area17cl.spc. FSC constants c_1 and b_1 are the same, not much difference is obtained for the pairs c_2 and b_2 and c_3 and b_3, either. For the following pairs, however, the difference shows. This tells that the FSC reproduction using five spectral components only will be slightly inferior to the NASVD reproduction with five spectral components. But the result is still very good. Please notice also the postulate above than under normal circumstances five spectral components are enough. Here are demonstrated errors using five components only and the errors are small both for four and five components. Using only four spectral components and four sets of FSC constants is therefore also reasonable under normal circumstances.

FSC has the advantage that a set of spectral components can be created once and then reused on future measurements with satisfactorily results (confer Section 4.3.3). The spectral components with the FSC method in this report originate from NASVD processed data. In principle it is also possible to obtain a set of standard spectra to be used with FSC without using NASVD.

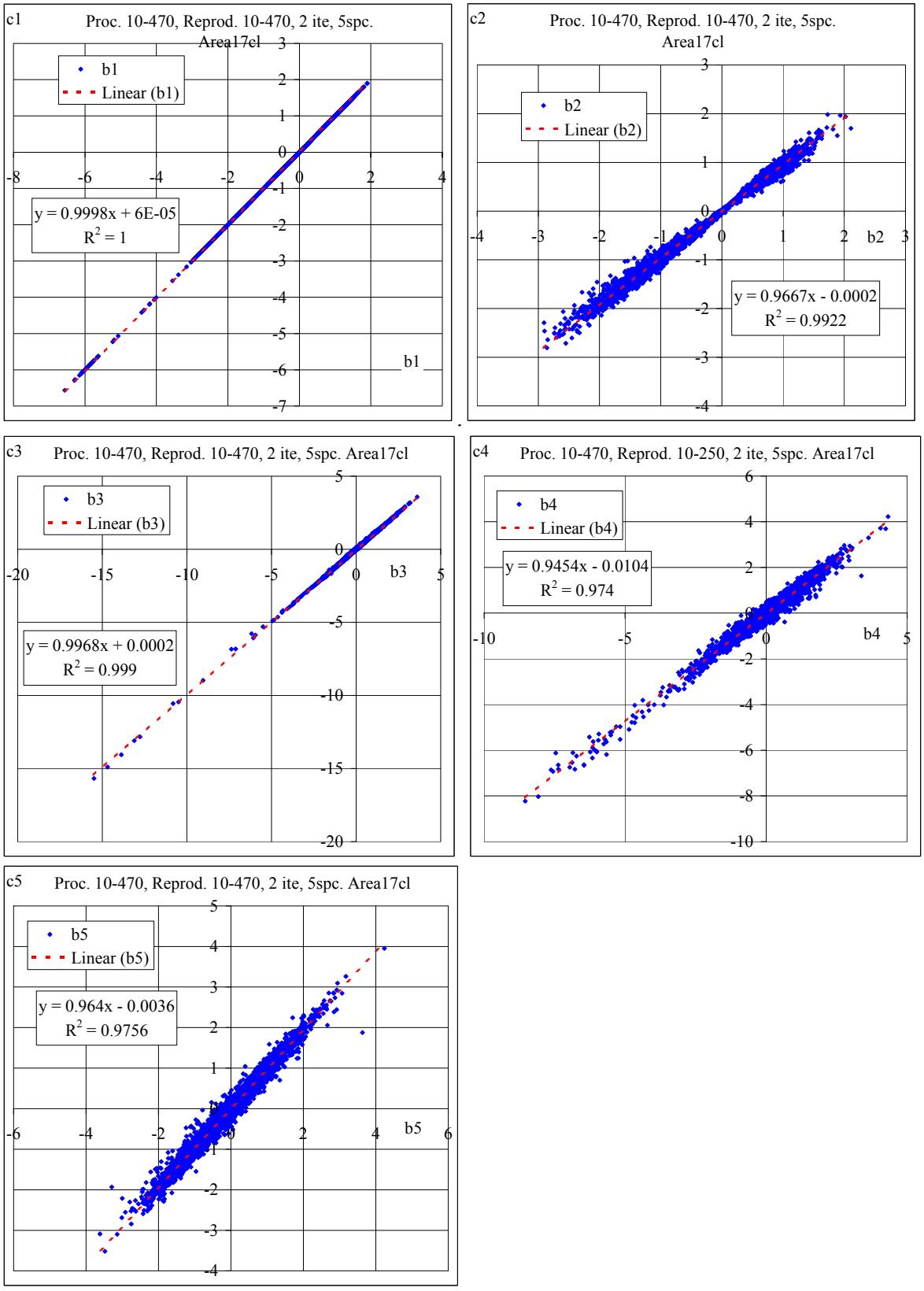

Figure 4.1.1. Cross plots of FSC fitting constants and NASVD amplitudes.

4.2 Iterations

In Section 3.3.3 is described the mathematics for the FSC method. The FSC program used can perform a number of iterations according to the users' choice. For each iteration a new set of weight factors ($w_{i,j}$ is selected as $1/var(n_{i,j})$) is calculated. But how many iterations are in fact necessary?

The data from file Area17cl.spc have been fitted with five spectral components from channel 10 to channel 470 using one, two, three, four and five iterations and five sets of fitting constants. In the first iteration, the weight factor is calculated from the mean spectrum, i.e. spectral component No. 0. This is of course not optimal for all spectra in the file. In the second fitting the weight factors for a spectrum is calculated from the reproduced spectrum from the first iteration, et cetera.

Table 4.2.1 shows the average fitting constants for one to five iterations. The differences are very small and the average starts to fluctuate very quickly. No more than two iterations are necessary. To iterate additional times does not improve the result. The values for each individual constant for each number of iterations are in fact quite similar. Figure 4.2.1 shows the c1 values for one iteration from which have been subtracted the values for two and five iterations, respectively. Figure 4.2.2 shows the corresponding c3 difference values.

There is not much to be gained from more than one iteration. However, a few differences are found, e.g. around measurement No. 3395 at Øster Søgade driving along the waterfront (canal) and around measurement No. 4449 driving around The Panum Institute (large brick walls).

Table 4.2.1. Average fitting constants for fitting of spectra with five spectral components in file Area17cl.spc.

No. Iterations	c1	c2	c3	c4	c5
1	0.0000	0.0000	0.0000	0.0000	0.0000
2	0.0001	-0.0002	0.0002	-0.0104	-0.0036
3	0.0001	-0.0008	-0.0002	-0.0039	-0.0029
4	0.0001	-0.0007	-0.0001	-0.0058	-0.0030
5	0.0001	-0.0008	-0.0002	-0.0046	-0.0030

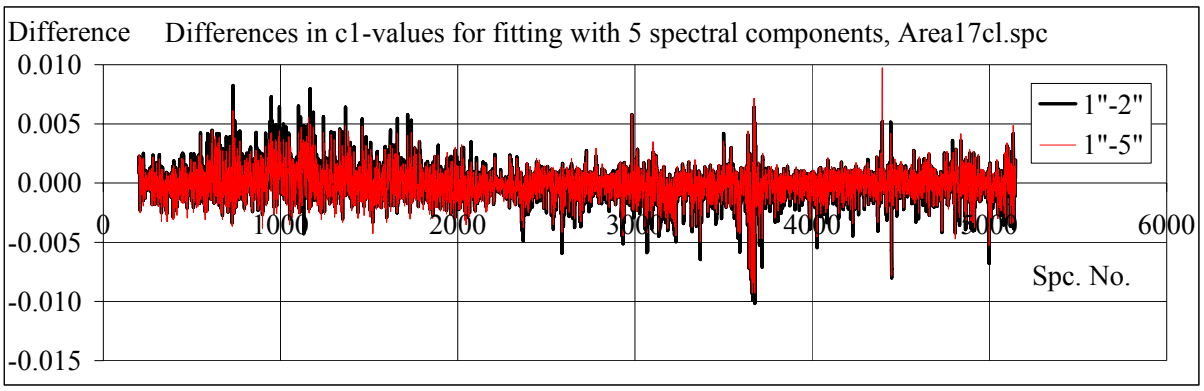

Figure 4.2.1. Fitting constant c_1-values. Values for 2 and 5 iterations subtracted from values for 1 iteration.

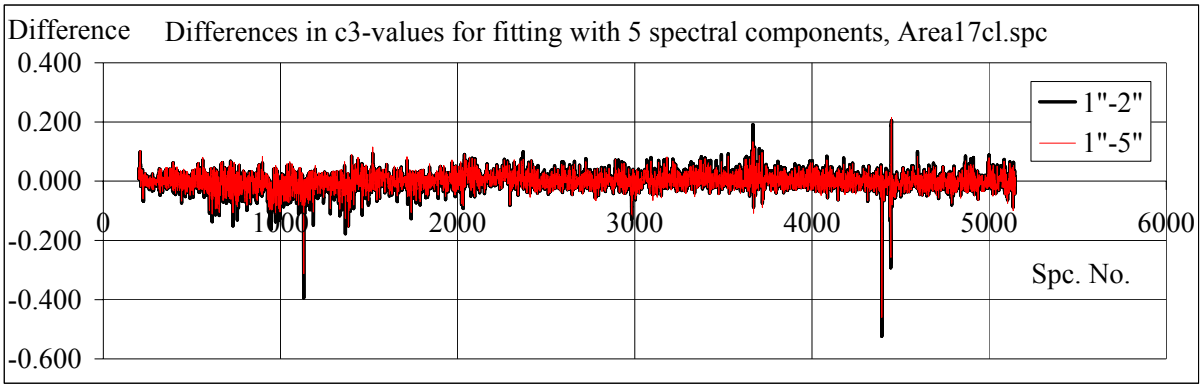

Figure 4.2.2. Fitting constant c3-values. Values for 2 and 5 iterations subtracted from values for 1 iteration.

To illustrate the order of magnitude of the FSC constants the c_1-values and c_3-values are shown for one and five iterations respectively. Spectral component $\mathbf{s}_3$ contains a potassium signal as its main feature.

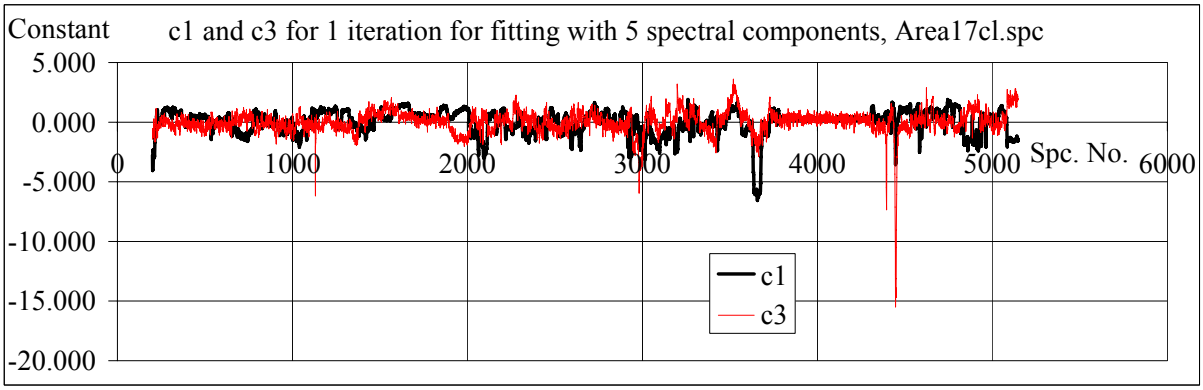

Figure 4.2.3. Fitting constants c_1- and c_3-values. Results for one iteration.

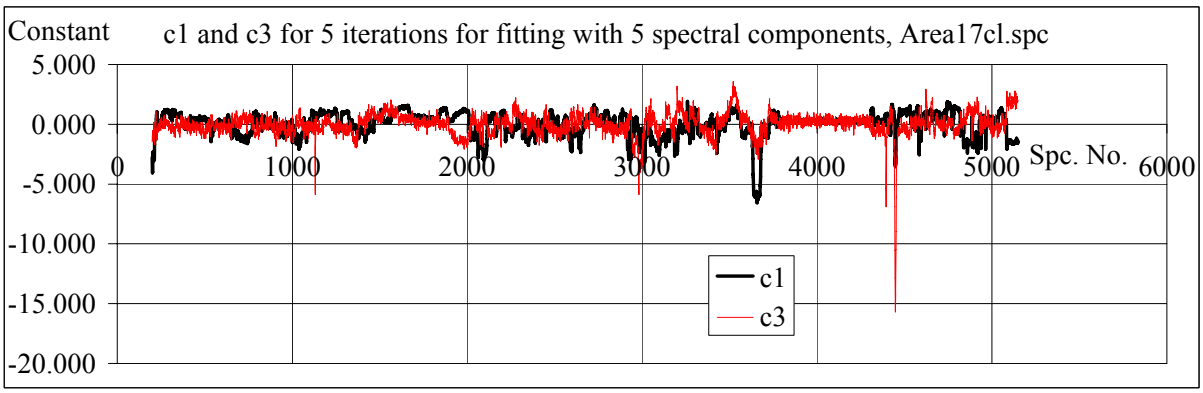

Figure 4.2.4. Fitting constants c_1- and c_3-values. Results for five iterations.

4.3 FSC for File Area052.spc

The FSC method was tested on the file Area052.spc with four different set of fitting constants. The fitting constants were calculated from the file itself or from other CGS data files. Two sets of fitting constants were calculated for the file itself: a set of constants using the standard (standard for DTU and DEMA) processing limits from channel 20 to channel 470 and a set of constants using a lower processing limit of 10 instead of 20. Another set of fitting constants were calculated from a file recorded earlier the same day, Area051.spc. This file was recorded approximately 1 hour after rainfall and the spectral components show a radon signal which is not found in file Area052.spc. Finally a set of constants were calculated from a 2-year old file, Area017cl.spc. This data file is of pooor quality with respect to spectrum stabilisation.

4.3.1 Count Rates for File Area052.spc

Results, however, does not necessarily indicate how good a method is if one does not know the "initial" material. Therefore plots of gross count rates in the analysed channel windows are presented here together with the count rates for the natural radionuclide windows. The file does not contain sources and for all low energy windows the natural radionuclide composition shows through.

A description of the survey is found in Section 3.4.4. The flat curve between approx. 500 and 1000 is due to a break (statistical fluctuations at a gasoline station). The peak at approx. 1500 is a result of driving under a viaduct. Nos. 1600 to 1630, approx., is Kastrup airport. In general, the highest count rates were found at Amalienborg (3650) and Lyngby Hovedgade (last part of the file) and were caused by pavings of paving stones.

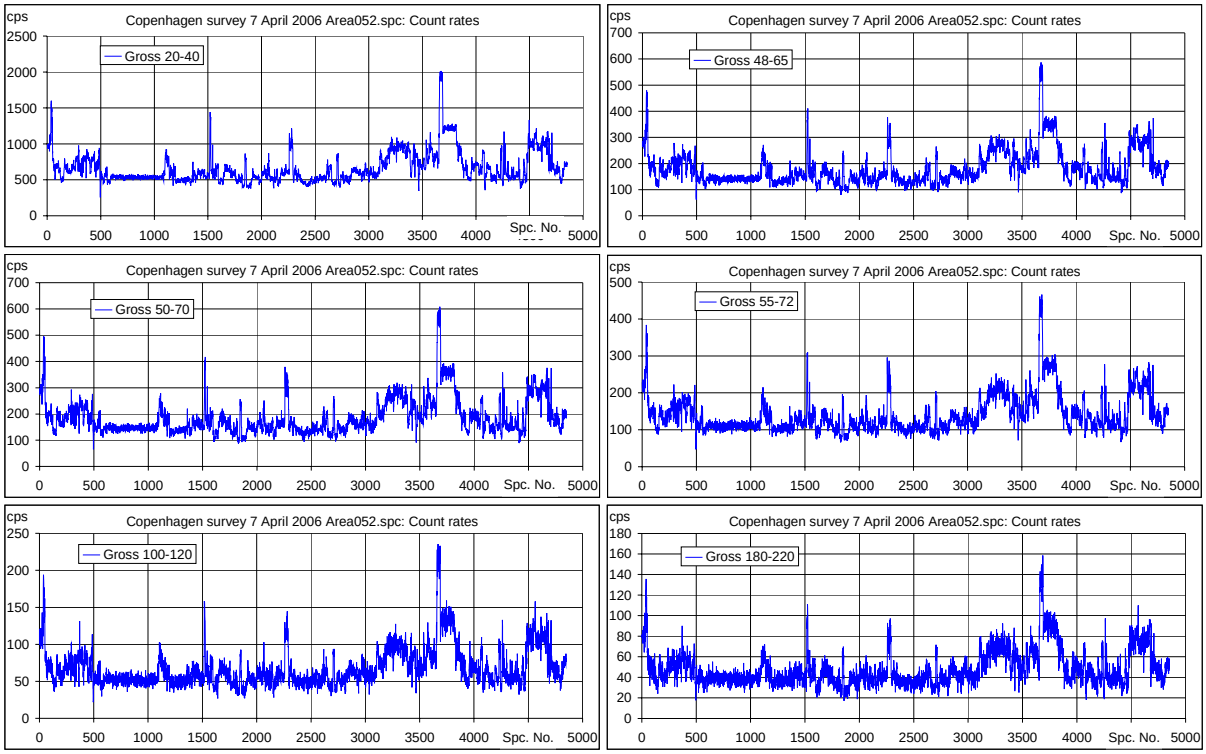

Figure 4.3.1.1. Count rates in low energy windows used with FSC, file Area052.spc.

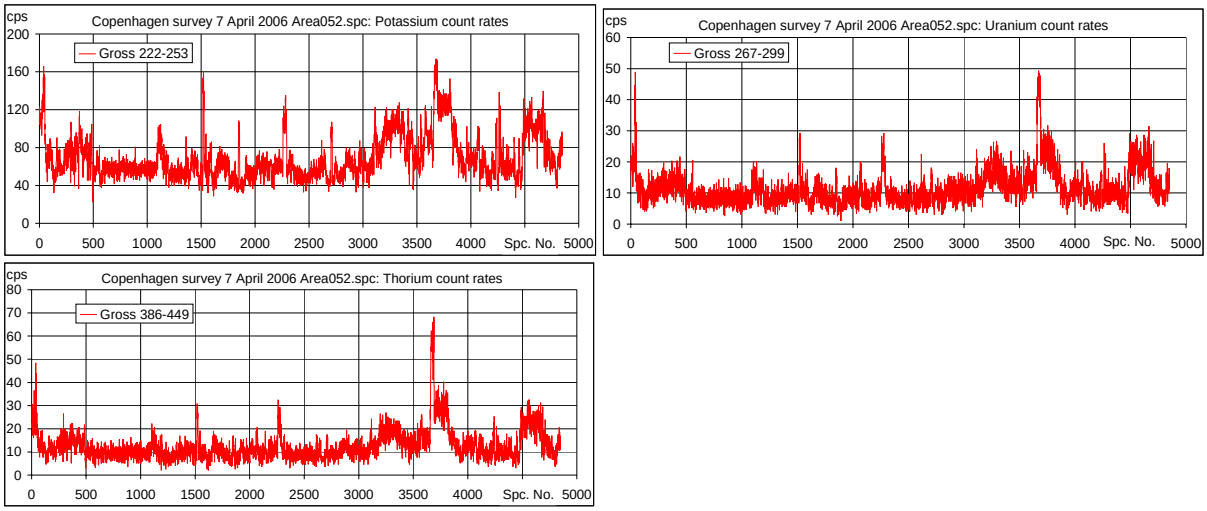

Figure 4.3.1.2. Count rates in natural radionuclide windows used with FSC, file Area052.spc.

4.3.2 FSC using Fitting Constants from File Area052.spc

If all necessary spectral components have been included in the calculation of the fitting constants the average of the fitting constants should be zero. The average fitting constants for Area052.spc were very close to zero, Table 4.3.2.1.

Table 4.3.2.1. Average FSC constants calculated from file Area052.spc.

Component file	c1	c2	c3	c4	c5
Ar52sc.txt	0.000	0.000	-0.002	0.000	0.000

A set of windows (defined in Section 3.1.1.4) was analysed for errors. The average errors were only slightly above what to expect from a χ^2 test (Expected, Table 4.3.2.1). Without going into minor detail analysis of each possible high value (or low value) error, the Figures 4.3.2.1 to 4.3.2.3 show no real indication of anything beyond the ordinary, i.e. a possible source signal. – Amalienborg, though, should probably be checked for natural anomalies.

The three plots shown are for a low energy window, a caesium window and a cobalt window. It is noticed, that the errors from the FSC calculations does not follow the count rate pattern for the natural radionuclides.

The plots are representative of the normal variations in a city the size of Copenhagen. One might choose to fix a 90% confidence level as a standard value for a possible source signal – or one might set the level based on source measurement. In Section 6 the FSC method will be used on the same data set to which source signals have been added.

Table 4.3.2.2. Average errors and expected errors for fitting of spectra in file Area052.spc.

Component file		20-40	48-65	50-70	55-72	100-120	180-220
Ar52sc.txt	Average	20.483	17.741	20.644	17.687	20.703	40.881
	Expected	20.3	17.3	20.3	17.3	20.3	40.3

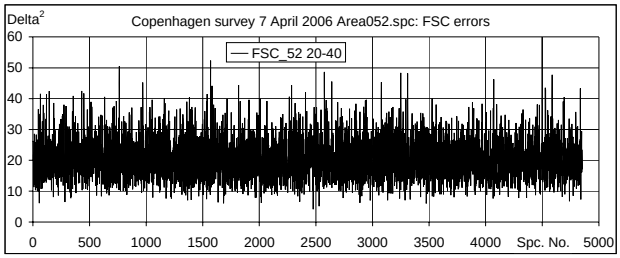

Figure 4.3.2.1. Low energy window errors.

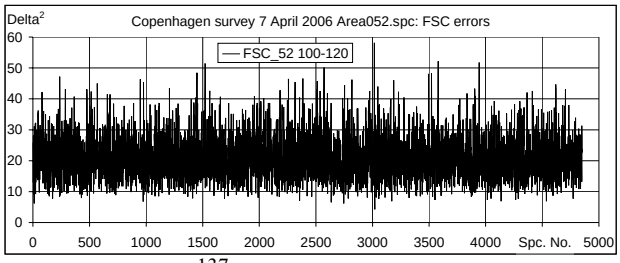

Figure 4.3.2.2. ^{137}Cs window errors.

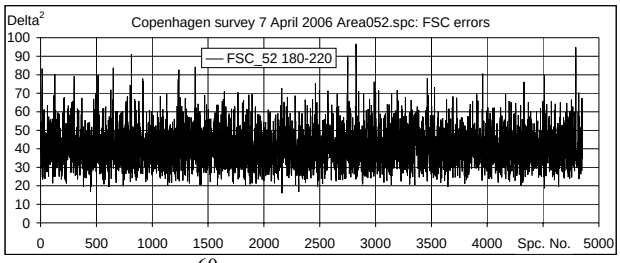

Figure 4.3.2.3. ^{60}Co window errors.

4.3.3 FSC using Fitting Constants from File Area051cl.spc

The file Area051cl.spc were made on the very same day but the radon content in the air was slightly different. Table 4.3.3.1 shows that the fit is not perfect. The average values of the fitting constants are not zero. So, what will the consequences be considering the calculated errors? Again three plots are shown: the low energy window, the caesium window and the cobalt window. And again no measurement stands out and presents itself as a possible source signal. The plots looks very much the same as had the analysed data file been used for the FSC constants calculations. In general the errors are 0.1-0.15 higher, Table 4.3.3.2.

Table 4.3.3.1. Average FSC constants calculated from file Area051cl.spc.

Component file	c1	c2	c3	c4	c5
Ar51clsc.txt	-0.499	0.327	0.009	-0.341	0.053

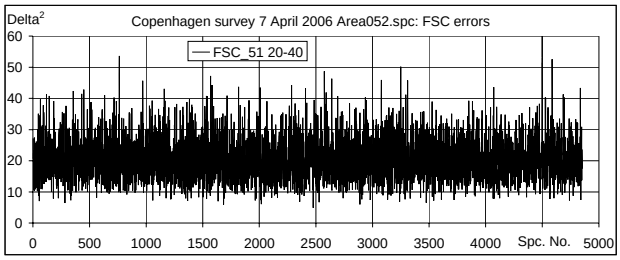

Figure 4.3.3.1. Low energy window errors.

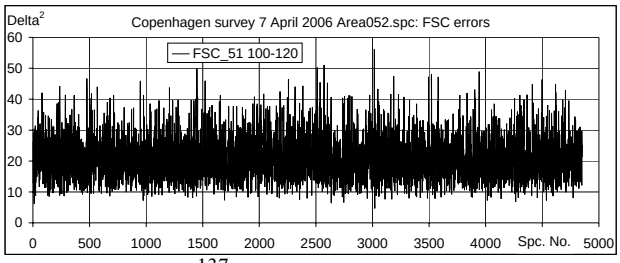

Figure 4.3.3.2. ^{137}Cs window errors.

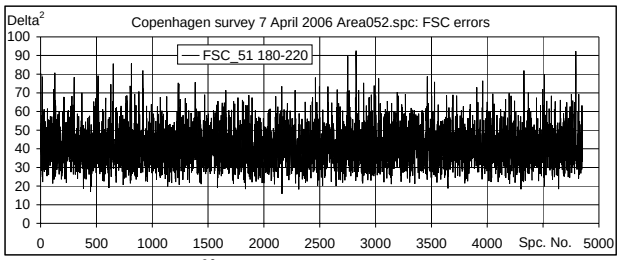

Figure 4.3.3.3. ^{60}Co window errors.

Table 4.3.3.2. Average errors and expected errors for fitting of spectra in file Area052.spc.

Component file		20-40	48-65	50-70	55-72	100-120	180-220
Ar51clsc.txt	Average	20.584	17.829	20.800	17.822	20.837	41.126
	Expected	20.3	17.3	20.3	17.3	20.3	40.3

4.3.4 FSC using Fitting Constants from File Area017cl.spc

File Area017cl.spc contains a large, spectrum drift signal in spectral component 2 that is not seen in the files Area052.spc or Area051cl.spc. When the file Area052.spc is fitted with the constants originating from this poor data file, information is lost. The average fitting constants are far from zero indicating, that more spectral components would be needed to obtain a proper fit. But how bad are the results? Table 4.3.4.2 shows the average errors that are seen to increase further compared to the average errors from Area051cl.spc – however, the errors for the caesium window and the cobalt window have decreased. Again, the error plots do not signify a source signal present somewhere in the surroundings.

Table 4.3.4.1. Average FSC constants calculated from file Area017cl.spc.

Component file	c1	c2	c3	c4	c5
Ar17clsc.txt	0.402	0.853	0.202	0.276	-0.342

Table 4.3.4.2. Average errors and expected errors for fitting of spectra in file Area052.spc.

Component file		20-40	48-65	50-70	55-72	100-120	180-220
Ar17clsc.txt	Average	20.761	17.921	20.882	17.863	20.601	40.820
	Expected	20.3	17.3	20.3	17.3	20.3	40.3

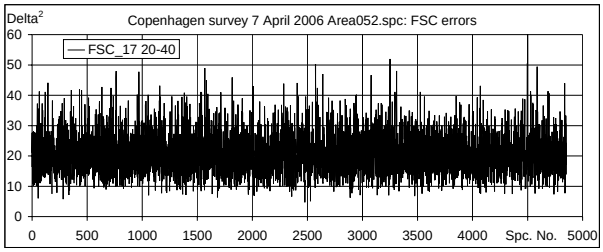

Figure 4.3.4.1. Low energy window errors.

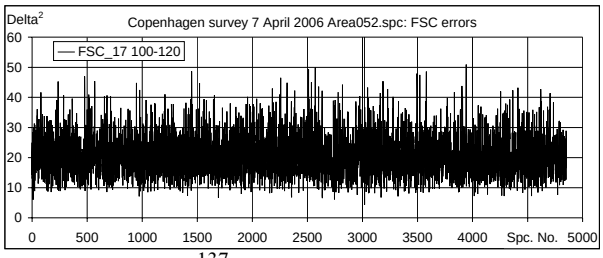

Figure 4.3.4.2. ^{137}Cs window errors.

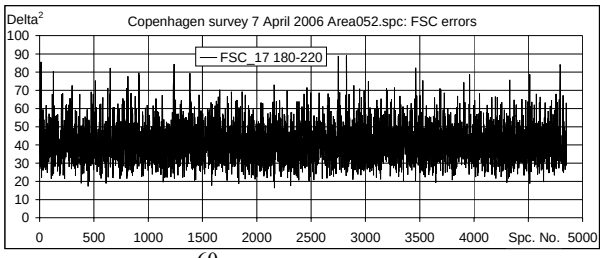

Figure 4.3.4.3. ^{60}Co window errors.

4.3.5 FSC using Fitting Constants from File Area052.spc: New NASVD Limits

The three previous fits were made with the lower NASVD processing limit very close to the cut-off detection limit which is, for the Danish system, approximately at the limit where a ^{241}Am may or may not be detected. When a very low limit is used one should be cautious not to fit too much of the "cut-off" energy tailing at the lowest energies. Will the results then be improved if the NASVD lower level is increased from channel 10 to channel 20?
Fittings similar to those of the three previous sections were made using a lower limit of 20. The resulting fitting constants are shown in Table 4.3.5.1. When fitting with a poor data quality file the average fitting constants do get closer to zero indicating a better fit. For the good quality data sets, no general tendency is seen. So what happens with the results? Table 4.3.5.2 shows that the average errors do decrease especially for the very low energy window (scattered radiation). In fact, the fitting for this window seemingly is better then what one should expect. A possible explanation for this has not yet been found.

Table 4.3.5.1. Average FSC constants calculated from file Area017cl.spc.

Component file	c1	c2	c3	c4	c5
Ar52sc20.txt	0.000	0.000	-0.001	0.000	0.001
Ar51clsc2.txt	-0.411	-0.381	-0.043	0.025	0.019
Ar17clsc2.txt	0.347	0.743	0.161	0.271	-0.317

Table 4.3.5.2. Average errors and expected errors for fitting of spectra in file Area052.spc.

Component file		20-40	48-65	50-70	55-72	100-120	180-220
Ar52sc20.txt	Average	20.071	17.673	20.565	17.625	20.628	40.719
Ar51clsc2.txt	Average	20.256	17.747	20.723	17.747	20.780	40.964
Ar17clsc2.txt	Average	20.344	17.944	20.902	17.894	20.647	41.015
	Expected	20.3	17.3	20.3	17.3	20.3	40.3

4.3.6 Comparison of FSC Results for File Area052.spc

It has been shown that it is possible to remove constributions from the natural radionuclides to an error level approximately the same size as one would achieve by a χ^2 test. It has also been shown that it is possible to fit a data set using information from other data sets recorded during different circumstances: radon remains, slight snow cover and rain.
Changing the data processing limit not to include the lowermost channels slightly improve the reults. Figure 4.3.6.1 shows the distribution of FSC errors for the caesium window. Apart from the very few, large errors (attributed to Amalienborg) the distribution of errors is close to a 50-50 distribution around the expected mean value.

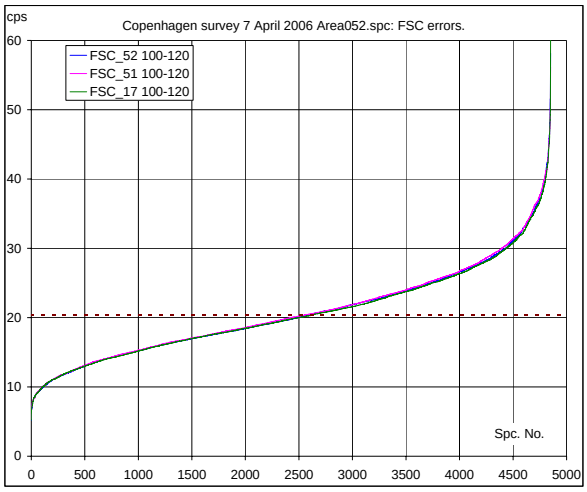

Figure 4.3.6.1. FSC errors in the caesium window for three different fitting files.

5 DANISH AREA SPECIFIC STRIPPING OF FILE AREA052.SPC

Although FSC was the proposed Danish analysis tool for the CGS project it was considered worth the effort to also test the method of ASSS on the same data. ASSS was first used by Danish CGS teams at the Barents Rescue exercise, and the method's ability to find weak source signals have previously been demonstrated.
FSC performs analysis on the entire spectrum whereas ASSS only uses window count rates.

Three sets of ASSS factors were calculated for the same files and same windows that were used in Section 4. Table 5.1.1 shows the ASSS factors. The different survey paths and the the different radionuclide compositions show as variations in A, B and C for the same windows. Table 5.1.2 shows the average measured count rate that should be compared to the stripped results presented in Table 5.1.3.
Are052.spc includes a drive in the courtyard of Amalienborg and rush hour traffic driving at Lyngby Hovedgade (paving stones). ASSS is not able to strip away the large contribution of

scattered photons originating from those paths. The result is positive count rates of approx. 2 cps in all windows.
Area051.spc includes post-rainfall signals and no measurements from the Island Amager where the measurement geometry is somewhat different from the main part of Copenhagen. Despite the spectrum drift in Area17cl.spc the average fit is remarkably good.

Table 5.1.1. Area Specific Spectrum Stripping Factors.

File		20-40	48-65	50-70	55-72	100-120	180-220
Area052.spc	A	6.960	2.260	2.388	1.814	0.923	0.530
	B	8.141	2.487	2.521	1.935	1.034	0.598
	C	7.023	1.777	1.832	1.378	0.622	0.487
Area51cl.spc	A	8.419	2.613	2.746	2.037	1.049	0.526
	B	11.190	2.893	2.947	2.249	0.954	0.574
	C	6.429	1.695	1.744	1.322	0.628	0.498
Area17cl.spc	A	9.385	2.809	2.904	2.246	1.165	0.581
	B	11.786	3.244	3.324	2.425	1.273	0.652
	C	6.026	1.609	1.660	1.260	0.588	0.485

Table 5.1.2. Average count rates for spectra in file Area052.spc.

222-253	267-299	386-449	20-40	48-65	50-70	55-72	100-120	180-220
68.662	11.438	12.584	665.295	181.119	186.867	141.574	67.909	48.279

Table 5.1.3.Average remaining count rates for area specific spectrum stripping of Area052.spc.

File	20-40	48-65	50-70	55-72	100-120	100-120 4-win.	180-220
Area052.spc	2.400	2.233	2.217	1.981	1.725	4.426	11.251
Area51cl.spc	-10.099	-1.203	-1.165	-0.569	0.706		11.030
Area17cl.spc	-1.391	-1.792	-1.693	-0.953	-1.709		10.115

The major difference between FSC and ASSS is seen when comparing the Figures 5.1.3.1-5.1.3.3 to the earlier FSC figures from Section 3. ASSS performs improper stripping that follows the count rates for natural radionuclides. If one wants to investigate if e.g. a ^{137}Cs or ^{60}Co signal is present a comparison with the natural radionuclides window count rates is necessary. This is not the case for the FSC method.

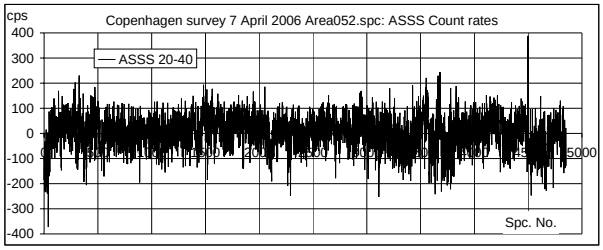

Figure 5.1.3.1. Low energy window errors. ASSS constants from file Area052.spc.

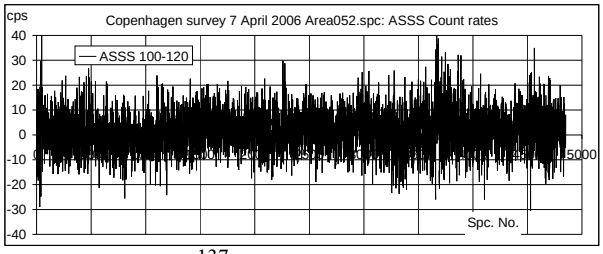

Figure 5.1.3.2. ^{137}Cs window errors. ASSS constants from file Area052.spc.

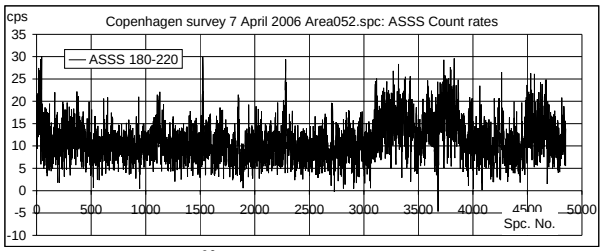

Figure 5.1.3.3. ^{60}Co window errors. ASSS constants from file Area052.spc.

Figure 5.1.3.4 shows the ASSS stripped count rate distribution for ASSS factors calculated for the file Area052.spc.

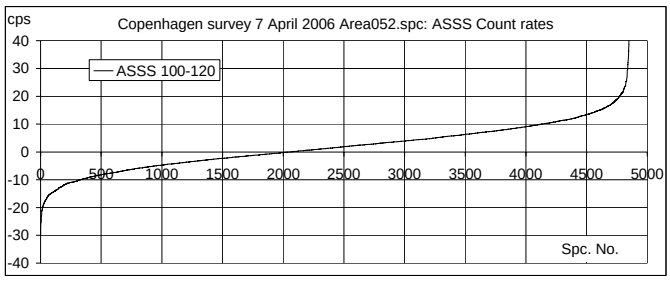

Figure 5.1.3.4. ASSS errors in the caesium window for fitting with Ar52sc.txt.

So far no source signals have been present in the data sets. In order to find out which method would be preferable to use source signals were added and the results for the two methods are compared in Section 6.

6 DANISH RESULTS FOR FILE AREA052.SPC WITH ADDED SOURCE SIGNALS

To each of the eight chosen files from file Area052.spc (Section 3.7.1) were added six different spectra containing source signals (Section 3.6).
Two of the spectra are ^{137}Cs spectra, CsPeak62 is an environmental spectrum whereas CsLab62 is a laboratory made spectrum with only few scattered photons. CoScat were made from measurements on a ^{60}Co source in containment and does not contain fulle energy signals as opposed to Bmb60Co. 15Ox62 and 99Tc62 are typical spectra associated with medical applications.
Each spectrum was only added to one measurement in the file Area052.spc at a time and only once, i.e. a total of 48 data files were analysed.

The FSC method and the ASSS methods both were tested using fitting constants and ASSS factors calculated from the file itself. (FSC component file Ar52clsc20.txt.) The FSC fitting constants are shown in Figure 6.1.

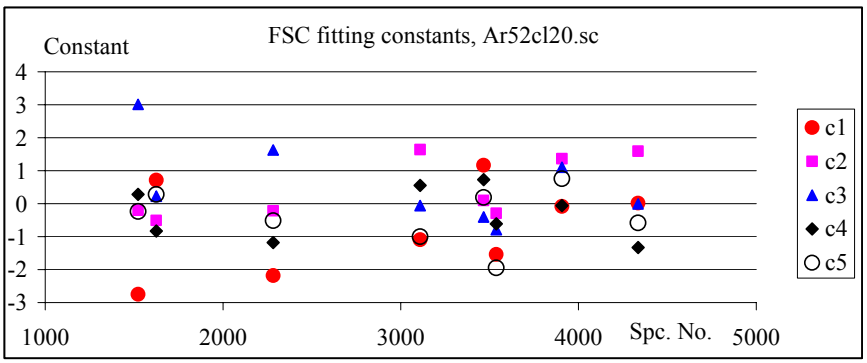

Figure 6.1. FSC fitting constants for eight spectra in file Area052.spc.

The results are presented graphically superimposed on FSC error plots and ASSS stripped count rate plots for the original data set containing no source signals.

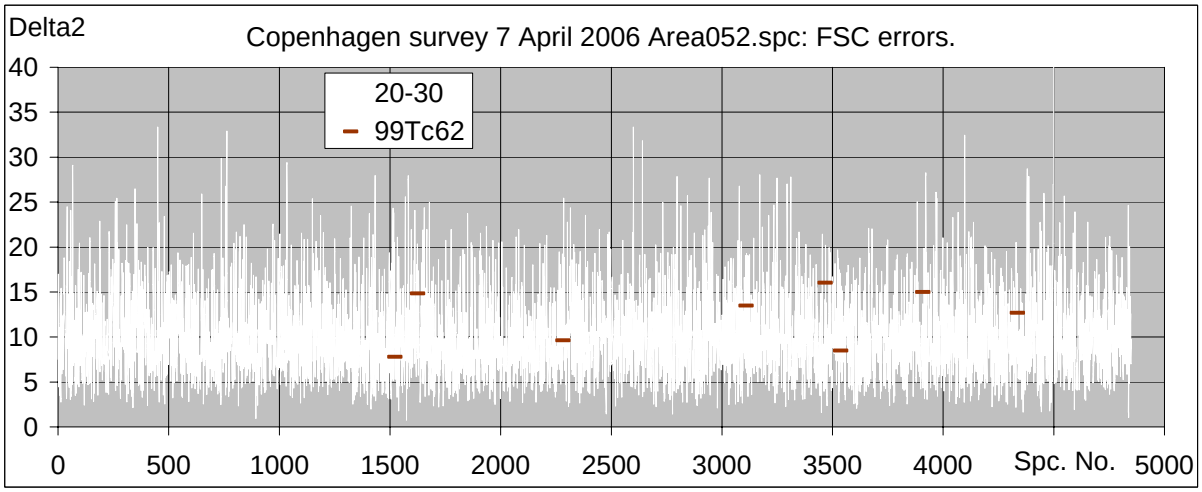

Figure 6.2. FSC errors for low energy window channel 20 to channel 30.

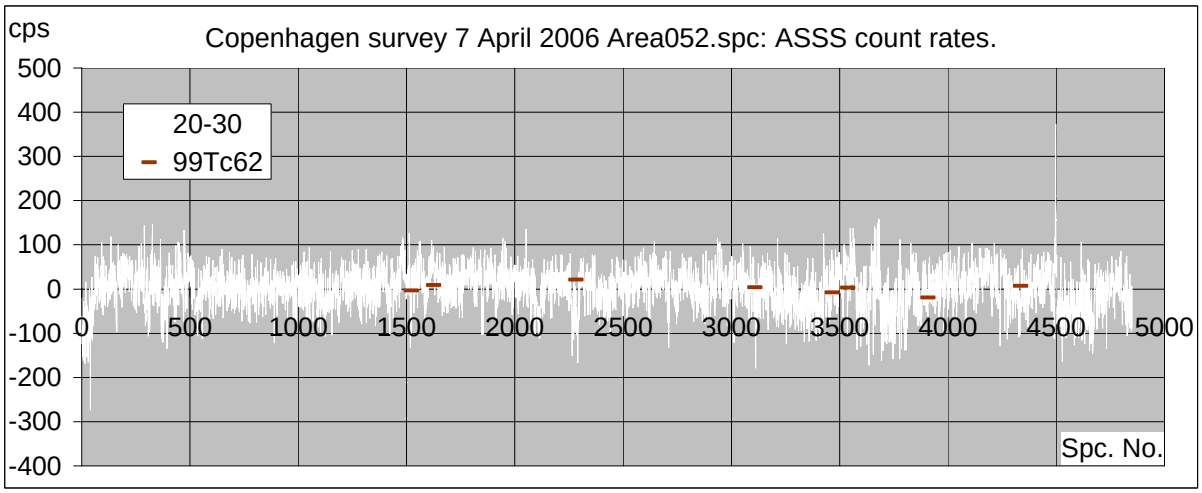

Figure 6.3. ASSS stripped count rates for low energy window channel 20 to channel 30.

The following observations were made:

99Tc62

This spectrum goes undetected with the ASSS method and the FSC method both. The peak in channel 23 fits too well with the normal spectrum shape at the low energies and FSC manages to fit the spectrum. ASSS actually shows slightly lower error values than before the addition of this spectrum. The introduction of a new window from channel 10 to channel 20 did not identify the source either.

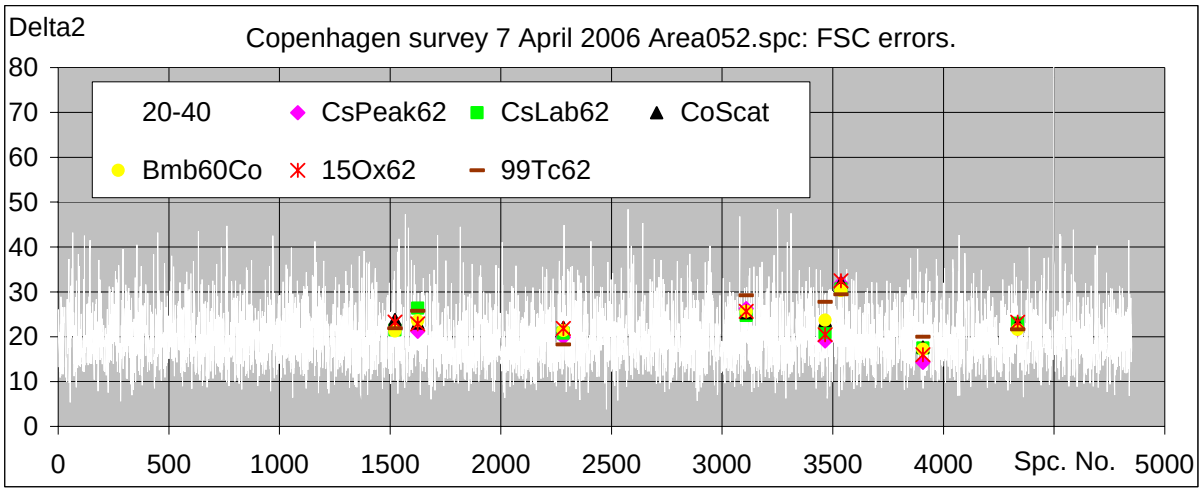

Figure 6.4. FSC errors for low energy window channel 20 to channel 40.

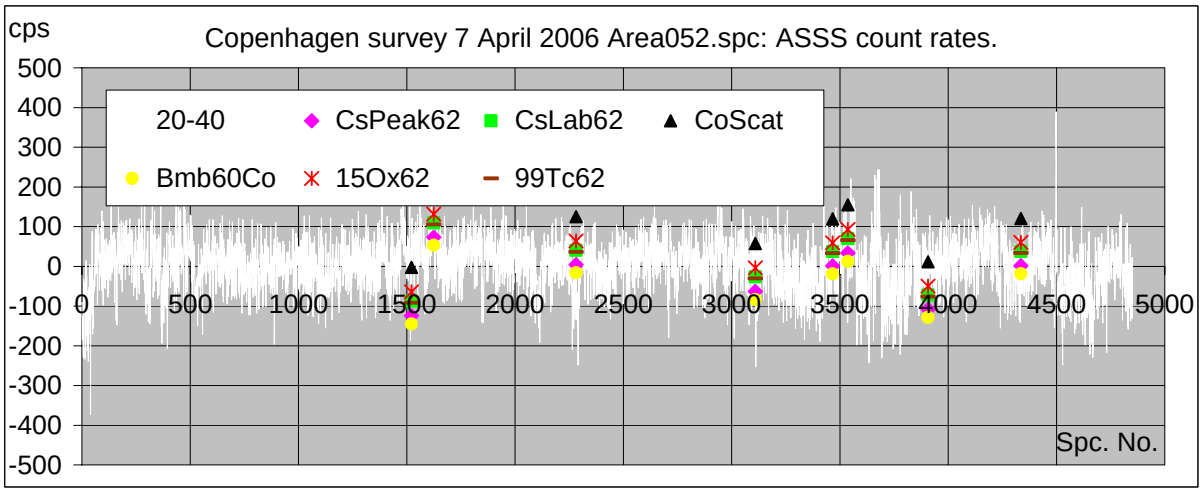

Figure 6.5. ASSS stripped count rates for low energy window channel 20 to channel 40.

15Ox62

The source signal is observed for spectrum Nos. 2282, 3644, and 4335 for ASSS in window 48-65 and for spectrum 4335 in window 500-70, also for ASSS only. Otherwise the source is undetected. The FSC method showed that for only one measurement, No. 1625, did the source signal rise above the general error fluctuations. For the ASSS method four measurements indicated a possible source. (One notices the peaks from Amamlienborg around the measurement No. 3540 that would also lead to suspisions of a possible source.)

An interesting detail is that ASSS for three of the measurements show significant low count rates in the cobalt window. A much too strong stripping also indicates a possible source. A source signal of twice the added amount would have been spotted for all measurements except for measurement No. 3607 using the FSC method.

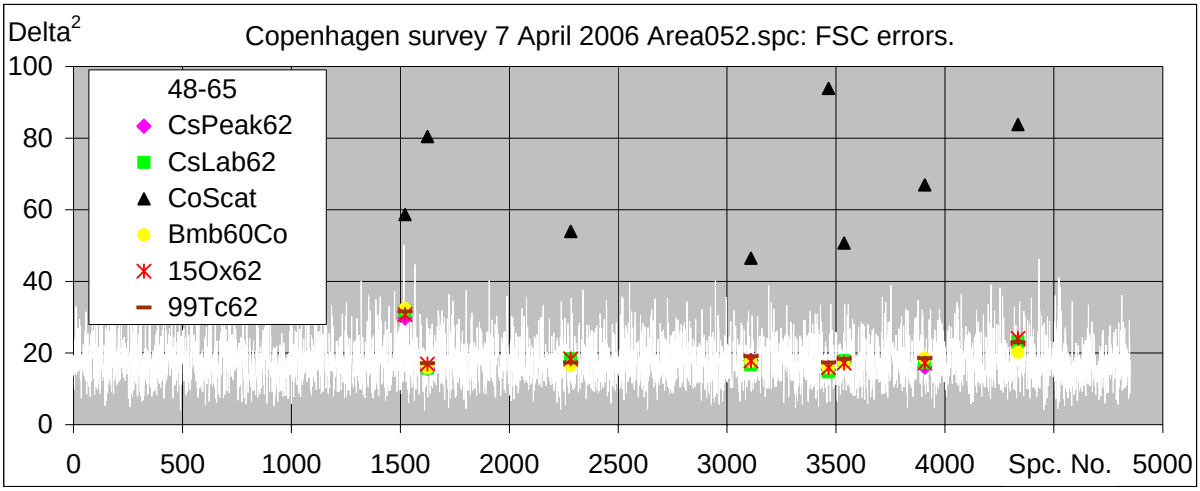

Figure 6.6. FSC errors for low energy window channel 48 to channel 65.

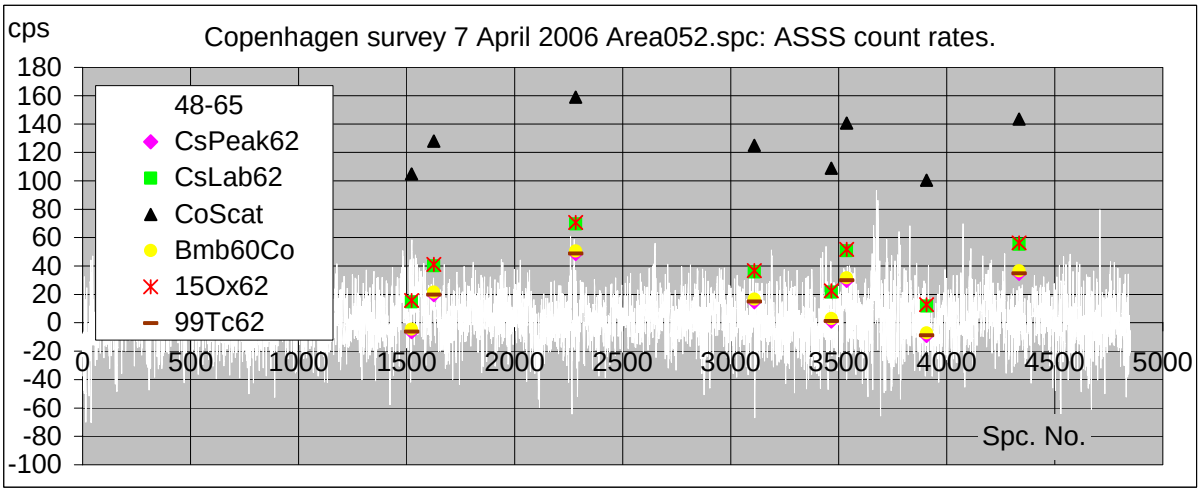

Figure 6.7. ASSS stripped count rates for low energy window channel 48 to channel 65.

CoScat

The low energy peak of this spectrum is not spotted by any of the two methods. In the windows 48-65, 50-70 , and 55-72, however, the source is seen for all eight measurements. Again ASSS shows strong negative stripped count rates in the cobalt window indicating that something is out of the ordinary for those measurements.

Bmb60Co

This spectrum only shows in the cobalt window for both methods. FSC only presents two significant results. ASSS presents three significant results and two "suspicious" results. Both methods find the signal in measurement No. 2282. FSC easily spots the signal in measurement No. 3466 (bridge) whereas ASSS do not.

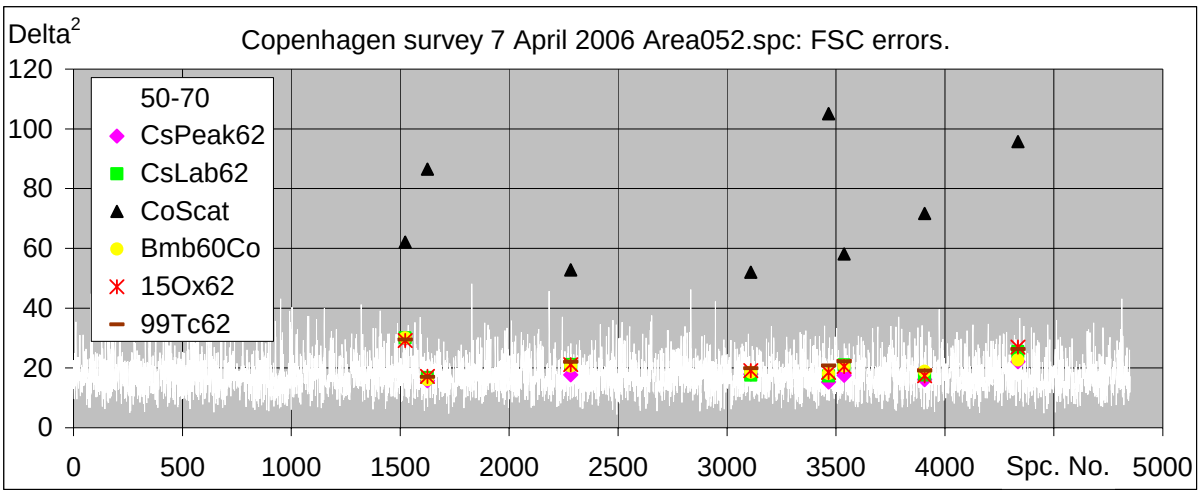

Figure 6.8. FSC errors for low energy window channel 50 to channel 70.

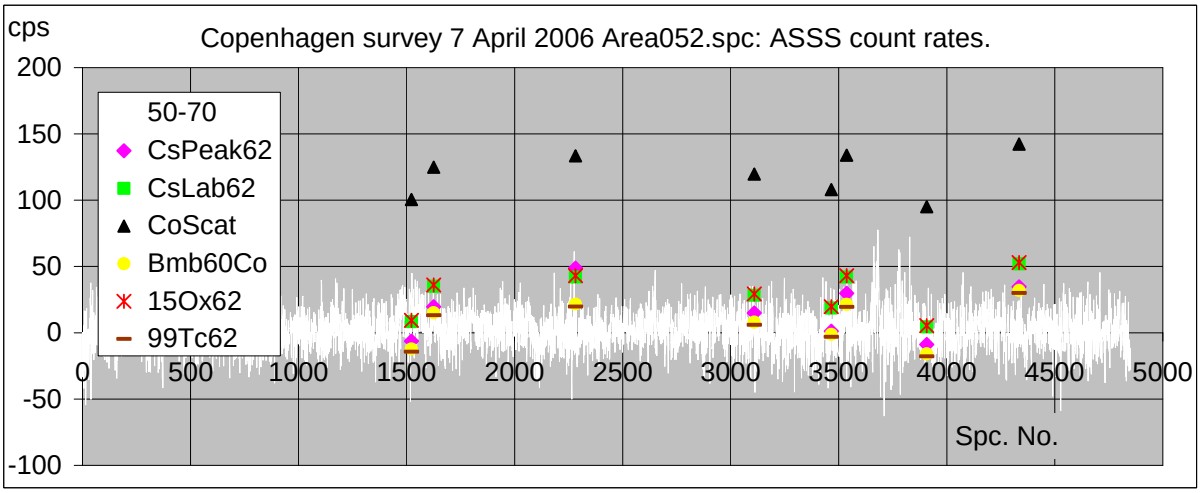

Figure 6.9. ASSS stripped count rates for low energy window channel 50 to channel 70.

CsPeak62

The source signal from this source does not show in the low energy windows and only the FSC method is able to find it. Two measurements, No. 1625 (airport) and No. 3466 (bridge) where the count rates are low are identified as containing source signals and one measurement, No. 3109, is “suspicious”.

The reason for not finding the source signals using ASSS has not been explained. That the FSC method is not able to find the signals in all the eight spectra is explained by the ratio of the low energy photons to the full energy peak photons. For measurements that have many counts in the 608 keV peak compared to the number of scattered photons in the low energy spectrum region, the measurements and the source signals resemble each other and most of the source signal is fitted as an expected radon signal.

CsLab62.

This laboratory made spectrum contains very few scattered photons but a distinct full energy peak. The signal only shows in the dedicated caesium window. The FSC method readily identifies three measurements, Nos. 1625, 3109, and 3466. The ASSS method finds almost all eight signales, the results for measurements Nos. 3466 and 3907 are slightly dubious.

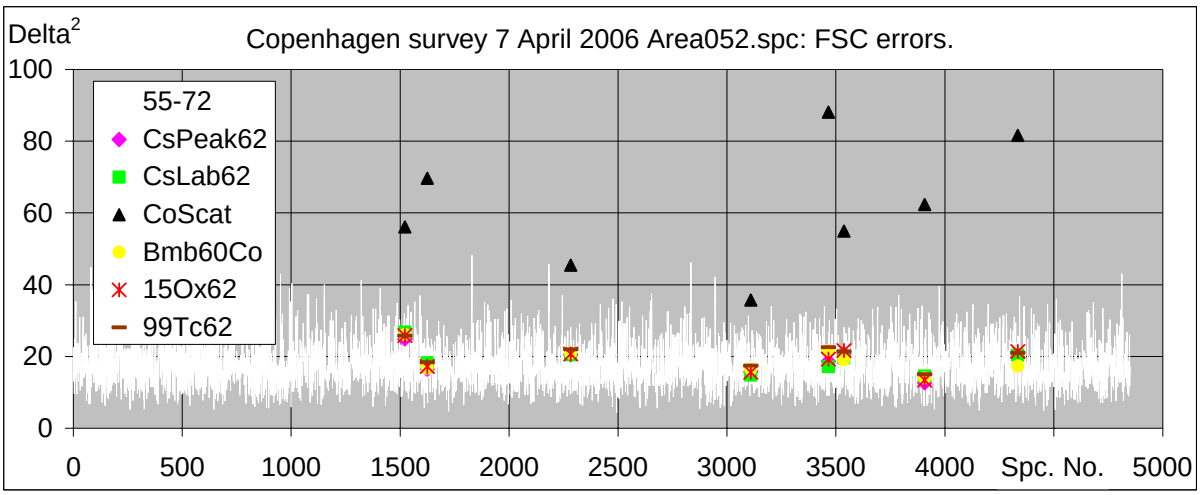

Figure 6.10. FSC errors for low energy window channel 55 to channel 72.

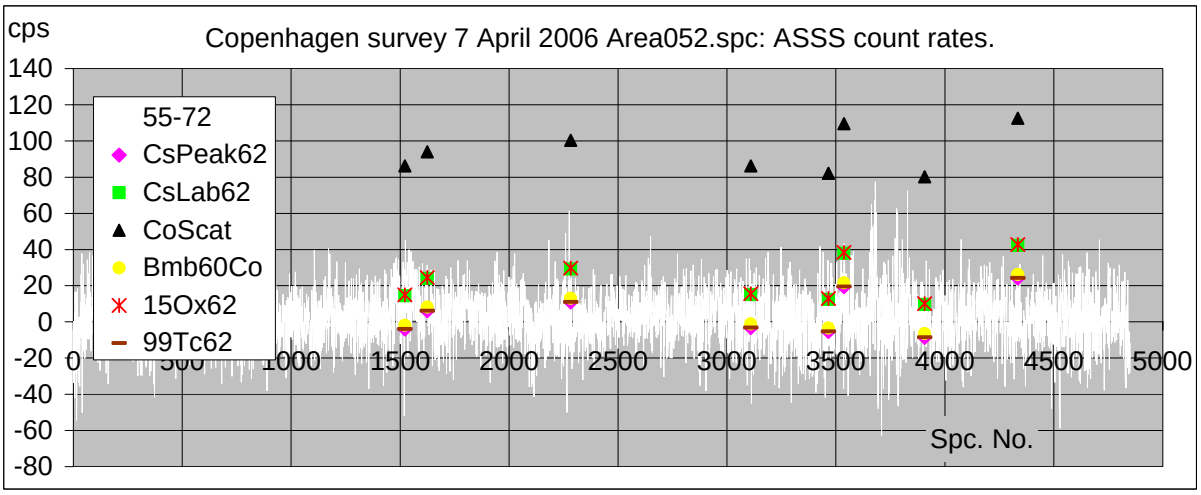

Figure 6.11. ASSS stripped count rates for low energy window channel 55 to channel 72.

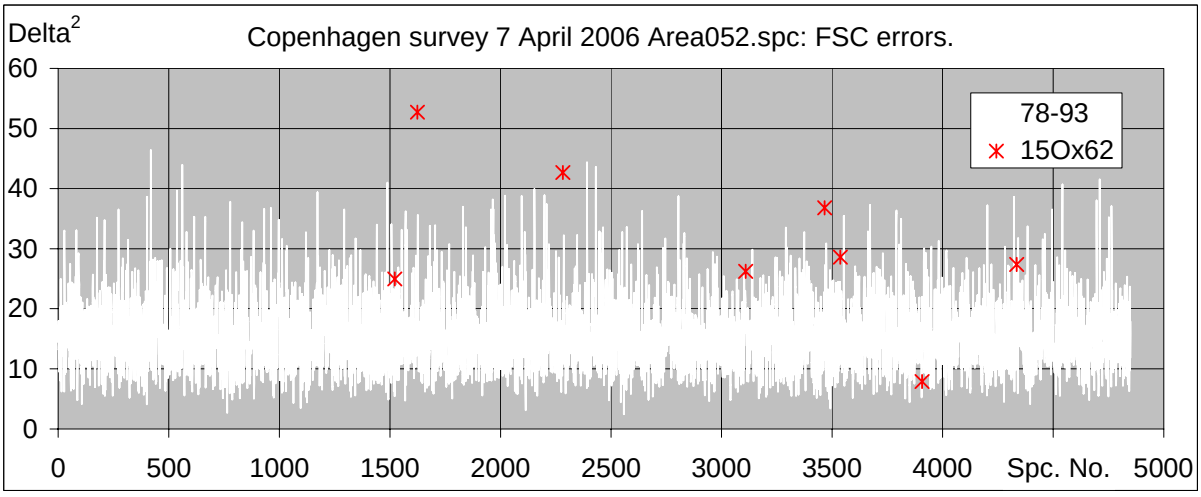

Figure 6.12. FSC errors for low energy window channel 78 to channel 93.

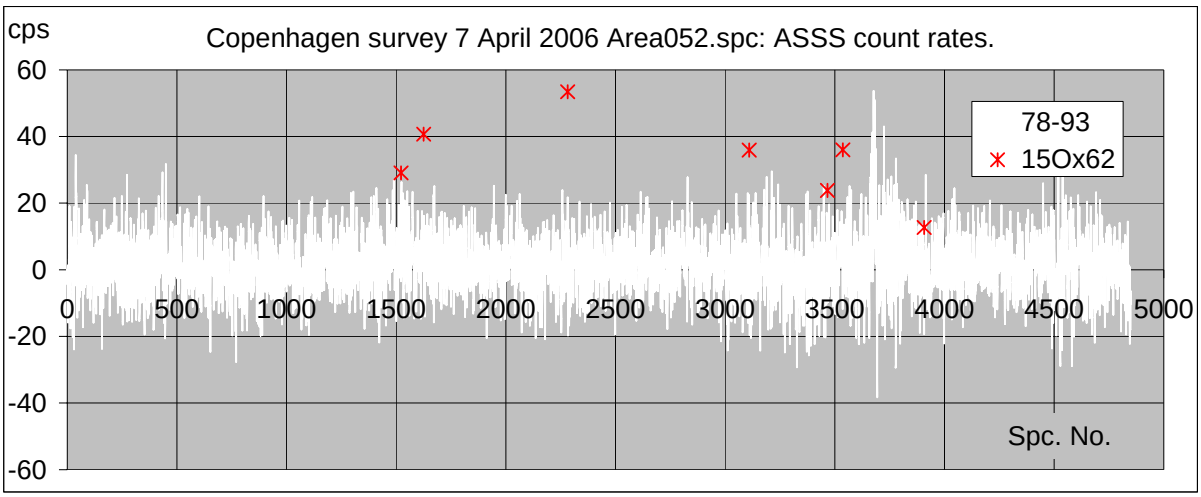

Figure 6.13. ASSS stripped count rates for low energy window channel 78 to channel 93.

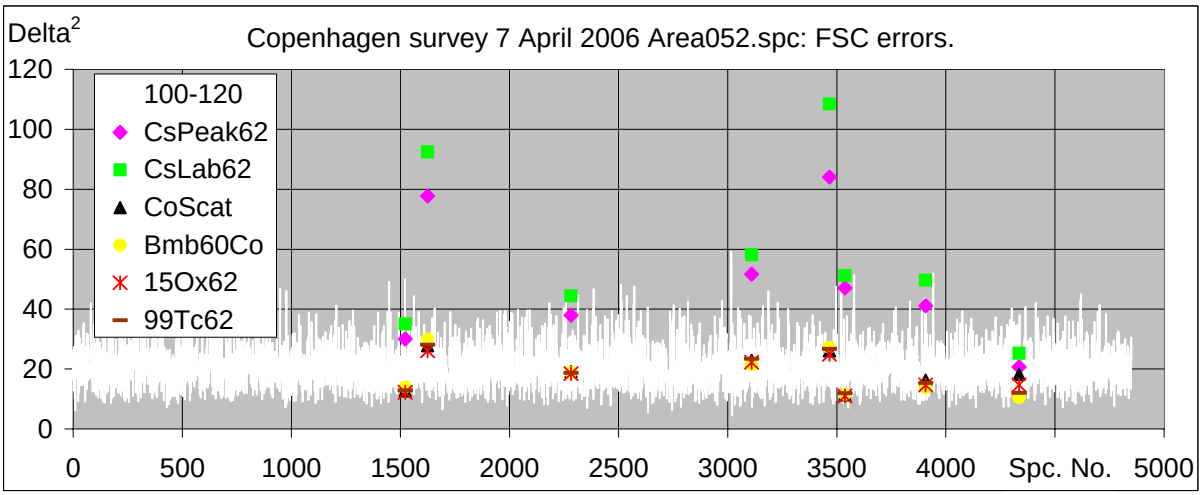

Figure 6.14. FSC errors for caesium window channel 100 to channel 120.

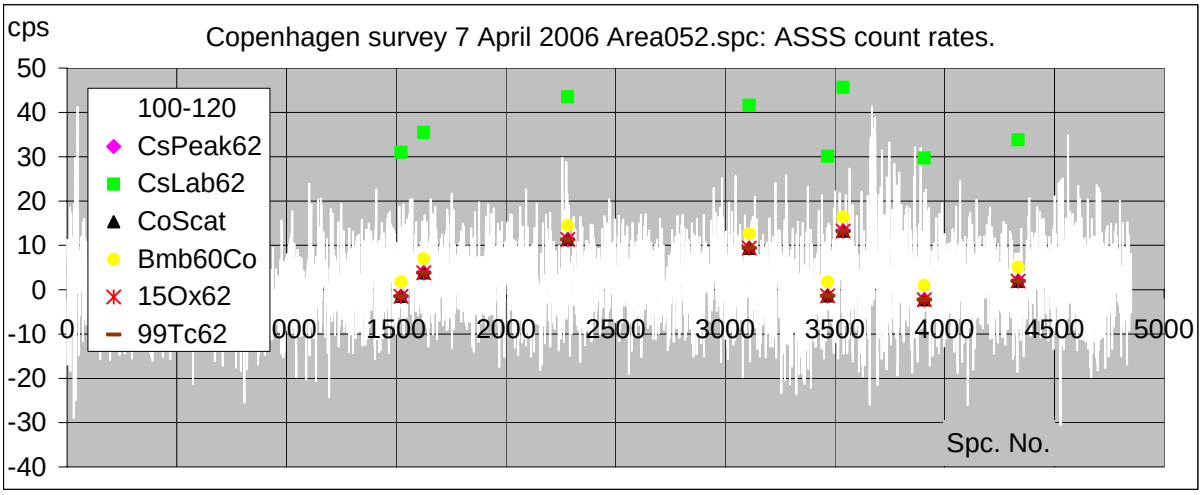

Figure 6.15. ASSS stripped count rates caesium window channel 100 to channel 120.

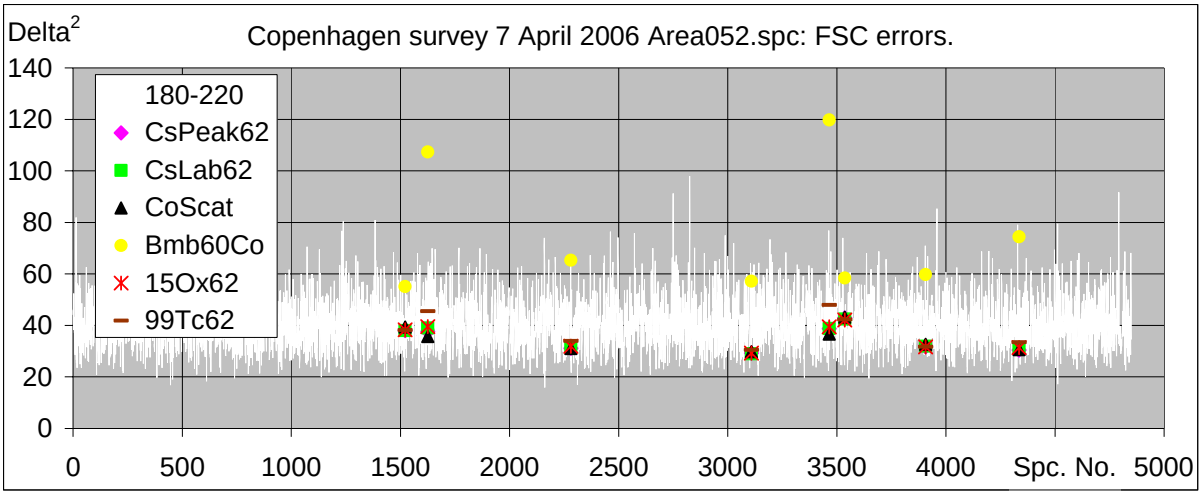

Figure 6.16. FSC errors for cobalt window channel 180 to channel 220.

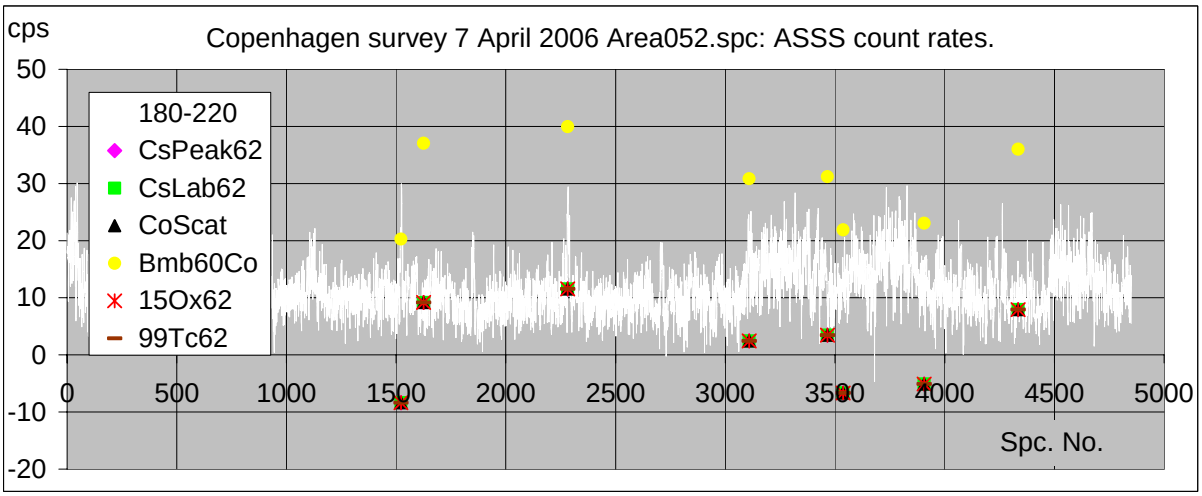

Figure 6.17. ASSS stripped count rates caesium window channel 180 to channel 220.

In general the following comments can be made:

When a source is found by the FSC method, the evidence is stronger than when a source is found by the ASSS method.
ASSS finds more signals but introduces also a lot of "false" source possibilites that could take a long time to investigate. This is caused by insufficient stripping of the natural radionuclides.

Data processing by the ASSS method is beyond doubt easier to do than data processing by the FSC method because the ASSS method only require the gross count rates for the measured spectra whereas the FSC method require that the user is able to extract a series of spectral shapes. ASSS therefore could be used also with simpler equipment as e.g. GM counters.
The ASSS method may be easier to apply but the interpretation of the results are more difficult. Some experience in comparison of natural radionuclide count rates to stripped count rates is needed. Another issue, that has not been discussed in this report but elsewhere (Ref.3, 4) is the possibility of obtaining very erroneous ASSS factors if measurements containing strong "high" energy source signals that give counts in the potassium windows (and possibly above if pile up), e.g. ^{60}Co, are not removed from the data sets before the ASSS factors are calculated.

7 FINNISH CGS MEASUREMENTS

7.1 The Finnish CGS System

The Finnish mobile laboratory (SONNI - Sophisticated On-Site Nuclide Identification system) has two electrically cooled coaxial HPGe detectors. Cooler units are mounted in a passively stabilized cradle, which counteracts the tilting of the vehicle while it is moving. The in-situ measurement crystal is mounted on the ceiling of the main operations section of the vehicle away from the bulk of the equipment. The lead shield of the sample measurement detector is securely fastened to the floor of the vehicle and the detector faces downwards. For added redundancy, the detector mountings are designed so that in case of a break down, the remaining detector can be installed in either position; thus, the function with the highest priority can be maintained.

SONNI has three NaI(Tl) scintillation detectors. Two large detectors (5" x 4") are mounted on the opposite walls of the main operation area facing the sides of the vehicle. Steel shields of 15 mm around the detectors create fields of view opening outwards. This type of configuration enables good detection and localization of radiation sources. One small detector (2" x 2") is mounted inside a 15 mm thick steel tube opening in the direction of travel. This type of collimation makes it possible to make a spatial scan of the incident site from a distance. In addition, it gives a capability to pinpoint target vehicles among the traffic. Time-stamped measurements can be used to identify the source of the radiation or the suspect vehicle from the simultaneous video recording.

Figure 7.1.1. Interior of Sonni. The two main NaI detectors can be seen on either side in the back. The HPGe detector is barely visible in the top of the picture.

7.2 The LINSSI Database

The Finnish data is collected to a relational database LINSSI <http://linssi.hut.fi/radphys/linssi/> running under MySQL. This database incorporates all relevant data, including raw spectrum data, positional data and analysis results. The general table layout of LINSSI is depicted in Figure 7.2.1.

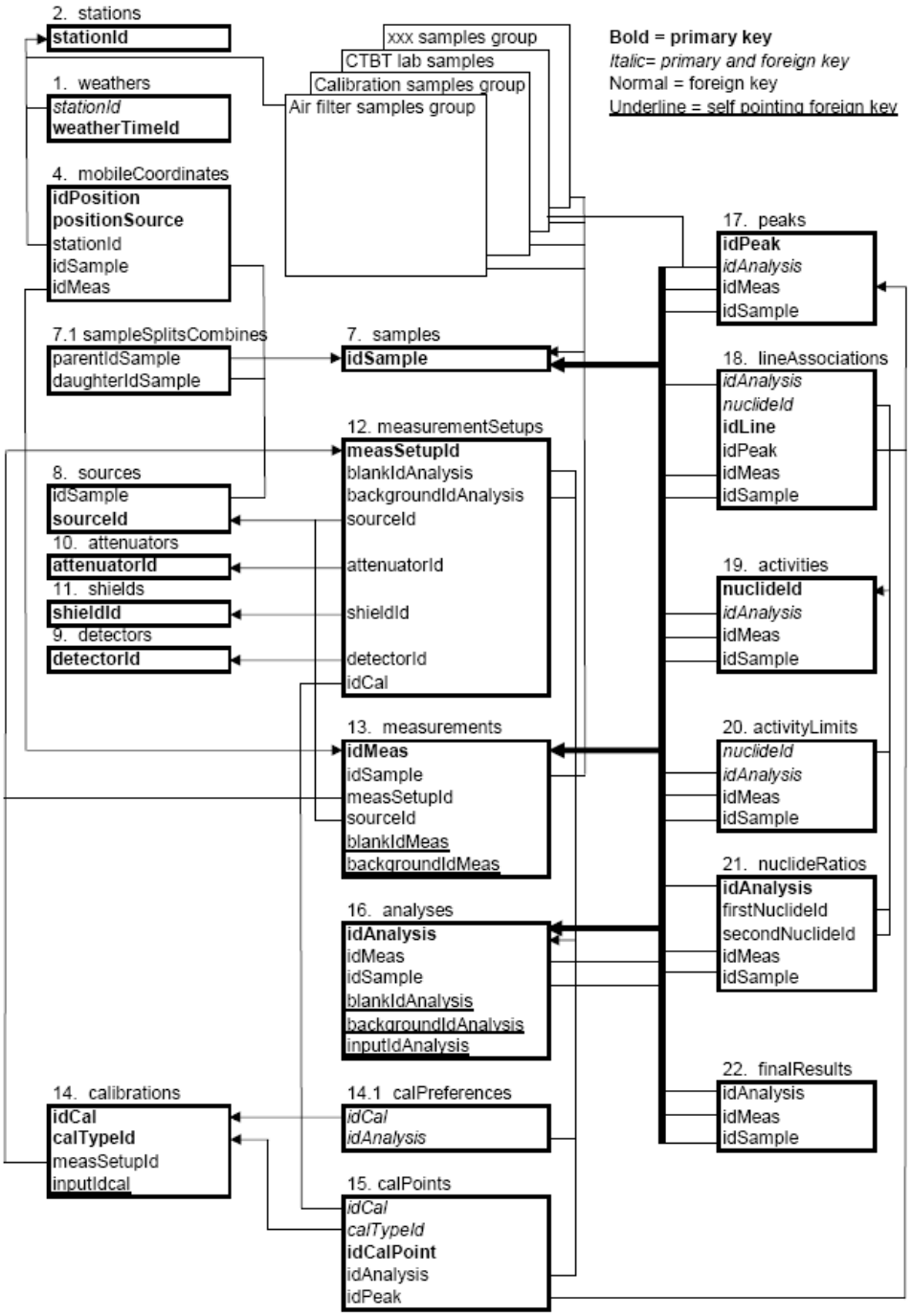

Figure 7.2.1. Table layout of the LINSSI database. For a complete description of LINSSI and all its fields please see <http://linssi.hut.fi/radphys/linssi/>.

7.3 XML-Format for Radiological Messages in In-Situ Measurements with Sonni

Data transfer between LINSSI databases in SONNI and at the STUK headquarters, is done through an XML format. This format is also used in this UGS project as an interim data format for transfer between the Danish CGS format and the LINSSI database.

A script has already been written for transferring the Danish data into this XML format.

7.3.1 Message Format - Example

```
<?xml version=”1.0”?>
<!DOCTYPE SONNI SYSTEM “insituSONNI.xsd”>
<message>
<defaultParams block="spatialData">
        <param pos="0" format=”UTC”>time</param>
        <param pos="1" unit="deg" datum="WGS84">xCoodinate</param>
        <param pos="2" unit="deg" datum="WGS84">yCoodinate</param>
        <param pos="3" unit=”m">altitude</param>
        <param pos="4" unit="deg">heading</param>
</defaultParams>
<defaultParams block="peakData">
        <param pos="0">nuclideId</param>
        <param pos="1" unit="keV">lineEnergy</param>
        <param pos=”2”>significance</param>
        <param pos=”3” unit=”cnts”>peakArea</param>
        <param pos=”4” unit=”cnts”>uncPeakArea</param>
</defaultParams>
<defaultParams block="roiData">
        <param pos="0">roiId</param>
        <param pos="1" unit="chn">ROIstart</param>
        <param pos=”2” unit=”chn">ROIend</param>
        <param pos=”3” unit=”cnts”>ROIarea</param>
</defaultParams>
<stationId>SONNI</stationId>
<idMessage>297</idMessage>
<hypothesisRiskLevel>1E-06</hypothesisRiskLevel>
<measurement>
        <idMeas>4208</idMeas>
        <acqStart>20060310101244</acqStart>
        <detectorName>L</detectorName>
        <liveTime>4.9</liveTime>
        <spatialData>
            <parameters>
                <param pos="0" format=”UTC”>time</param>
                <param pos="1" unit="deg" datum="WGS84">xCoodinate</param>
                <param pos="2" unit="deg" datum="WGS84">yCoodinate</param>
                <param pos="3" unit=”m">altitude</param>
                <param pos="4" unit="deg">heading</param>
                </parameters>
                <values>
                20060310101249 25.0159 60.12456 50 0.6
                ...Next position during measurement..
                </values>
        </spatialData>
```

<peakData>

<parameters>

<param pos="0">nuclideId</param>
<param pos="1" unit="keV">lineEnergy</param>
<param pos="2">significance</param>
<param pos="3" unit="cnts">peakArea</param>
<param pos="4" unit="cnts">uncPeakArea</param>

</parameters>

<values>

Am-241	**59.5**	**-0.232**	**-32.067**	**29.043**
Tc-99m	**140.5**	**0.432**	**127.078**	**61.861**
Ra-226	**186.2**	**0.431**	**135.392**	**66.076**
Ir-192	**316.5**	**0.089**	**21.823**	**51.669**
I-131	**364.5**	**0.050**	**12.074**	**50.424**
Ir-192b	**468.1**	**0.345**	**75.534**	**46.084**
Cs-137	**661.7**	**2.931**	**652.019**	**46.801**
Co-60	**1173.2**	**0.212**	**10.977**	**10.889**
Co-60b	**1332.5**	**-0.187**	**-9.204**	**10.373**
K-40	**1460.8**	**0.686**	**33.673**	**10.333**

</values>

</peakData>

<roiData>

<parameters>

<param pos="0">roiId</param>
<param pos="1" unit="chn">ROIstart</param>
<param pos="2" unit="chn">ROIend</param>
<param pos="3" unit="cnts">ROIarea</param>

</parameters>

<values>

TcLow	**6**	**40**	**1950**
TcHigh	**53**	**93**	**4945**
hiEnd	**933**	**1021**	**6**
total	**6**	**1024**	**15985**

</values>

</roiData>

<spectralData>

<firstChannel>201</firstChannel>
<lastChannel>266</lastChannel>
<firstValidChannel>201</firstValidChannel>
<lastValidChannel>266</lastValidChannel>
<spectrum>
0 0 0 0 0 1 5 7 6 20 22 50 60 ....
</spectrum>

</spectralData>

<comments>Is this specification OK?</comments>

</measurement>

<measurement>
...Data from another measurement....
</measurement>

</message>

Fields used with SONNI are written in **bold.** Required parameter definitions can be written in <*defaultParams*>-blocks or within the corresponding <data>-block in <*parameters*>-block. A minimum of one <Data>-block per message is required. The <spectralData>-block is not used in automated messaging from SONNI but can be used with other applications on demand. Spectrum is given within the <spectrum>-tags as counts per each channel, separated with one or many white space characters.

7.4 CGS Analysis Tools

7.4.1 Standard Software

Sonni is equipped with the Unisampo-Shaman (USS) spectrum analysis package. Unisampo is capable of mobile in-situ spectrum acquisition and real-time analysis. It also is equipped with waterfall and roi area display functionalities for data visualisation in the vehicle. A picture of the Unisampo waterfall spectrum is shown in Fig. 7.4.1.1.

The USS package can also be used for in depth analysis of interesting spectrums. USS is specialised on HPGe analysis, but Unisampo can also handle NaI spectra.

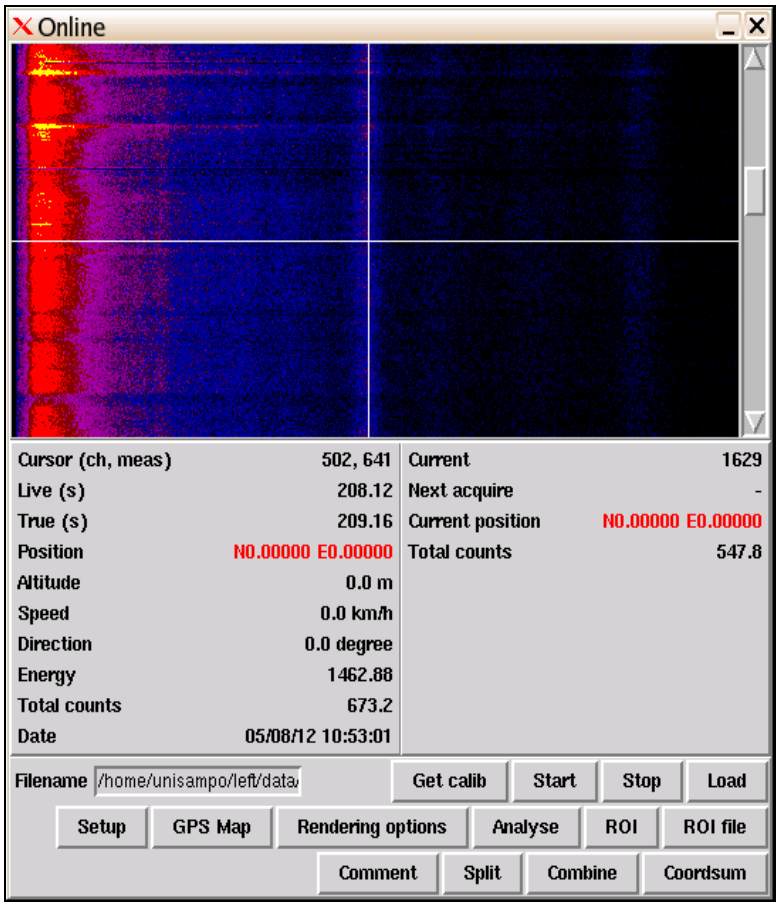

Figure.7.4.1.1. Unisampo Waterfall plot. The thin yellow streak just above the crosshair is from a ^{99m}Tc source detected during the 2005 Athletics World Championship (Radiology patient outside a hospital).

7.4.2 In-house data Processing Methods

Measured spectra are analyzed in real time with a script using a simple summation algorithm over predefined areas of interest. The analysis assumes that the spectrum contains peaks of the predefined nuclides and tests this hypothesis by calculating the peak significance for each nuclide. The peak significance S is defined as:

$$S = \frac{A}{L_C(\alpha)} = \frac{A}{k_\alpha D(A)} \qquad (7.4.2.1)$$

where A is peak area, $D(A)$, the standard deviation of the peak area, L_C Currie's decision limit (Ref. 11) and k_a sets the risk level of detecting false positives in terms of the Gaussian abscissa. With $k_a = 4.753$, $S>1$ once in a million measurements (type I error risk $\alpha = 10^{-6}$). Exceeding the decision limit S=1 triggers an automatic alarm.

The summation algorithm is presented in Figure 7.4.2.1. The baseline B is calculated from both sides of the assumed peak by summing up the counts in both baseline calculation areas B_1 and B_2 and by scaling with the number of channels under the peak (W) and the baseline ($2n$):

$$B = \frac{B_1 + B_2}{2n} W \,, \qquad (7.4.2.2)$$

The peak area is then calculated simply with equation:

$$A = \frac{C - B}{g} \,, \qquad (7.4.2.3)$$

where C is the total counts in the peak calculation area. If the peak calculation area does not span over the whole Gaussian peak, the total counts in a peak is gained by scaling with the area correction parameter g.

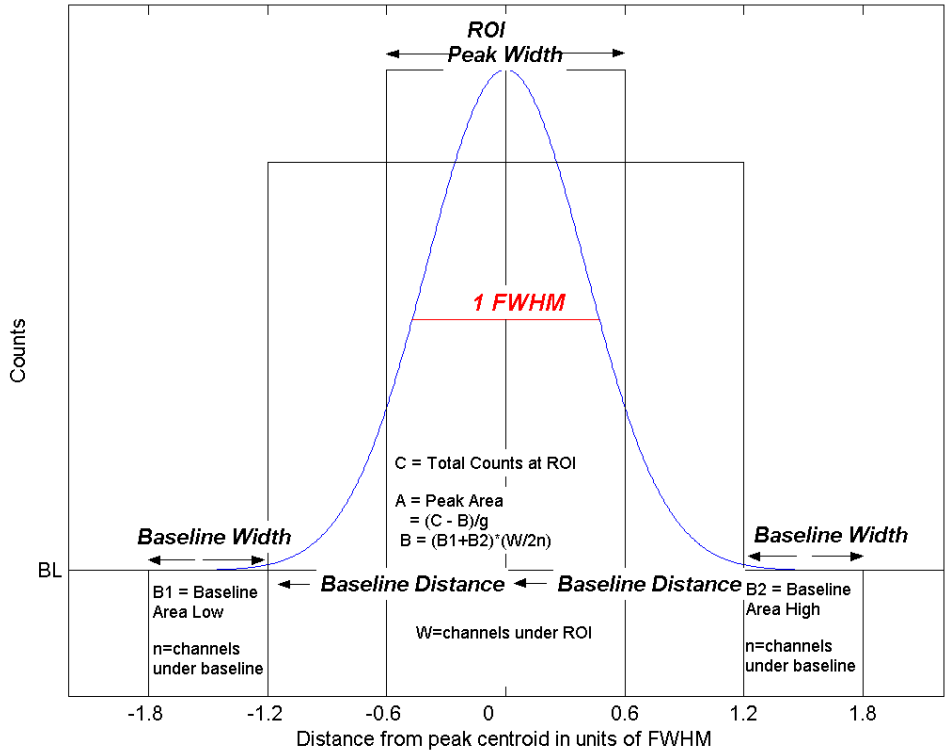

Figure 7.4.2.1. Gaussian peak and the summation algorithm used for hypothesis testing. All parameters are given in units of FWHM. Parameters used for NaI(Tl) spectra are Peak Width = 1.2, Baseline Width = 0.6, Baseline Distance = 1.2 and g = 0.842.

The variance of the peak area $D^2(A)$ is then estimated with:

$$D^2(A) = \frac{1}{g^2}\left|A + B\left(1 + \frac{W}{2n}\right)\right| \qquad (7.4.2.4)$$

All calculations are done in channels. The statistical behaviour of this method is described in detail in reference (Ref. 12).

7.5 Finnish Data Sets

The main Finnish dataset to be used in this project is the more than 25000 NaI spectra measured in the Helsinki region during the Athletics World Championship in 2005. During a period of two weeks, Sonni made daily routes around the Helsinki Stadium and the Otaniemi area, where the athletes had their lodgings. These routes are shown with thick blue lines in the maps in figures 7.5 and 7.6. Additionally Sonni measured the area along the Marathon route before the event. This route is shown in green in fig 7.6. The dataset also includes measurements made during transition between the two areas, and to or from the headquarters in eastern Helsinki.

All mobile measurements in this dataset are 5 sec long. The spectrums consist of 1024 channels. Sonni is equipped with a climate control system and the energy calibration was adjusted manually several times each day, to counteract the effects of temperature drift. The resolution of the NaI detectors is approximately 8% when driving in the field.

Furthermore, another dataset with signals from artificial radionuclides is available as test and comparison data. This dataset consists of measurements made at the Vesivehmaa airfield during driving past artificial radionuclides (^{241}Am, ^{99m}Tc, ^{137}Cs and ^{60}Co) at different distances ranging from 20 to 160 m and at different speeds (30km/h and 60 km/h). The measurements are of 2 and 5 sec duration.

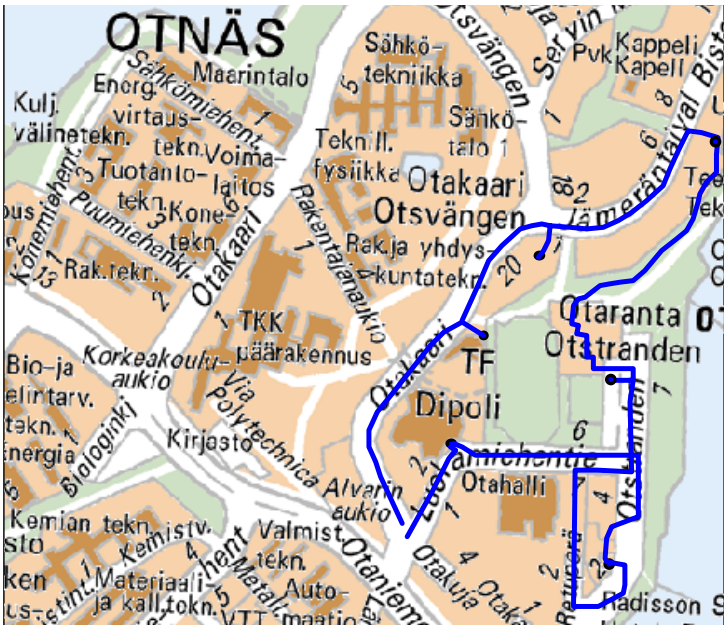

Figure 7.5.1. The daily route in the Otaniemi area.

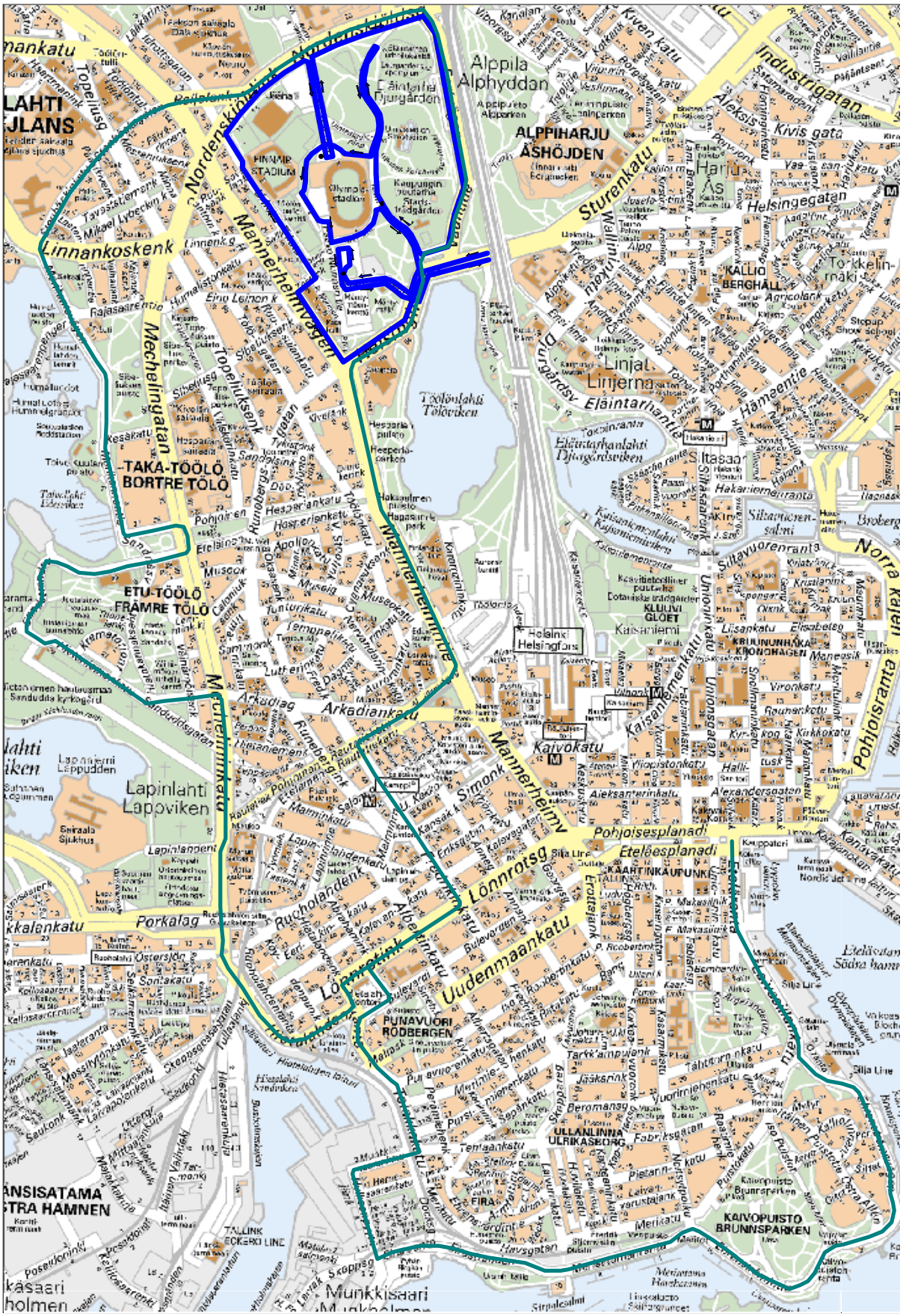

Figure 7.5.2. The daily route around the Helsinki Stadium (thick blue line) and The Marathon route (thinner green line).

7.6 Finnish data processing

All measurements in Sonni are analysed in real time using the hypothesis test method described in Section 7.4.2. The algorithm searches for certain key nuclides, that are expected to be found in possible orphan sources or that can be obtained and used for malicious purposes.

In Figure 7.6.1 is an example of the hypothesis test outcome for the left NaI detector for three nuclides (^{99m}Tc, ^{137}Cs and ^{241}Am), during a time period of slightly less than half an hour. The significance of ^{99m}Tc has a small positive bias, due to the shape of the spectrum in the area of the 141 keV peak. This offset is taken into account when setting the alarm levels in Sonni (not shown in picture), so for this nuclide a significance of 1.2, must be achieved for an alarm to go off. The same method is used when measuring in areas with real background (e.g. searching for a ^{137}Cs orphan source, in an area with significant ^{137}Cs fallout). As explained in Section 7.4.2, the risk level is set at 10^{-6} so the ^{99m}Tc measurement with a high significance close to 10:51:40 is a real finding (probably an isotope patient, as the finding was made right outside a big hospital).

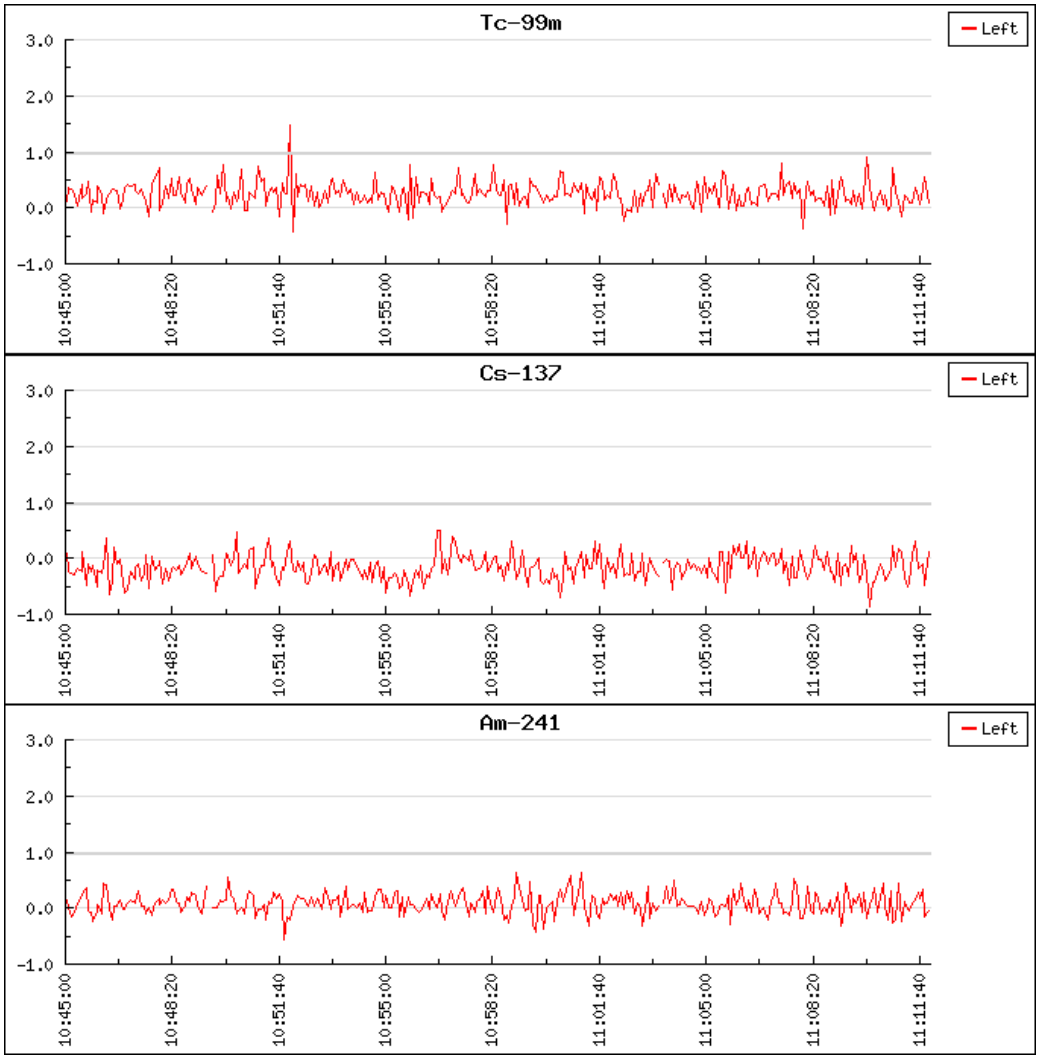

Figure 7.6.1. Significances output by the hypothesis test method used in Sonni. In this data period one finding of ^{99m}Tc can be seen.

From the Vesivehmaa data, STUK calculated peak efficiencies and MDA's for the measured nuclides, at different distances from the car. One example of this can be seen in Figure 7.6.2.

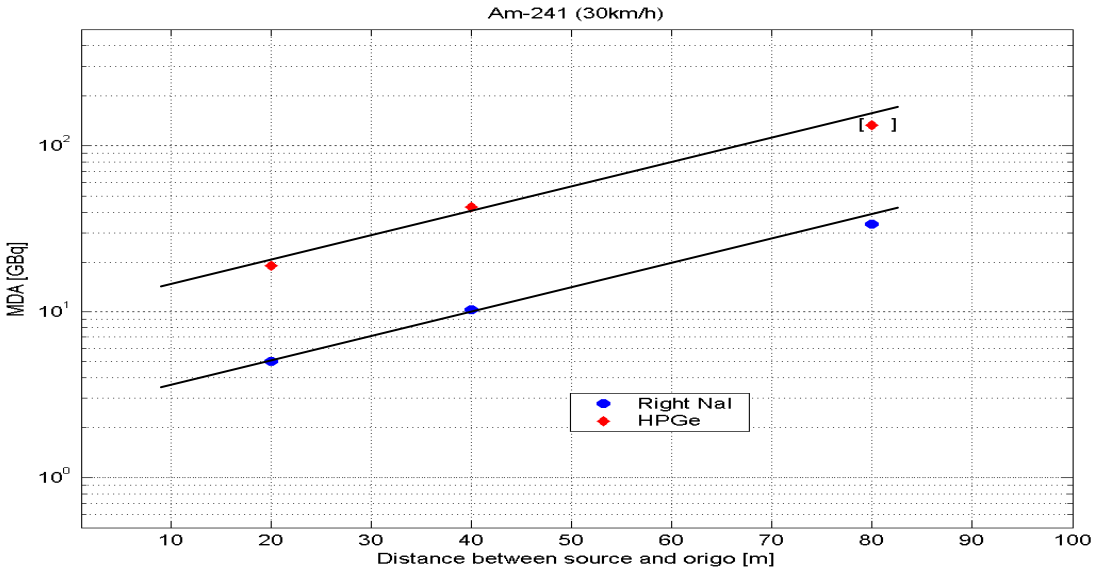

Figure 7.6.2. Minimum detectable activity, MDA, for ^{241}Am with data acquisition interval of 5 s and driving speed of 30 km/h as a function of distance between the source and the road. Measurements with low statistics are marked with square brackets ([ ]) (Ref. 13).

8 ACRONYMS

AGS	Airborne Gamma Spectrometry
ASSS	Area Specific Spectrum Stripping (previously ASS)
CGS	Carborne Gamma Spectrometry
DEMA	Danish Emergency Management Agency
DTU	Technical University of Denmark
FSC	Fitting with Spectral Components
LINSSI	LInux System for Spectral Information
MDA	Minimum Detectable Activity
NASVD	Noise Adjusted Singular Value Decomposition
NRPA	Norwegian Radiation Protection Agency
SONNI	Sophisticated On Site Nuclide Identification
SSI	Swedish Radiation Protection Authority
STUK	Radiation and Nuclear Safety Authority, Finland
UGS	Urban Gamma Spectrometry
USS	Unisampo-Shaman

9 REFERENCES

1. Karlsson, S., Mellander, H., Lindgren, J., Finck, R., and Lauritzen, B. (eds.). RESUME99 Rapid Environmental Surveying Using Mobile Equipment. NKS-15, ISBN 87-7893-065-0 (2000).
2. Aage, H. K., Korsbech, U.: Search for orphan sources using CGS equipment - a short handbook. (Made for CGS measuring teams in Balticum, Poland, Russia and Denmark, restricted). Ørsted-DTU, Measurement & Instrumentation Systems, Technical University of Denmark, Report IT-NT-59, November 2001.
3. Korsbech, U., Aage, H.K., Byström, S., Wedmark, M., Thorshaug, S. and Bargholz, K. Area specific stripping of lower energy windows for AGS and CGS systems. Nordic AGS and CGS data, NKS-109, ISBN 87-7893-168-1, May 2005.
4. Aage, H. K., Korsbech, U., Bargholz, K., Bystöm, S. Wedmark, M., and Thorshaug, S., 2006. Experience with area specific spectrum stripping of NaI(Tl) gamma spectra. ASSS paper. Radiation Protection Dosimetry, doi:10.1093/rpd/ncl010.
5. Aage, H. K., Korsbech, U. and Bargholz, K. Early detection of radioactive fall-out by gamma-spectrometry. Radiation Protection Dosimetry, 106 (2), 155-164, (2003).
6. Aage, H. K., Korsbech, U.: Fitting of new CGS spectra with base spectral components. Report NT-67, December 2004, Øersted-DTU.
7. Hovgaard, J., 1997a. Airborne Gamma-Ray Spectrometry. Statistical Analysis of Airborne Gamma-Ray Spectra. Ph. D. Thesis, Technical University of Denmark.
8. Aage, H. K., and Korsbech, U. Search for lost or orphan radioactive sources based on NaI gamma spectrometry. Appl. Radiat. Isot., 58 (1), 103-113 (2003).
9. Aage, H. K., Korsbech, U., Bargholz, K., Hovgaard, J.: A new technique for processing airborne gamma ray spectrometry data for mapping low level contaminations. Applied Radiation and Isotopes, Volume 51, pp. 651-662, December 1999.
10. Tsoulfanides, N. Measurement and Detection of Radiation, University of Missouri-Rolla, Hemisphere Publishing Corporation, 1983.
11. Currie L. A. Limits for Qualitative Detection and Quantitative Determination - Application to Radiochemistry.
    Analytical Chemistry 1968, Vol 40, no. 3, pp.586 - 593.
12. Kuukankorpi S., Toivonen H., Moring M. and Smolander P. Mobile Spectrometry System for Source Finding and Prompt Reporting (to be published in 2006).
13. Toivonen H, Kuukankorpi S, Moring M. Smolander P. Radionuclide source finding using a mobile laboratory for supporting counter terrorism actions. Symposium on chemical, biological, nuclear and radiological threats, Tampere 2006 (to be published in 2006).

Title	Urban Gamma Spectrometry: Report 1
Author(s)	[1]Helle Karina Aage, [2]Satu Kuukankorpi, [2]Mikael Moring, [2]Petri Smolander and [2]Harri Toivonen
Affiliation(s)	1) Technical University of Denmark, Kgs. Lyngby, Denmark 2) Radiation and Nuclear Safety Authority, Helsinki, Finland
ISBN	978-87-7893-257-0
Date	June 2009
Project	NKS-B / UGS
No. of pages	62
No. of tables	17
No. of illustrations	65 (some of which are composites)
No. of references	13

Abstract

This report contains the present status and results for the NKS UGS-project per 1 June 2006 for NKS partners DTU, Denmark, and STUK, Finland.
The Danish and Finnish CGS systems are not of similar types. The Danish CGS system(s) only make use of one NaI(Tl) detector whereas the Finnish CGS system consists of several detectors, NaI(Tl) and HPGe both and as an additional feature the Finnish detectors have position dependent different fields of view.
Furthermore, the Finnish system is equipped with an air sampling system. In terms of operation, the Danish detector is located r on the rooftop whereas the Finnish detectors are located inside the vehicle.
The Finnish and the Danish team use different methods for data processing.
STUK uses a hypothesis test method to get robust real time alarms (within 10 seconds) when significant peaks from a previously defined set of nuclides are detected. An alarm for a significantly elevated total pulse rate is sent if none of the predefined nuclides is identified. All data are stored to the LINSSI database, which facilitates easy data retrieval for post processing.
DEMA/DTU bases their calculations on full spectrum fitting using NASVD and the Danish software NucSpec. Source signals are found from spectrum fitting residuals or from stripping of energy windows – either by the standard 4-windows method or by a measurement based method where stripping factors for any window of interest can be derived from the measurements themselves.
A thorough description of the two systems and data processing methods (including mathematics) are described in this report.
For the Danish methods of data processing some comparisons have been made, but no final conclusion has been reached yet. Raw urban data has been investigated along with urban data sets to which source signals have been added and searched for.
For the Finnish method calibration plots of the minimum detection limits for two different detector types have been made so far, and survey significance plots from drives around Helsinki during the Athletics World Championship in 2005 are presented.

Key words

Urban Carborne Gamma Spectrometry, Spectrum Stripping, Peak hypothesis, LINSSI, FSC, ASSS, NASVD

Available on request from the NKS Secretariat, P.O.Box 49, DK-4000 Roskilde, Denmark.
Phone (+45) 4677 4045, fax (+45) 4677 4046, e-mail nks@nks.org, www.nks.org